UNIVERSITÀ
DEGLI STUDI
DI PADOVA

Sede Amministrativa: Università degli Studi di Padova

Dipartimento di Biologia

SCUOLA DI DOTTORATO DI RICERCA IN BIOSCIENZE E BIOTECNOLOGIE

INDIRIZZO BIOLOGIA CELLULARE

CICLO XXV

A Novel Ca^{2+} Release Channel in Mitochondria of *Drosophila melanogaster*: Properties and Role in Ca^{2+} Homeostasis

Direttore della Scuola: Ch.mo Prof. Giuseppe Zanotti

Coordinatore d'indirizzo: Ch.mo Prof. Paolo Bernardi

Supervisore: Ch.mo Prof. Paolo Bernardi

Dottorando: Sophia von Stockum

31 DICEMBRE 2012

"We must not forget that when radium was discovered no one knew that it would prove useful in hospitals. The work was one of pure science. And this is a proof that scientific work must not be considered from the point of view of the direct usefulness of it. It must be done for itself, for the beauty of science, and then there is always the chance that a scientific discovery may become like the radium a benefit for humanity. "

- Marie Curie, Lecture at Vassar College, 1921-

The scientist is not a person who gives the right answers, he's one who asks the right questions.

-Claude Lévi-Strauss, Le Cru et le cuit, 1964-

dedicated to my parents

TABLE OF CONTENTS

LIST OF FIGURES

LIST OF TABLES

SUMMARY

Mitochondrial Ca^{2+} uptake and release play a pivotal role in different physiological processes such as intracellular Ca^{2+} signaling and cell metabolism, while their dysregulation can lead to cell death induction. In energized mitochondria the Ca^{2+} uniporter (MCU) mediates Ca^{2+} uptake across the inner mitochondrial membrane (IMM) while the Na^{+}/Ca^{2+} exchanger and the H^{+}/Ca^{2+} exchanger are responsible for Ca^{2+} efflux. However, when mitochondrial matrix Ca^{2+} load exceeds the capacity of the efflux pathway by exchangers, an additional pathway for Ca^{2+} release from mitochondria may exist through opening of the permeability transition pore (PTP). The mitochondrial permeability transition (PT) describes a process of Ca^{2+}-dependent, tightly regulated increase in the permeability of the IMM to solutes with molecular masses below 1500 Da, due to the opening of a high-conductance channel, the PTP. Prolonged PTP opening causes several effects, such as depolarization, osmotic swelling, outer mitochondrial membrane rupture and release of apoptogenic proteins like cytochrome *c* (cyt *c*). Transient openings of the PTP on the other hand, might be involved in physiological Ca^{2+} homeostasis and may protect mitochondria from Ca^{2+} overload. Several studies allowed a thorough characterization of the functional properties and regulation of the putative channel, but its molecular nature remains still elusive. One of the best defined modulators of the PTP is the mitochondrial peptidyl-prolyl-*cis-trans*-isomerase (PPIase) Cyclophilin D (Cyp-D), that plays an important role in protein folding and can be selectively inhibited by the immunosuppressant drug Cyclosporin A (CsA).

In spite of its importance as a model organism and as a genetic tool, remarkably little is known about the properties of Ca^{2+} transport in mitochondria of the fruit fly *Drosophila melanogaster*, and on whether these mitochondria can undergo a PT. In this study we have characterized the pathways of Ca^{2+} transport in the digitonin-permeabilized embryonic *Drosophila* cell line S_2R^{+}. We demonstrated the presence of ruthenium red-sensitive Ca^{2+} uptake, and of Na^{+}-stimulated Ca^{2+} release in energized mitochondria, which match well characterized Ca^{2+} transport pathways of mammalian mitochondria. Furthermore we identified and characterized a novel mitochondrial Ca^{2+}-dependent Ca^{2+} release channel in *Drosophila.* Like the mammalian PTP, *Drosophila* Ca^{2+} release is inhibited by tetracaine and opens in response to matrix Ca^{2+} loading, IMM depolarization and thiol oxidation. As the yeast pore (and at variance from the

mammalian PTP), the *Drosophila* channel is inhibited by Pi and insensitive to CsA. A striking difference between the pore of *Drosophila* and that of mammals is its selectivity to Ca^{2+} and H^{+} and the lack of mitochondrial swelling and cyt *c* release during the opening of the channel.

The apparent absence of a mitochondrial Cyp in *Drosophila* prevents an investigation based on the effects of CsA, a classical inhibitor of the mammalian PTP. Thus, in the second part of this study we expressed human Cyp-D in *Drosophila* S_2R^{+} cells in order to investigate its impact on the Ca^{2+}-induced Ca^{2+} release channel. Preliminary Ca^{2+} retention capacity studies demonstrated that human Cyp-D induces opening of the *Drosophila* Ca^{2+} release channel in a rotenone-sensitive but CsA-insensitive manner. If the Cyp-D in *Drosophila* cells changes selectivity, size and properties of the Ca^{2+}-induced Ca^{2+} release channel can now be addressed.

We conclude that *Drosophila* mitochondria possess a selective Ca^{2+} release channel with features intermediate between yeast and mammals that is probably involved in Ca^{2+} homeostasis but not in Ca^{2+}-mediated cell death induction. In this study we paved the way for the application from the sophisticated genetic strategies that *Drosophila* provides to define the molecular nature of the PTP and its role in pathophysiology of Ca^{2+} homeostasis.

SOMMARIO

L'accumulo e il rilascio di Ca^{2+} da parte dei mitocondri svolge un ruolo centrale in diversi processi fisiologici, come nelle vie di segnalazione intracellulari e nel metabolismo cellulare, mentre la loro disregolazione può indurre la morte cellulare. In mitocondri energizzati, l'uniporto del Ca^{2+} (MCU) media l'accumulo di Ca^{2+} attraverso la membrane mitocondriale interna (MMI) mentre gli scambiatori Na^{+}/Ca^{2+} e H^{+}/Ca^{2+} sono responsabili del suo efflusso. Tuttavia, quando il carico di Ca^{2+} nella matrice mitocondriale supera la capacità di efflusso attraverso gli scambiatori, potrebbe attivarsi una via aggiuntiva di rilascio di Ca^{2+}, attraverso l'apertura del poro di transizione di permeabilità (PTP). La transizione di permeabilità (TP) consiste nell'aumento della permeabilità della MMI a soluti con massa molecolare inferiore a 1500 Da, è un processo Ca^{2+}-dipendente, strettamente regolato, e dovuto all'apertura di un canale ad alta conduttanza, il PTP. La prolungata apertura del PTP provoca diversi effetti, come la depolarizzazione, il rigonfiamento osmotico, la rottura della membrana mitocondriale esterna e il rilascio di proteine pro-apoptotiche come il citocromo *c* (cit *c*). L'apertura transiente del PTP, invece potrebbe essere coinvolta nell'omeostasi fisiologica del Ca^{2+} e potrebbe proteggere i mitocondri da un sovraccarico dello stesso. Diversi studi hanno consentito una caratterizzazione accurata delle proprietà funzionali e della regolazione del canale putativo, ma la sua natura molecolare rimane ignota. Uno dei miglior modulatori caratterizzati del PTP è la peptidil-prolil-*cis*-*trans*-isomerasi mitocondriale Ciclofilina D (Cip-D), che svolge un ruolo importante nel ripiegamento delle proteine e può essere selettivamente inibita dal farmaco immunosoppressore Ciclosporina A (CsA).

Nonostante la sua importanza come organismo modello e come strumento genetico, poco si conosce a proposito delle proprietà di trasporto di Ca^{2+} mitocondriale del moscerino della frutta *Drosophila melanogaster* e dell'eventualità che i suoi mitocondri possano subire una TP. In questo studio abbiamo caratterizzato le vie di trasporto di Ca^{2+} mitocondriale nella linea cellulare embrionica di *Drosophila* S_2R^{+}, permeabilizzata con la digitonina. Abbiamo dimostrato la presenza di un effettivo accumolo di Ca^{2+}, sensibile al rosso rutenio, come anche il rilascio di Ca^{2+} stimolato dal Na^{+} in mitocondri energizzati, processi che corrispondono alle ben caratterizzate vie di trasporto di Ca^{2+} in mammiferi. Inoltre, abbiamo identificato e caratterizzato un nuovo canale di rilascio del Ca^{2+} indotto dal Ca^{2+} stesso in *Drosophila*. Come il PTP dei mammiferi, il canale di

rilascio di Ca^{2+} in *Drosophila* è inibito da tetracaina e apre in risposta al carico di Ca^{2+} nella matrice, depolarizzazione della MMI ed ossidazione di tioli. Come il poro in lievito (e in contrasto con il PTP dei mammiferi), il poro di *Drosophila* è inibito da Pi e insensibile alla CsA. Le principali differenze il poro di *Drosophila* e quello dei mammiferi sono la sua selettività per Ca^{2+} e H^{+}, e la mancanza di rigonfiamento mitocondriale e il rilascio di cit *c* conseguente all'apertura del canale.

L'apparente assenza di una Cip mitocondriale in *Drosophila* impedisce uno studio basato sugli effetti della CsA, un classico inibitore del PTP dei mammiferi. Perciò, nella seconda parte di questo studio abbiamo espresso la Cip-D umana nelle cellule S_2R^{+} di *Drosophila* al fine di indagare il suo impatto sul canale di rilascio del Ca^{2+}. Preliminari studi di capacità di ritenzione del Ca^{2+} hanno dimostrato che la Cip-D umana induce l'apertura del canale di rilascio del Ca^{2+} in *Drosophila* in modo rotenone-sensibile ma CsA-insensibile. Se la Cip-D in *Drosophila* cambia la selettività, la grandezza e le proprietà del canale di rilascio del Ca^{2+} può ora essere investigato.

Concludiamo che i mitocondri di *Drosophila* possiedono un canale selettivo di rilascio di Ca^{2+} con caratteristiche intermedie tra il lievito e i mammiferi che probabilmente è coinvolto nell'omeostasi del Ca^{2+}, ma non nell'induzione della morte cellulare mediata dal Ca^{2+}. In questo studio abbiamo spianato la strada per l'applicazione delle strategie di genetica sofisticate, che la *Drosophila* offre per definire la natura molecolare del PTP ed il suo ruolo nella patofisiologia dell'omeostasi del Ca^{2+}.

LIST OF PUBLICATIONS

- **Luca Azzolin, Sophia von Stockum, Emy Basso and Paolo Bernardi.** The mitochondrial permeability transition from yeast to mammals. FEBS Letters (2010), vol. 584; p. 2504-2509

- **Sophia von Stockum, Emy Basso, Valeria Petronilli, Patrizia Sabatelli, Michael A. Forte and Paolo Bernardi.** Properties of Ca^{2+} transport in mitochondria of *Drosophila melanogaster.* The Journal of Biological Chemistry (2011), vol. 286; p. 41163-41170

- **Paolo Bernardi and Sophia von Stockum.** The permeability transition pore as a Ca^{2+} release channel: New answers to an old question. Cell Calcium (2012), vol. 52(1); p. 22-27

- **Sophia von Stockum, Gabriella Mazzotta, Rodolfo Costa and Paolo Bernardi.** Expression of human Cyclophilin D in *Drosophila melanogaster* – impact on regulation of the *Drosophila* mitochondrial Ca^{2+}-induced Ca^{2+} release channel. Manuscript in preparation

LIST OF ABBREVIATIONS

$\Delta\Psi_m$: mitochondrial membrane potential

ΔpH: pH gradient

$\Delta\tilde{\mu}$: electrochemical gradient

ANT: adenine nucleotide translocator

ADP: adenosine diphosphate

AIF: apoptosis inducing factor

Apaf-1: apoptotic protease-activating factor-1

ATP: adenosine triphosphate

BH3: Bcl-2 homology 3

CsA: Cyclosporin A

CsH: Cyclosporin H

Cyp-D: Cyclophilin D

cyt *c*: cytochrome *c*

CRC: calcium retention capacity

Diablo: direct inhibitor of apoptosis binding protein with low pI

DISC: death-inducing signaling complex

DNP: 2,4-Dinitrophenol

EGTA: ethylene glycol tetraacetic acid

endoG: endonuclease G

ER: endoplasmatic reticulum

FADH2: reduced form of flavin adenine dinucleotide

FBS: fetal bovine serum

FCCP: carbonyl cyanide-p-trifluoromethoxyphenylhydrazone

HBSS: Hank's balanced salt solution

hUCP2: human uncoupling protein 2

IAP: inhibitor of apoptotic proteins

IF1: inhibitor protein 1

IMM: inner mitochondrial membrane

MCU: mitochondrial Ca^{2+} uniporter

MDR: multi drug resistance

MnSOD: manganese superoxide dismutase

MOMP: mitochondrial outer membrane permeabilization

mtDNA: mitochondrial DNA

NADH: reduced form of nicotinamide adenine dinucleotide

NCLX: Na^{+}/Ca^{2+} exchanger

NEM: *N*-ethylmaleimide

OMM: outer mitochondrial membrane

OSCP: oligomycin sensitivity conferring protein

PBR: peripheral benzodiazepine receptor

PBS: phosphate buffered saline

PCR: polymerase chain reaction

Pi: inorganic phosphate

PiC: phosphate carrier

PMCA: plasma membrane Ca^{2+}-ATPase

PPIase: peptidyl-prolyl-*cis*-*trans*-isomerase

PT: permeability transition

PTP: permeability transition pore

Q: ubiquinone

ROS: reactive oxygen species

RR: ruthenium red

SDS: sodium dodecyl sulfate

Smac: second mitochondrial-derived activator of caspases

TMRM: tetramethyl rhodamine methyl ester

TNF: tumor necrosis factor

Ub_0: ubiquinone 0

UCP 2: uncoupling protein 2

VDAC: voltage-dependent anion channel

XIAP: X-linked inhibitor of apoptosis proteins

YMUC: yeast mitochondrial unselective channel

INTRODUCTION

1 Mitochondria

Mitochondria are organelles found in the cytoplasm of every eukaryotic cell with the exception of red blood cells and of amitochondrial eukaryotic organisms such as *Giardia intestinalis* and *Trachipleistophora hominis*[1,2]. Their most prominent roles are the supply of energy in form of the high-energy molecule ATP and the regulation of cellular metabolism. In addition, mitochondria are involved in a wide range of other processes, such as Ca^{2+} homeostasis, cellular differentiation, control of cell cycle, cell growth and cell death[3].

1.1 Mitochondrial morphology

During live cell imaging it becomes immediately apparent that mitochondrial morphology is far from static and that mitochondria are mobile and plastic organelles, constantly changing their shape. They can undergo fission and fusion, events which in mammals are regulated by the proteins OPA1, MFN1, MFN2 and DRP1[(4)], or move along the cytoskeleton via specific motor proteins[5], a process of critical importance in axons. Thus, mitochondrial morphology varies widely among different cell types depending on the balance between the rates of fission and fusion. In some cells they form long filaments or chains as in fibroblasts. In others they remain fixed in one position where they provide ATP directly to a site of high ATP consumption, e.g. in myofibrils.

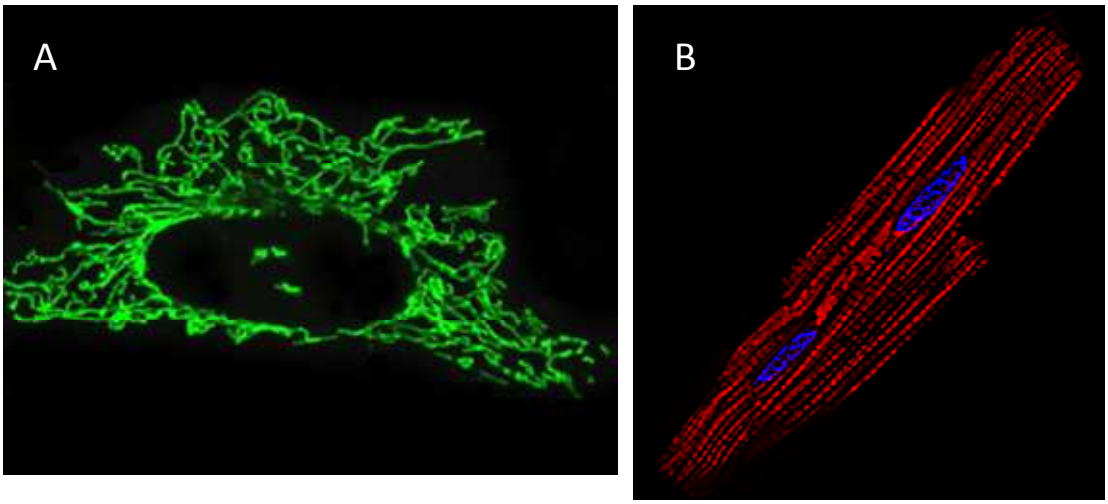

Figure 1. Mitochondrial morphology in fibroblasts and cardiomyocytes. (A) Fluorescence imaging of reticular mitochondrial network in human fibroblasts (green) composed of filamentous tubules that frequently change shape due to high rates of fission and fusion; from[6]. (B) Mitochondrial morphology in cardiomyocytes. Fluorescence live-cell imaging of adult rat cardiomyocyte mitochondria (red). The mitochondria account for about 35% of total cell volume and are arranged longitudinally along the myofibrils at the sarcomeric A-band, providing the majority of ATP needed for contraction and ion homeostasis; from[7].

Mitochondria possess their own genome consisting of a single circular DNA molecule[8] encoding for 2 ribosomal RNAs (rRNAs), 22 transfer RNAs (tRNAs), and 13 polypeptides (all of them components of the respiratory chain/oxidative phosphorylation system). The majority of mitochondrial proteins, however, are encoded by the nuclear genome, requiring import into the mitochondria following translation.

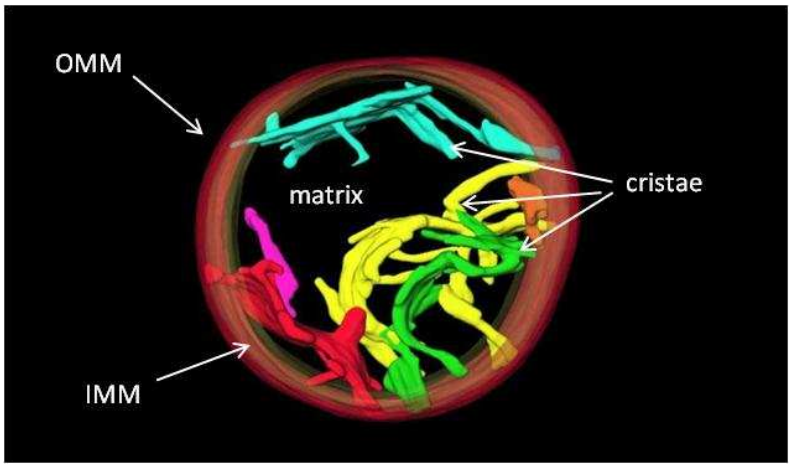

Figure 2. Cryotomogram from isolated rat liver mitochondrion. OMM: outer mitochondrial membrane, IMM: inner mitochondrial membrane; modified from[9].

Each mitochondrion has two highly specialized membranes, the inner and the outer membrane, which have very distinct functions. Together they create two separate mitochondrial compartments: the internal matrix and a narrow intermembrane space (IMS). The inner mitochondrial membrane (IMM) is folded into numerous cristae, which expand its surface area. The outer mitochondrial membrane (OMM) contains many copies of the voltage-dependent anion channel (VDAC), which forms large aqueous channels through the lipid bilayer and allows ions, metabolites and small molecules to move between the cytoplasm and the mitochondria. Such molecules can enter the IMS, but most of them cannot pass the impermeable IMM, which contains a high proportion of the phospholipid cardiolipin, making it especially impermeable to ions. IMM permeability is mediated by a variety of specialized membrane channels, transporters and exchangers that make the latter selectively permeable to ions and small molecules which are metabolized or required by the mitochondrial enzymes located in the matrix. The IMM is a very good electric insulator and can keep a potential difference of -180 mV[10]. Proton pumping driven by electron flow through the respiratory chain constantly

generates an electrochemical gradient ($\Delta\tilde{\mu}H$), which is composed of a membrane potential difference ($\Delta\Psi$) and a proton concentration difference (ΔpH). The proton gradient provides the driving force for ATP synthesis and for ion and metabolite transport. The IMM contains also the energy transducing macromolecular complexes of the respiratory chain.

1.2 Mitochondrial energy production

Living organisms require a constant input of energy to carry out movement like muscle contraction, active transport of molecules and ions as well as the synthesis of biomolecules from simple precursors. In most processes the carrier of free energy is adenosine triphosphate (ATP). Ingested glucose is converted to pyruvate in a process known as glycolysis, taking place in the cytoplasm of any cell. In this process only a very small fraction of the total free energy potentially available from glucose is used to synthesize ATP. The metabolism of the sugar is completed in the mitochondria, where pyruvate is imported and eventually oxidized to CO_2 and H_2O through the combined operation of the Krebs cycle, the respiratory chain and the F_OF_1 ATP synthase, whereby 15 times more energy is converted to ATP than in glycolysis. Initially, pyruvate is metabolized to the intermediate acetylCoA and afterwards oxidized in the citric acid cycle by a series of enzymatic reactions taking place in the mitochondrial matrix. End products of this oxidation are CO_2, which is released from the cell as waste, and the activated electron carrier molecules NADH and $FADH_2$, the sources of electrons for transport along the respiratory chain. The enzymes of the electron transport chain are located in the IMM and most of them are arranged into three large enzymatic complexes, which as described later function also as H^+-pumps. Each complex is composed of electron carriers, associated with and held in close proximity by different protein molecules. The three intermembrane complexes are linked by two mobile electron carriers. The main purpose of making electrons pass through a chain of electron carriers with increasing reduction potential (increasing affinity for electrons), is to divide the energetically favorable reaction $H_2 + ½\ O_2 \rightarrow H_2O$ into small steps, so that most of the energy released can be stored instead of being lost to the environment as heat. Thus, the electrons start with high energy and gradually lose it as they pass along

the chain. The flow of electrons from the energy-rich molecules NADH and $FADH_2$ to the final acceptor O_2 can be subdivided into the following steps.

Complex I: (NADH Dehydrogenase complex) accepts electrons from NADH and passes them through a flavin and several iron-sulfur centers to ubiquinone (Q). The electrons emerge in QH_2, the reduced form of Q. This highly mobile hydrophobic molecule then transfers its electrons to a second respiratory enzyme complex, the Cytochrome b-c_1 complex. Complex I can be specifically inhibited by rotenone. Q also receives electrons from $FADH_2$ produced by the oxidation of succinate in the citric acid cycle by an enzyme complex called Succinate Dehydrogenase (**Complex II**). Complex II is the only respiratory complex which does not pump protons.

Complex III: (Cytochrome *b*-c_1 complex) functions as a dimer. Each monomer contains three hemes bound to cytochromes and an iron-sulfur protein. The complex accepts electrons from Q and passes them on to cytochrome *c* (cyt *c*), a water-soluble peripheral membrane protein, which is like Q a mobile electron carrier. It passes its electrons to the Cytochrome Oxidase complex. Complex III can be specifically inhibited by antimycin A which blocks the respiratory chain between cytochrome *b* and cytochrome c_1.

Complex IV: (Cytochrome Oxidase complex) is also composed of a dimer; each monomer contains two cytochromes and two copper atoms. The complex accepts one electron at a time from cyt *c* and passes them four at a time to oxygen, the ultimate electron acceptor to form H_2O. Complex IV can be specifically inhibited by cyanide, which prevents respiration with all substrates.

The flow of electrons across the respiratory chain and the thereby released energy is coupled to proton pumping across the IMM, from the matrix to the IMS. This generates a proton gradient, which is largely contributed by the inside negative $\Delta\Psi$. The resulting proton motive-force is the link between the electron flow in the respiratory chain and the synthesis of ATP. The F_OF_1 ATP synthase (complex V) localized in the IMM uses the

$\Delta\tilde{\mu}H$ to drive the energetically unfavorable reaction between ADP and P_i to synthesize ATP.

Structure of the ATP synthase (complex V)

The mitochondrial F_OF_1 ATP synthase is a multi-subunit protein localized in the IMM and composed of a catalytic F_1 and a membrane-bound F_O part. The F_1 region comprises the subunits α, β (3 of each), γ, δ and ε whereas the F_O region comprises subunits a, b, c (multiple subunits, 8 in mammals), d, e, f, g, A6L and F6[11, 12]. The F_1 and F_O parts are connected by a central stalk formed by the subunits γ, δ, and ε as well as by a peripheral stalk, comprised of the oligomycin sensitivity conferring protein (OSCP) and subunits b, d, and F6[13]. ATP synthesis is based on a rotary catalytic mechanism. H^+ translocation through the F_O region induces rotation of the membrane-bound c-ring, which is organized like a barrel within the membrane. Spinning of the c-ring induces the rotation of the central stalk (which is attached to the c-ring) inside the $\alpha_3\beta_3$ hexamer of the F_1 part[14]. This process drives ATP synthesis by inducing conformational changes in three catalytic nucleotide binding sites located at interfaces between α- and β-subunits[11]. During rotation, the F_1 region is held stationary relative to the F_O region by the peripheral stalk, a connection which is essential for the proper function of the enzyme[15]. In absence of a proton gradient the ATP synthase can function in reverse, pumping protons into the IMS and hydrolyzing ATP in order to create a mitochondrial membrane potential ($\Delta\Psi_m$). Furthermore ATP synthase can associate with the inhibitor protein 1 (IF1) which inhibits hydrolysis of the enzyme. IF1 acts as a dimer and binds to the α-β interfaces of two F_1-ATPases via its N-terminal inhibitory sequence[16]. Binding of IF1 requires ATP and is favored by low pH and $\Delta\Psi_m$. The restoration of $\Delta\Psi_m$ favoring ATP synthesis displaces IF1 from the F_OF_1 ATP synthase[17].

In eukaryotic mitochondria oligomycin can inhibit F_OF_1 ATP synthase, by binding to subunit c[18]. It thereby blocks synthesis as well as hydrolysis of ATP and abolishes ADP-stimulated respiration in intact mitochondria.

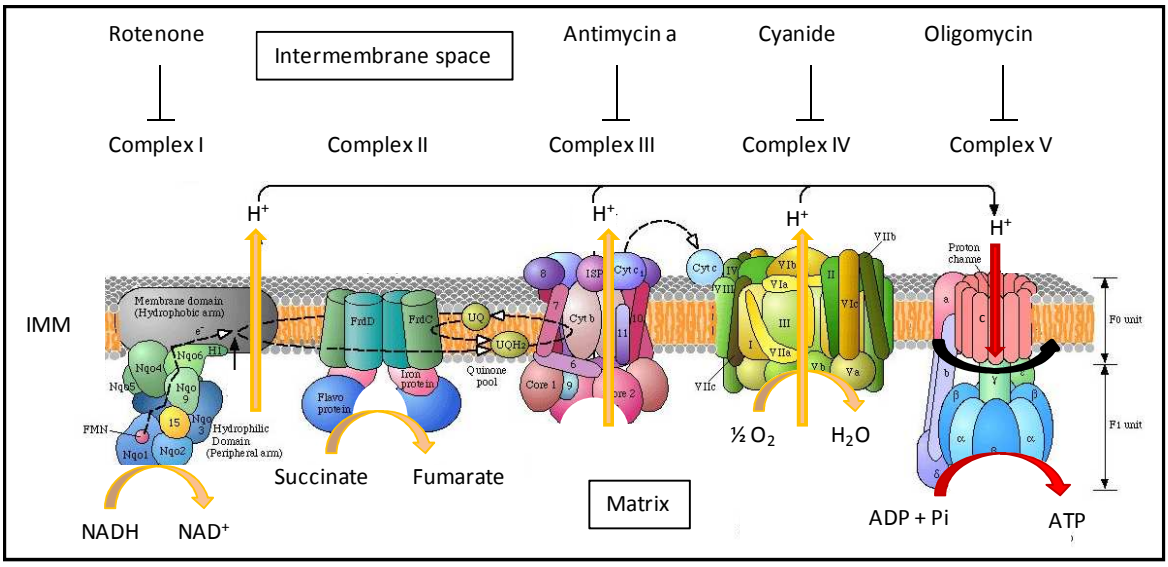

Figure 3. Schematic representation of the mitochondrial respiratory chain, composed of four multimeric complexes, and of the ATP synthase (complex V). Shown are the set of reactions that transfer electrons from reduced cofactors to oxygen, obtaining water (yellow curved arrows). Electron transport between complexes I to IV is coupled to extrusion of protons from complexes I, III and IV into the intermembrane space (yellow straight arrows), creating an electrochemical gradient ($\Delta\tilde{\mu}H$) across the inner mitochondrial membrane (IMM). Protons then enter in the c-subunit (red straight arrow) of complex V, the ATP synthase, causing the ring of c-subunits to spin (black curved arrow) and driving the synthesis of ATP from ADP and Pi (red curved arrow). Some common specific inhibitors for complex I, III and IV as well as for the ATP synthase are shown (black arrows on top); modified from[19].

1.3 Mitochondrial control of apoptosis

Mammalian cell death is most widely classified into two processes, apoptosis or necrosis. Cells undergoing a sudden stress situation such as infection or exposure to toxins die by necrosis resulting in loss of plasma membrane integrity, uncontrolled release of cellular components and inflammation. On the contrary, apoptosis is a genetically encoded and highly regulated form of cell death that governs normal body sculpture, defense against pathogen invasion and developmental processes. Exposure of the cell to an apoptotic stimulus leads to a series of morphological changes such as rounding up of the cell, pseudopod retraction, cell shrinkage, chromatin condensation and nuclear fragmentation[20]. Thus, apoptosis enables the body to eliminate a damaged cell without affecting the neighboring environment. Its abnormal regulation is associated with many human pathologies such as degenerative diseases (too much apoptosis) or cancer (too little apoptosis). Until recently necrosis and apoptosis were considered to be two distinct phenomena. However, there is now evidence that both

processes can be interconnected and that necrosis can be initiated by death receptors usually involved in apoptototic cell death in a process called necroptosis[21].

The key player in the execution of apoptosis is a family of cysteinyl aspartate-directed proteases called caspases. These enzymes are synthesized as inactive zymogens (called pro-caspases) in healthy cells and can be activated by proteolytic cleavage upon triggering by a diverse range of internal and external stimuli[22]. Upon receipt of apoptotic stimuli, cells activate initiator caspases (such as caspase-2, -8, -9, and -10) that, in turn, proteolytically activate effector caspases (such as caspase-3, -6, and -7). Once active, effector caspases cleave different substrates, eventually leading to the dismantling of the dying cell[23]. Activation of the initiator caspases may occur through either an extrinsic or an intrinsic pathway.

Extrinsic pathway

The extrinsic pathway of apoptosis is mediated by activation of the so called death receptors TNF, FAS or TRAIL. Upon binding of death ligands (such as members of the tumor necrosis factor receptor superfamily) on the plasma membrane, conformational changes in the receptors lead to the recruitment of adapter proteins on the cytoplasmic side and thus the formation of the death-inducing signaling complex (DISC) and subsequent activation of pro-caspase-8. Active caspase-8 in turn proteolytically processes effector caspases (-3, -6 and -7) leading to further caspase activation events which result in substrate proteolysis and cell death. Caspase-8 can also engage the intrinsic apoptotic pathway through cleavage of the Bcl-2 homology 3 (BH_3)-only protein Bid[24]. Truncated Bid (tBid) translocates to the mitochondria, where it triggers activation of the intrinsic apoptotic pathway by promoting mitochondrial outer membrane permeabilization (MOMP) and release of apoptogenic proteins[25].

Intrinsic pathway

The intrinsic pathway of apoptosis can be induced by many different stimuli such as oxygen radicals, γ-irradiation, hypoxia or ischemia-reperfusion and converges on the central death machinery at the mitochondria. The key event in the intrinsic pathway is MOMP and release of mitochondrial apoptogenic proteins, usually located in the IMS,

into the cytosol. Once in the cytosol, apoptotic proteins such as cyt *c*, apoptosis inducing factor (AIF), second mitochondria-derived activator of caspases (Smac)/direct inhibitor of apoptosis binding protein with low pI (Diablo), and endonuclease G (endoG), are able to initiate caspase-dependent or caspase-independent mechanisms that promote apoptosis. In caspase-dependent signaling, the most critical apoptogen cyt *c* binds to the adapter protein apoptotic protease-activating factor-1 (Apaf-1), changing its conformational state and leading to its oligomerization as well as to the recruitment of the effector caspase-9. The complex built of cyt c, Apaf-1 and caspase-9 is called apoptosome and its formation is highly ATP-dependent[26]. The apoptosome in turn leads to the downstream activation of other effector caspases and proteolytic cleavage of target proteins. The function of active caspases can be blocked by the inhibitors of apoptotic proteins (IAPs), whereas Smac/Diablo once released from the IMS binds to and inhibits the effects of IAPs, thereby indirectly enhancing the activation of caspases. In addition, AIF and endoG translocate to the nucleus where they induce nuclear chromatin condensation and DNA fragmentation in a caspase-independent manner[27].

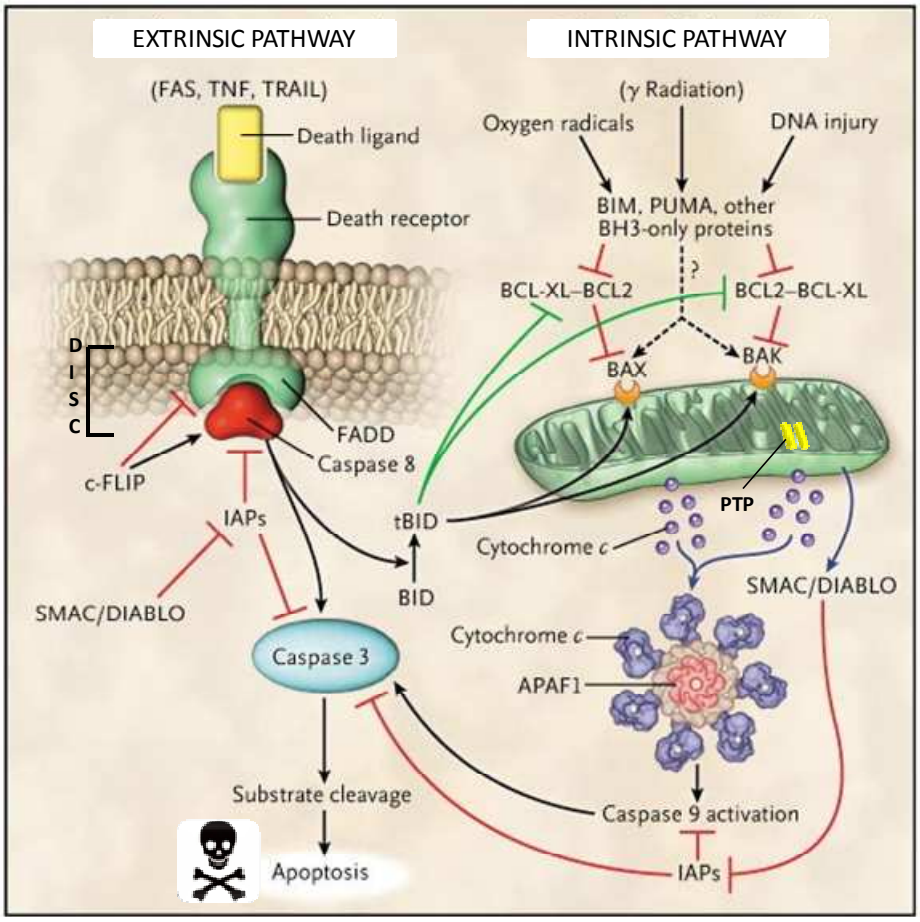

Figure 4. Intrinsic and extrinsic pathway of apoptosis. In the intrinsic apoptotic pathway, pro-apoptotic BH3 proteins of the Bcl-2 family are activated by diverse noxious stimuli, and inhibit anti-apoptotic proteins (Bcl-2 or Bcl-x_L). Thus, Bax and Bak are free to induce mitochondrial permeabilization with release of cytochrome *c*, which ultimately results in formation of the apoptosome and subsequent activation of the caspase cascade. The outer membrane permeabilization can be induced by the permeability transition pore (PTP) as well. SMAC/DIABLO is also released after mitochondrial permeabilization and acts to block the action of inhibitors of apoptosis proteins (IAPs), which inhibit caspase activation. In the extrinsic apoptotic pathway, ligation of death receptors recruits the adaptor protein FAS-associated death domain (FADD) to form the death-inducing signaling complex (DISC). This in turn recruits caspase-8, which ultimately activates caspase-3, the key effector caspase. There is a cross-talk between the two pathways, which is mediated by the truncated form of Bid (tBid) that is produced by caspase-8-mediated Bid cleavage; tBid acts to inhibit the Bcl-2-Bcl-x_L pathway and to activate Bax and Bak. Apaf1: apoptotic protease-activating factor 1, TNF: tumor necrosis factor, TRAIL: TNF-related apoptosis-inducing ligand; modified from[28].

The mechanisms by which MOMP occurs and mitochondrial apoptogenic factors are released into the cytosol are still unresolved and different models which are not mutually exclusive have been proposed. One of these models involves members of the Bcl-2-family, which can be grouped into pro-apoptotic or anti-apoptotic proteins. All of them contain one or more Bcl-2 homology (BH) domains, which are important for heterodimeric interactions among the different members of the family[29]. Anti-apoptotic Bcl-2 proteins (such as Bcl-2, Bcl-x_L or Bcl-w) and pro-apoptotic Bcl-2 proteins

(such as Bax, Bak, or Bok/Mtd) display four BH domains. The proapoptotic BH_3-only proteins (such as Bid, Bad, Noxa or Puma/Bbc3), on the other hand, possess only a short motif called the BH_3 domain as their name indicates. Through their BH_3 domain, these proteins either inhibit anti-apoptotic proteins or stimulate oligomerization of the multidomain proteins Bax and Bak leading to MOMP. Bax proteins can be found as monomers in the cytosol. Upon activation the latter translocate to and insert into the OMM[30], while Bak is present in the OMM even if not activated[31]. Following activation, Bax and Bak undergo conformational changes, oligomerize and form pores in the OMM, inducing thus the release of the previously described apoptogenic proteins[32].

This mechanism remains only poorly characterized and it seems unlikely that Bax-/Bak channels are large enough to release the bigger pro-apoptotic proteins such as the serine protease Omi-Htr2. Another mechanism leading to MOMP through opening of the mitochondrial permeability transition pore (PTP) will be discussed in more detail below.

2 Cellular Ca^{2+} homeostasis

Ca^{2+} ions are among the most important second messengers and play a key role in cell signaling. Most cell types are able to translate the information obtained by a variety of stimuli through an increase in intracellular [Ca^{2+}] with highly defined spatial and temporal patterns. This can be achieved by the storage of Ca^{2+} in specialized compartments such as the endoplasmic reticulum (ER), by the low permeability of the plasma membrane to ions and by the activity of the plasma membrane Ca^{2+}-ATPase (PMCA, pumping Ca^{2+} outside the cell) and of the Na^{+}/Ca^{2+} exchanger (NCLX)[33]. Due to these mechanisms the cell is able to keep very low cytoplasmic free [Ca^{2+}] levels in resting conditions (~100 nM). Upon stimulation, local changes in cytoplasmic [Ca^{2+}] due to fast release from the Ca^{2+} stores via highly selective channels can be sensed by Ca^{2+} dependent enzymes (such as kinases or phosphatases) or target proteins with direct Ca^{2+}-binding sites, that in turn induce specific cellular responses (e.g. contraction, secretion, proliferation or cell death).

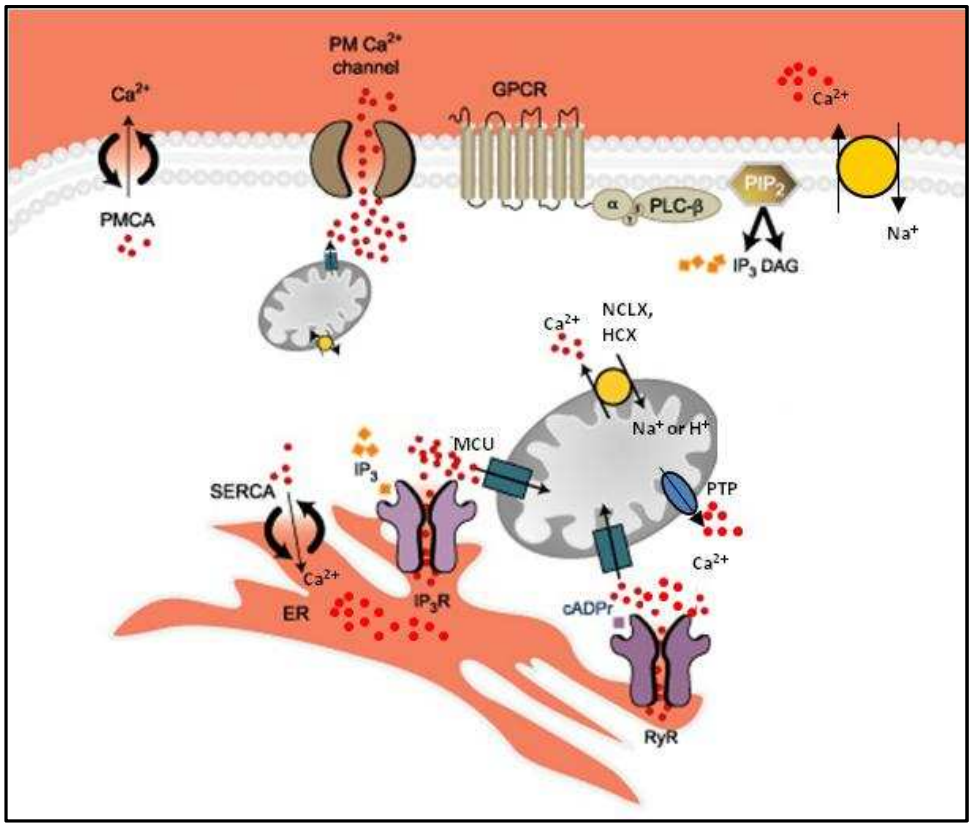

Figure 5. Schematic representation of the Ca^{2+} homeostatic network between endoplasmatic reticulum, mitochondria and cytosol. cADPr, cyclic ADP ribose receptor; CICR, calcium-induced calcium release channel; DAG, diacylglycerol; DHPR, dihydropyridine receptor; GPCR, G protein-coupled receptor; IP3, inositol triphosphate; PLC-β, phospholipase C-β; PM Ca^{2+} channel, plasma membrane calcium channel; PMCA, plasma membrane channel pump; RyR, ryanodine receptor; SERCA, sarco/endoplasmic reticulum Ca^{2+} ATPase; modified from[33].

2.1 The role of mitochondria

The first hint on the important role of mitochondria in Ca^{2+} handling was the demonstration of Ca^{2+} accumulation in isolated energized rat kidney mitochondria half a century ago[34]. Today it is known that mitochondria play a pivotal role in cellular Ca^{2+} homeostasis and that they are thereby involved in a wide field of physiological processes such as buffering of cytoplasmic Ca^{2+} signals, excitation-contraction coupling and induction of cell death. In healthy cells the mitochondrial matrix [Ca^{2+}] is low. When Ca^{2+} is released from the Ca^{2+} stores into the cytoplasm, microdomains of high [Ca^{2+}] (10-20μM) can transiently form in regions of close proximity between mitochondria and Ca^{2+} channels of the ER or the plasma membrane[35]. Mitochondria in these regions rapidly accumulate Ca^{2+} and then gradually release it when plasma membrane ion pumps have lowered the cytoplasmic free [Ca^{2+}], thus amplifying and sustaining signals arising from cytoplasmic [Ca^{2+}] increases. Furthermore, mitochondrial Ca^{2+} uptake can

profoundly influence cell survival, as excess matrix [Ca^{2+}] can initiate cell death through opening of the PTP (as discussed below). Thus, the mechanisms controlling cellular and mitochondrial Ca^{2+} homeostasis, metabolism and bioenergetics have to be tightly integrated in the overall cellular Ca^{2+} homeostatic network[36].

2.2 Mitochondrial Ca^{2+} influx and efflux mechanisms

Ca^{2+} uptake into respiring mitochondria is an energy dependent, electrophoretic process driven by the Ca^{2+} electrochemical gradient $\Delta\tilde{\mu}Ca$, favored by the inside-negative $\Delta\Psi_m$ and mediated by the mitochondrial Ca^{2+} uniporter (MCU). In the last four decades the MCU has been characterized in terms of thermodynamic properties and inhibitor specificity (with ruthenium red and lanthanides being the most potent inhibitors) and was recently shown to be a highly selective, low conductance channel by electrophysiology[37]. In 2011 two groups independently identified a 40kD protein with two transmembrane domains to be the MCU[38, 39]. The influx of Ca^{2+} via the MCU is charge-compensated by increased H^+ pumping of the respiratory chain, resulting in increased matrix pH, which lowers the $\Delta\Psi_m$ and prevents further uptake of Ca^{2+}[(40)]. Uptake of substantial amounts of Ca^{2+} therefore requires buffering of matrix pH (to allow regeneration of the $\Delta\Psi_m$) as well as buffering of matrix Ca^{2+} (to prevent the buildup of a Ca^{2+} concentration gradient)[41-43]. Buffering of matrix pH is achieved by the simultaneous uptake of protons and anions via diffusion of the undissociated acid through the IMM (as in the case of acetate), of CO_2 (which then regenerates bicarbonate and H^+ in the matrix) or through transport proteins (like the H^+–Pi symporter)[44]. The buildup of a Ca^{2+} concentration gradient may be prevented by the cotransport of Pi. Indeed, under physiological conditions the parallel accumulation of Pi and Ca^{2+} leads to the formation of a Ca^{2+}/Pi complex in the matrix which effectively buffers matrix free [Ca^{2+}][45]. However, the [Ca^{2+}] inside the mitochondrial matrix is not exclusively dictated by $\Delta\tilde{\mu}Ca$, but is rather governed by a kinetic steady state between Ca^{2+} influx via the uniporter and Ca^{2+} efflux by antiporters (Na^+/Ca^{2+} and H^+/Ca^{2+} exchanger) that extrude Ca^{2+} from the matrix using the concentration gradients of H^+ and Na^+. The Na^+/Ca^{2+} exchanger NCLX, which mediates Ca^{2+} efflux with a stoichiometry of 3 Na^+- 1 Ca^{2+}, has been recently identified at the molecular level[46], whereas the Na^+-insensitive Ca^{2+}

extrusion pathway via a putative H^+/Ca^{2+} exchanger has been studied only functionally in isolated mitochondria and has a predicted stoichiometry of 3 H^+-1 Ca^{2+} [47].

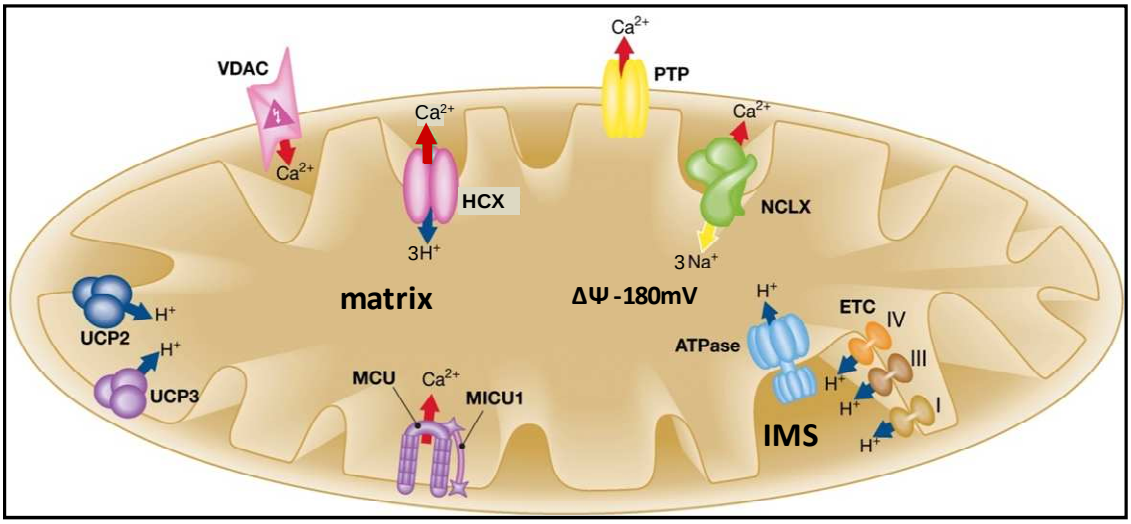

Figure 6. Schematic representation of mitochondrial Ca^{2+} uptake and efflux mechanisms. Ion fluxes are indicated by arrows. Red arrow, Ca^{2+}; blue arrow, H^+; yellow arrow, Na^+. ETC: electron transport chain; NCLX: Na^+/Ca^{2+} exchanger; HCX: H^+/Ca^{2+} exchanger; PTP: permeability transition pore; UCP2/3: uncoupling protein 2/3; VDAC: voltage-dependent anion channel; IMS: intermambrane space; MCU: mitochondrial Ca^{2+} uniporter; MICU1: mitochondrial Ca^{2+} uptake 1; modified from [48].

2.3 The problem of Ca^{2+} overload: a constant threat for mitochondria

The coupling of Ca^{2+} uptake with Ca^{2+} efflux in energized mitochondria on distinct pathways allows the regulation of both cytoplasmic and matrix [Ca^{2+}]. However, a kinetic imbalance is apparent because the V_{max} of the MCU is about 1400 nmol Ca^{2+} per mg protein per min while the combined V_{max} of the efflux pathways is about 20 nmol Ca^{2+} per mg protein per min. What is the reason for such an imbalance? The rate of Ca^{2+} uptake via the MCU is a steep function of extramitochondrial [Ca^{2+}] [49]. If mitochondria could release Ca^{2+} at a comparable rate this would increase extramitochondrial [Ca^{2+}], stimulate Ca^{2+} uptake by the MCU and increase overall Ca^{2+} cycling resulting in energy dissipation [50]. Thus, net Ca^{2+} efflux through stimulation of the efflux pathways would have a high energetic cost for the cell, which can be avoided with the previously described low V_{max} and early saturation of the efflux pathways. However, this energy-saving strategy exposes mitochondria to another dangerous problem. According to the above described kinetic model, increase of extramitochondrial Ca^{2+} goes along with

increase of matrix Ca^{2+} when the rate of Ca^{2+} uptake exceeds that of the efflux pathways and thus mitochondria are constantly exposed to the danger of Ca^{2+} overload. To prevent this scenario mitochondria need a system to achieve transient, fast and regulated Ca^{2+} release in situations of high matrix [Ca^{2+}]. It was hypothesized that this mechanism could be provided by transient openings of the PTP and there is more and more evidence that this plays a relevant role in *in vivo* Ca^{2+} homeostasis and signalling processes, as will be discussed more in detail below.

3 The permeability transition pore (PTP)

The mitochondrial permeability transition (PT) describes a process of Ca^{2+}-dependent, regulated increase in the permeability of the inner mitochondrial membrane to solutes with molecular masses below approximately 1500 Da. This event, which plays a major role in cell death, is due to the opening of the mitochondrial PTP, a high-conductance inner membrane channel. The PTP was discovered and studied mostly in mammals where it was shown to play a role in different cellular processes, depending on the open time of the channel. PTP opening causes collapse of $\Delta\Psi_m$ and Ca^{2+} release through the pore itself, an event that for short open times may be involved in physiological Ca^{2+} homeostasis[51] and might play a role in cell signaling[52]. Prolonged opening of the PTP, on the other hand, causes stable depolarization, loss of ionic homeostasis, depletion of pyridine nucleotides and respiratory inhibition. During the PT ions and osmotically active molecules (up to 1500 Da) can enter the mitochondria and consequently lead to influx of water into the matrix and thus mitochondrial volume increase. Matrix swelling in turn can lead to rupture of the OMM, release of apoptogenic proteins such as cyt *c* and cell death via apoptosis or necrosis depending on a variety of additional factors, among which cellular ATP and Ca^{2+} levels play a major role[53]. For a long time the PTP was considered to be an *in vitro* artifact of little pathophysiological relevance. However, the role of the PTP in disease has been reevaluated in the context of both programmed and accidental cell death[39] and there is increasing evidence that it might function as a Ca^{2+} release channel in physiological Ca^{2+} homeostasis, as will be discussed below.

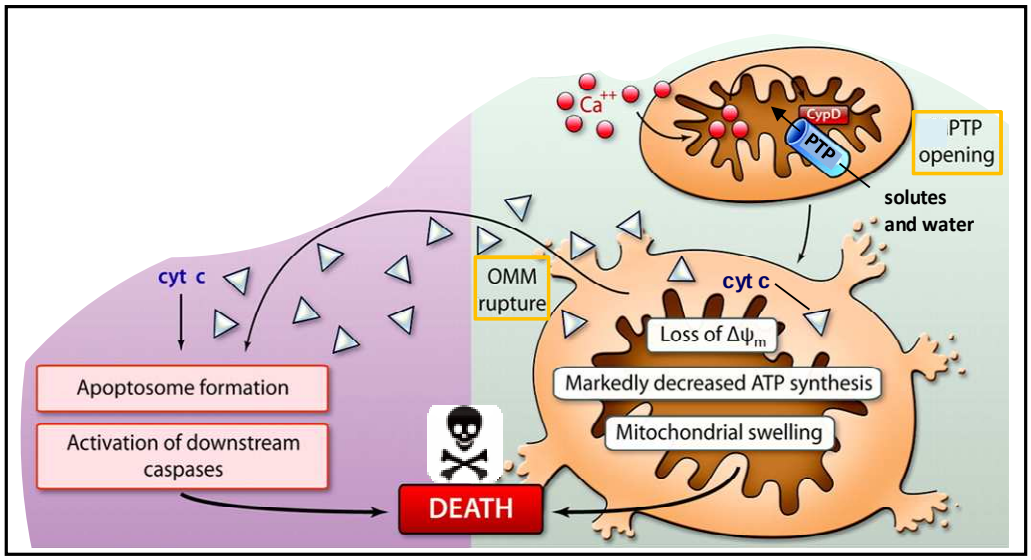

Figure 7. Mechanisms of mitochondrial permeabilization and release of intermembrane space proteins due to the opening of the permeability transition pore. Opening of the permeability transition pore (PTP) can be triggered by different stimuli and results in loss of mitochondrial membrane potential ($\Delta\psi_m$), decreased ATP production and entry of solutes and water into the mitochondrial matrix. This causes mitochondrial swelling, outer mitochondrial membrane (OMM) rupture and release of apoptogenic proteins, such as cytochrome *c* (cyt *c*) from the intermembrane space into the cytosol. Cyt *c* in turn leads to formation of the apoptosome and subsequent activation of the caspase cascade, thus inducing cell death. Cyp-D: Cyclophilin D; modified from[54].

3.1 Features and regulation of the PTP in mammals

Most classical studies of the PT were carried out in mitochondria obtained from mammalian cells or tissues. These studies allowed a thorough characterization of the functional properties and regulation of the putative channel, but its molecular nature remains still elusive. The transition between the "open" and "closed" state of the PTP can be modulated by many different compounds, ions or conditions. These PTP effectors can be subdivided into inducers, that increase the probability of the pore to open; and inhibitors, that increase the probability of the pore to close. Perhaps the single most important factor, which is essential for opening of the PTP and therefore is called a "permissive factor", is **matrix Ca^{2+}**. Importantly, all the other divalent metals, such as Mg^{2+}, Mn^{2+} and Sr^{2+} instead decrease the PTP open probability. Another important modulator of the PTP is **matrix pH**, with an optimum for PTP opening at pH 7.4. More basic as well as more acidic pH desensitizes the PTP to opening[55]. The PTP is a voltage-dependent channel, in the sense that a decrease in **$\Delta\Psi_m$** favors PTP opening, whereas a high inside-negative $\Delta\Psi_m$ tends to stabilize the pore in the closed conformation[56]. This led to the hypothesis that a specific sensor, which is able to

perceive the threshold potential necessary to open the PTP, does exist. Many PTP modulators appear to modify the threshold potential, bringing it closer (inducers) or moving it further away (inhibitors) from the resting potential[50]. Thus, an inducer brings the threshold potential needed for PTP opening closer to the resting potential, and makes mitochondria more susceptible to PTP opening even after slight depolarizations. Inhibition of PTP can also be observed with **bongkrekate**[57], whereas **atractylate** opens the pore[58]. Since atractylate and bongkrekate are selective inhibitors of the adenine nucleotide translocase (ANT), these results led to the suggestion that the PTP may be entirely or partially formed by the ANT[59], an issue that will be discussed below.

The PTP can be directly regulated by electron flux within complex I of the respiratory chain, with an increased open probability when flux increases[60]. This led to the discovery that **quinones** can modulate the PTP, with some of them acting as inhibitors (such as ubiquinone 0 (Ub_0) or decylubiquinone) and others as inducers (such as 2,5-dihydroxy-6-undecyl-1,4-benzoquinone). A third class of PTP-inactive quinones (such as ubiquinone 5) are able to counteract the effects of both inhibitors and inducers. However, despite a large number of studies, the exact relationship between quinone structure and effect on the pore remains unsolved[61].

Opening of the PTP is strongly favored by an oxidized state of the pyridine nucleotides **NADH** and **NADPH** as well as of critical **thiol groups** at distinct matrix or membrane sites. Both of these effects can be reversed by reducing agents[62, 63]. The interconversion between dithiol and disulfide groups correlates with the redox state of glutathione, suggesting that there is a redox equilibrium between the dithiols and matrix glutathione. This finding explains the effect of thiol reacting agents such as *N*-ethylmaleimide (NEM)[64, 65] and monobromobimane[66] on the pore.

Inorganic phosphate (Pi) is a powerful PTP inducer in mammalian mitochondria, whereas it has an inhibitory effect in yeast mitochondria. As Pi is also taken up following Ca^{2+} uptake into the matrix, where it leads to the formation of a Ca^{2+}-Pi complex, an increased threshold of the PTP to Ca^{2+} should be expected when Pi is present, due to its lowering effect on free matrix [Ca^{2+}]. The unexpected inducing effect of Pi on the PTP has been explained by the fact that an increase of Pi also produces a decrease in matrix free [Mg^{2+}] (a PTP inhibitor), as well as buffering of matrix pH at ~7.2, and it may

generate polyphosphate[67], all of which would favor PTP opening. Recently, our group demonstrated that Pi can also act as an inhibitor of the PTP in case of genetic ablation of the matrix peptidyl-prolyl-*cis-trans*-isomerase (PPIase) Cyclophilin D (Cyp-D) or its displacement from the pore by its specific inhibitor Cyclosporin A (CsA). We hypothesized that Cyp-D might mask a Pi-regulatory site, which becomes only accessible when Cyp-D is detached from the pore[68].

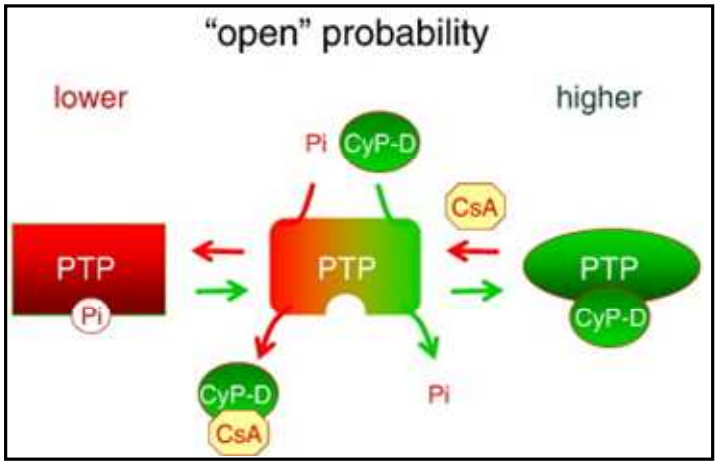

Figure 8. Modulation of the permeability transition pore by Cyclophilin D and Phosphate in mammalian mitochondria. The permeability transition pore (PTP) displays a higher probability of opening (right) when it binds to Cyclophilin D (Cyp-D); treatment with Cyclosporin A (CsA) displaces Cyp-D and unmasks a cryptic site for inorganic Phosphate (Pi) (center); if the Pi concentration is sufficiently high, Pi binding decreases the probability of pore opening (left), in a reaction that can be readily reversed if the Pi concentration decreases; from[69].

Opening of the PTP is inhibited by the immunosuppressive drug **CsA**[70] through the binding to its matrix target CyP-D. CsA acts on Cyp-D by inhibiting its PPIase activity, but whether this is essential for the modulating effect of Cyp-D on the PTP is still unclear[71]. Likewise (and at variance from immunosuppression), the effect of CsA does not involve inhibition of calcineurin[72]. However, CsA cannot be regarded as a true PTP blocker but rather as a desensitizer, as pore opening still occurs in presence of CsA, even if the threshold Ca^{2+} needed for PTP opening increases two to three-fold. Furthermore, sensitivity to CsA highly depends on the expression level of Cyp-D and is thus tissue- and cell type-specific. Tissues or cell lines expressing low levels of Cyp-D were shown to be less sensitive to CsA but more sensitive to another potent PTP inhibitor, **rotenone**[73]. On the other hand, high expression levels of Cyp-D correlate with a high sensitivity to

CsA and a low sensitivity to rotenone. Inhibition of the PTP by rotenone requires Pi in a striking analogy with the effect of CsA, suggesting that both might act on the same binding site. Thus, inhibition of complex I by rotenone and detachment of Cyp-D by CsA might affect the PTP through a common mechanism[73].

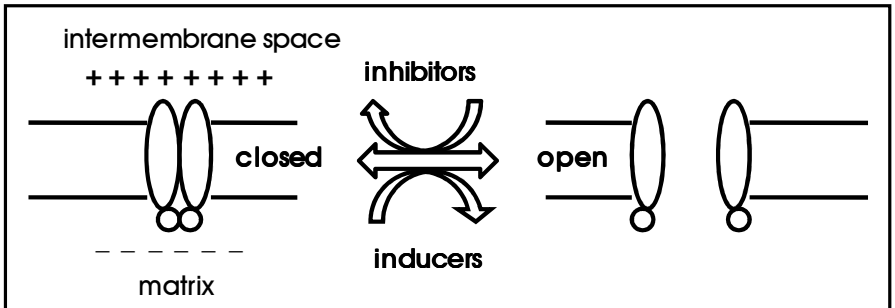

Inhibitors:	Inducers:
Ub_0	2,5-dihydroxy-6-undecyl-1,4-benzoquinone
Mg^{2+}	matrix Ca^{2+}
NAD(P)H	$NAD(P)^+$
-SH HS-	-S-S-
GSH	GSSG
ADP, ATP, bongkrekate	atractylate
Pi (in presence of CsA or in absence of Cyp-D)	Pi
high $\Delta\Psi_m$	low $\Delta\Psi_m$
matrix pH < 7.4, or > 7.4	matrix pH ~ 7.4
CsA	
rotenone	

Figure 9. Modulators of the permeability transition pore in mammals. All modulators are grouped in inhibitors which promote the closed and inducers which promote the open state of the pore, signs denote transmembrane electrical potential, Ub_0: Ubiquinone 0, Cyp-D: Cyclophilin D, CsA: Cyclosporin A, $\Delta\Psi_m$: mitochondrial membrane potential; modified from[74].

3.2 Structure

Many hypotheses on the molecular nature of the PTP have been put forward over the years. Based on many pharmacological studies, the PTP has been supposed to be a multiprotein-channel created by defined components.

VDAC: (voltage dependent anion channel, located in the OMM). Several data led to the hypothesis that VDAC is a component of the PTP. Purified VDAC when incorporated in phospholipid bilayer membranes forms channels with size and electrophysiological properties similar to those of the PTP[75, 76]. In addition it has been found that VDAC can be modulated by some of the stimuli that regulate the PTP, e.g. Ca^{2+}, NADH, glutamate[77-79], and binding of hexokinase II[80]. In mammals there are three VDAC isoforms (VDAC 1, 2 and 3), and each of them is able to form channels when incorporated in phospholipid bilayers[81]. However, characteristics of permeability transition have been studied in VDAC1$^{-/-}$ mice, but the properties of the PTP in mutants and wild-type mice were identical[82]. Studies in cells lacking all of the three isoforms finally led to the conclusion that VDAC is not essential for the mitochondrial PT[83].

ANT: The adenine nucleotide translocator was supposed to be a component of the pore, as the PTP can be modulated by inhibitory ligands of ANT and by adenine nucleotides themselves[84]. Studies in ANT knock-out mitochondria isolated from mouse liver, however, showed that ANT as well is not essential for PTP formation. ANT$^{-/-}$ mitochondria undergo a PT which is Ca^{2+}- and oxidant-dependent as well as CsA-sensitive. This indicates that ANT is neither the binding partner of Cyp-D nor it is the target for the oxidants[85]. Furthermore, isolated hepatocytes of wild-type and ANT knock-out mice show an identical response to death receptor-mediated activation of apoptosis. Thus, experimental data based on genetic ablation of the relevant proteins support the conclusion that also ANT is not an essential component of the PTP.

Phosphate carrier: The phosphate carrier (PiC) is a member of the mitochondrial carrier family and promotes the transport of Pi across the IMM. Uptake of Pi into the mitochondria is essential for the production of ATP from ADP. Different studies hypothesized a role for PiC in the PTP composition due to the fact that some inhibitors of the PTP such as NEM[65], Ub_0[86] and Ro 68-3400[87], are also PiC inhibitors[88, 89]. However, these studies were performed with de-energized mitochondria incubated in the presence of 40 mM Pi, conditions that are far from physiological. Thus, it is questionable how relevant the obtained results are to an *in vivo* situation. Another critical point is the inseparable relationship between Ca^{2+} and Pi uptake in

mitochondria. Inhibition of PiC by NEM in respiring mitochondria blocks Pi uptake and consequently limits Ca^{2+} uptake to amounts that may be below the threshold level for PTP opening[42]. Thus, the effect of PTP inhibition due to decreased Pi or decreased Ca^{2+} uptake is hard to sort out. Furthermore, the ubiquinone analogues Ub_0 and Ro 68-3400 desensitize the PTP to Ca^{2+} even when Pi is replaced by arsenate or vanadate[68]. Whether the PiC is a component of the PTP should be addressed by knock-out approaches as used for studying the role of ANT and VDAC. A recent attempt to elucidate the role of PiC in pore formation by siRNA down-regulation of both splice variants (PiC-A and PiC-B) failed, since maximal knock down efficiency was 65-80% and the remaining protein was sufficient to maintain maximal rates of Ca^{2+} uptake without any detectable decrease in PTP opening[89].

Cyclophilin D: The regulatory role of the mitochondrial peptidyl-prolyl-*cis-trans*-isomerase Cyp-D on the PTP has been discovered through the finding that the immunosuppressant drug CsA, a potent inhibitor of the intrinsic apoptotic pathway, also inhibits the PTP at concentrations very similar to those needed to inhibit the enzymatic activity of Cyp-D[72, 90]. Several genetic studies have demonstrated that Cyp-D is a regulator of the PTP, sensitizing it to Ca^{2+}, rather than being a component of the pore[68, 91, 92]. Further details on structure and function of Cyclophilins and in particular Cyp-D will be provided in chapter 4.

Additional proteins may play a regulatory role on the PTP. Amongst these the anti-apoptotic and pro-apoptotic proteins of the Bcl-2-family in the OMM[93], mitochondrial creatine kinase (which produces ATP from ADP by converting creatine phosphate to creatine)[94], mitochondrial hexokinase (which catalyze the first step of glycolysis)[95, 96] and the peripheral benzodiazepine receptor (PBR or TSPO), located in the OMM and involved in steroidogenesis[97].

3.3 The PTP as a Ca^{2+} release channel

Besides its well accepted role in cell death induction, the PTP was hypothesized to be a Ca^{2+} release channel whose transient opening protects mitochondria from Ca^{2+} overload. This idea could be corroborated through recent studies in isolated

cardiomyocytes, adult cortical neurons and Cyp-D KO mice. In 1992, R. Altschuld et al. demonstrated that CsA significantly increases net Ca^{2+} uptake and decreases Ca^{2+} efflux in isolated cardiomyocytes, without having any impact on cell morphology or viability[98]. The effect of CsA was concentration dependent and specific to mitochondria, as ATP-dependent Ca^{2+} uptake by the sarcoplasmatic reticulum was not affected. This was the first piece of evidence that the PTP might contribute to Ca^{2+} cycling in the mitochondria of functional cardiomyocytes and that reversible pore opening may be a normal process in heart cells. However, a direct role for the PTP in regulation of mitochondrial total Ca^{2+} *in situ* remained controversial, as Eriksson et al. demonstrated that fluxes of Ca^{2+}, Mg^{2+} and adenine nucleotides in perfused rat livers following hormonal stimulation were unaffected by CsA[99]. The authors concluded that regulation of mitochondrial ion and metabolite homeostasis is independent of the PTP. Two recent publications based on a knock-out mouse model lacking the *Ppif* gene encoding for the mitochondrial Cyp-D do provide clear support for a role of the PTP in Ca^{2+} homeostasis[100, 101]. Barsukova et al. treated adult cortical neurons from wild type and *Ppif*$^{-/-}$ mice with either ATP (to activate P2Y purinergic receptors) or with depolarizing concentrations of KCl (to open plasma membrane voltage-dependent Ca^{2+} channels), and demonstrated that both stimuli cause a robust increase of both cytosolic and mitochondrial [Ca^{2+}] that is indistinguishable in neurons of the two genotypes[101]. Application of the two stimuli together, however, resulted in much higher levels of mitochondrial [Ca^{2+}] in the *Ppif*$^{-/-}$ neurons, suggesting that the threshold for PTP activation had been reached in the wild type but not in the Cyp-D null mitochondria *in situ*. The higher resistance to mitochondrial Ca^{2+} overload and thus the capacity to blunt *in vivo* cytoplasmic Ca^{2+} increases might explain the neuroprotective effect of Cyp-D ablation in many neurodegenerative disease models and underlines the high physiological importance of transient, rather than persistent PTP opening[102-104]. The implication of Cyp-D and the PTP in pathologic conditions *in vivo* was further investigated by Elrod et al. Cyp-D KO mice were more susceptible to cardiac hypertrophy, fibrosis and reduction in myocardial function upon treatment with stimuli such as transaortic constriction, overexpression of Ca^{2+}/calmodulin-dependent protein kinase IIδc and swimming exercise[100]. Myocardial dysfunction was not due to altered cell viability indicating an additional role of the PTP beyond cell death induction. Indeed, the authors showed that

heart mitochondria lacking Cyp-D had higher resting Ca^{2+} levels resulting in metabolic alterations such as activation of Ca^{2+}-dependent dehydrogenases and increased glucose oxidation, thus limiting the heart's ability to maintain contractility during stress situations. This was the first *in vivo* study demonstrating that the PTP is an important regulator of Ca^{2+} homeostasis and of signaling events critically involved in metabolic adaptation to disease states such as heart failure. For further discussion and more detailed analysis of this topic see **Publication 3**.

3.4 The PTP in other species: a channel conserved through evolution?

Classical studies on the PTP were carried out mostly in mitochondria obtained from mammals, although permeability changes have also been described in yeast mitochondria[105-109]. However, due to the increasing interest on the PT in cell death, studies have emerged also in mitochondria from other organisms, e.g. plants[110-114], fish[115, 116] and amphibians[117, 118]. Until recently, though, it was not clear whether the permeability changes observed in these organisms can be ascribed to the same molecular events. Our recent findings in *Drosophila* might bridge the gap between the pore of yeast and that of mammals, and support our proposal that channels in different species actually possess unifying features[119], as will be described below.

3.5 Ca^{2+} transport and PT in yeast mitochondria

Cell signaling roles of Ca^{2+} are less developed in lower eukaryotes, explaining why mitochondria may be less critical in the maintenance of Ca^{2+} homeostasis. In addition, ATP production in yeast seems to be independent of the regulation of Ca^{2+}[120]. This can be explained by the fact that mitochondria from most yeast strains do not possess a rapid Ca^{2+} uptake system as the MCU[106, 121] (although there are strain-specific differences, as *Endomyces magnusii* does have a Ca^{2+} uniporter[122]) or a Na^{+}-stimulated Ca^{2+} release pathway as NCLX. Nevertheless, they do contain a mitochondrial Ca^{2+}:$2H^{+}$ antiporter extruding Ca^{2+} from the matrix, which is highly active in presence of free fatty acids[123], suggesting that matrix Ca^{2+} may serve some regulatory role.

Yeast mitochondria also possess a fast Ca^{2+} release channel called yeast mitochondrial unselective channel (YMUC), which can be opened by respiration or nucleotides and has

similar electrophysiological properties as the mammalian PTP[105-109, 124]. For a long time yeast was considered to be a poor model for studying the PTP, as the regulation of this channel seemed to be too different, particularly because it is inhibited rather than activated by Pi, and insensitive to CsA[107]. Several new results, however, suggest that the PTP of yeast and mammals may be closer than previously thought. One issue concerns the Ca^{2+}-dependence of YMUC in the presence of the Ca^{2+} ionophore ETH129, which allows electrophoretic matrix Ca^{2+} accumulation in yeast mitochondria[106]. A recent study shows that in optimized conditions, i.e. using low concentrations of Pi (an inhibitor of the yeast pore), the opening of the channel becomes Ca^{2+}-dependent[109]. The opposing effects of Pi (which is an inducer of the mammalian PTP and an inhibitor of the yeast pore) could be recently explained in a study showing that Pi may become an inhibitor in mammalian mitochondria that are treated by CsA or in which Cyp-D had been genetically ablated[68]. We suppose that Cyp-D is masking an inhibitory Pi binding site which becomes accessible only when Cyp-D is removed. Thus, we hypothesize that the yeast mitochondrial cyclophilin CYP3[125] may not be able to bind the PTP, and thereby to hinder the binding site for Pi. This scenario would explain the inhibitory function of Pi as well as the lack of CsA-sensitivity in yeast. Additional points are the lack of effect of several inducers of the mammalian PTP like carboxyatractylate (inhibitor of the ANT), ligands of the PBR, and prooxidants in yeast[107]. However, some of these differences might depend on experimental conditions as e.g. the dithiol crosslinker phenylarsine oxide, one of the most important PTP-inducers, is able to sensitize the yeast pore to Ca^{2+}[126]. Based on these observations, we believe that the yeast and mammalian PT may be the expression of very similar events, although they differ in modulation through mechanisms that will be fully understood only after the molecular nature of the PTP is defined.

For further description of PT in other species and comments on the conservation of the PTP during evolution see **Publication 2**.

4 Cyclophilins

The cyclophilins are a family of highly conserved PPIases with a crucial role in protein folding. The peptide bonds of any protein can exist in two different isomeric forms, *cis* or *trans.* Protein folding as well as refolding processes following cellular membrane traffic require isomerization and the interconversion between the *cis* and the *trans* form of prolines relative to the nascent polypeptide chain is catalyzed by cyclophilins and other PPIases. All cyclophilins share a common domain of about 109 amino acids, the cyclophilin-like domain (CLD), surrounded by domains unique to each member of the family that are associated with subcellular compartmentalization and functional specialization[127]. All cyclophilins can bind the immunosuppressant drug CsA. The cytoplasmic Cyclophilin A (Cyp-A) is the main intracellular receptor for CsA[128]. The immunosuppressive action of CsA is carried out via a ternary complex between CsA, Cyp-A and calcineurin, a calcium-calmodulin-activated serine/threonine-specific protein phosphatase. The CsA-Cyp-A complex inhibits calcineurin preventing dephosphorylation, hence nuclear translocation of the nuclear factor of activated T cells (NFAT), thus preventing the transcription of genes encoding cytokines[129].

4.1 Cyclophilin D

Cyp-D, which in the mouse is encoded by the *Ppif* gene, possesses a mitochondrial targeting sequence and is imported into the mitochondrial matrix upon translation. Cyp-D has a series of binding partners inside mitochondria. In the matrix it interacts with a complex chaperone network involving Hsp90 and its related molecule TRAP-1[130]. Capturing of Cyp-D to this complex makes it no longer available for binding to, and inducing, the PTP, which might be a strategy to protect from cell death. Treatment of tumor cells with shepherdin, an Hsp90 antagonist, leads to replacement of Cyp-D from the Hsp90–TRAP-1–Cyp-D complex and selective killing of tumor cells[130]. Another target of Cyp-D is the F_OF_1-ATP synthase, as recently documented in bovine heart and liver mitochondria[131]. Giorgio et al. demonstrated that Cyp-D binds to the lateral stalk of the enzyme, forming a complex with the OSCP, b, and d subunits, and that this binding is favored by Pi. Association of Cyp-D to the F_OF_1-ATP synthase decreases the ATPase activity while treatment with CsA increases the latter and displaces Cyp-D from the

ATP synthase. A recent study also demonstrated a CsA-sensitive interaction of Cyp-D with the anti-apoptotic protein Bcl2[132].

Cyp-D binds to the IMM in a process that is associated with PTP opening, promoted by increased intramitochondrial levels of Ca^{2+} and/or reactive oxygen species and inhibited by CsA. The first pharmacological tool used to demonstrate the relationship between Cyp-D and the PTP was CsA. Later this interaction was confirmed by other Cyp-D ligands such as sanglifehrin A, NIM-811, Debio-025 and antamanide[133-136]. However, only after the generation of *Ppif*$^{-/-}$ mice lacking Cyp-D, a final evidence for Cyp-D in PTP regulation could be provided. Several studies analyzed fibroblasts, thymocytes and hepatocytes isolated from *Ppif*$^{-/-}$ mice and evaluated in particular the response to different apoptotic stimuli[91, 102, 137, 138]. Basso et al. showed that the PTP in *Ppif*$^{-/-}$ mitochondria still forms, consistent with its role as a pore regulator, but not as a structural component. The propensity of PTP opening in Cyp-D null mitochondria is strikingly reduced in that the opening requires about twice the Ca^{2+} load necessary to open the PTP in wild type mitochondria. PTP opening in *Ppif*$^{-/-}$ mitochondria was insensitive to CsA, as expected. Studies in cells lacking Cyp-D showed that they were more resistant to oxidative stress and increased cytoplasmic Ca^{2+}[(102)]. On the other hand, increased Cyp-D expression in a neuronal cell line[139] and in mitochondria from rat hearts with volume overload-induced compensated hypertrophy[140] were more susceptible to PTP opening and cell death. Recently, Basso et al. have shown that the desensitizing effect of Cyp-D ablation or CsA treatment on the pore is only present when Pi is used, but not when the latter is replaced by its analogues arsenate or vanadate. As already mentioned, these results suggest that when Cyp-D does not bind to the PTP (because of genetic ablation or of the binding to CsA) Pi can bind to an inhibitory site on the pore thereby delaying pore opening[68].

There is a striking analogy between the regulation of the PTP and the ATP synthase by Cyp-D and CsA. Indeed, Pi favors binding of Cyp-D to ATP synthase and PTP opening, while CsA promotes Cyp-D unbinding from the ATP synthase and PTP closure. Whether this is due to a link between the two processes is currently under investigation in our laboratory. Our recent studies have shown that the PTP might form from dimers of the ATP synthase (Giorgio et al, submitted).

5 The fruit fly *Drosophila melanogaster*

The ecdysozoan arthropod *Drosophila melanogaster* belongs to a sub-species of the Drosophilidae, dipteran insects found all over the world. The species is known generally as the common fruit fly. The life cycle of *Drosophila* varies with temperature, as is the case for many ectothermic species. At **25°C** the developmental time (egg to adult) is about 10 days. Females lay about 400 eggs into rotting fruit or other suitable material. The eggs, which are about half a millimeter long, hatch after about one day into a worm-like larva. The larva grows for about 4 days, molting at day 1, day 2, and day 4 after hatching (first, second and third instar larva). After another two days the larva molts one more time to form an immobile pupa and undergoes a four-day-long metamorphosis, in which the body is completely remodeled to give rise to the adult winged form. The life cycle is concluded with the hatching from the pupal case after which the fly becomes fertile within about 12 hours.

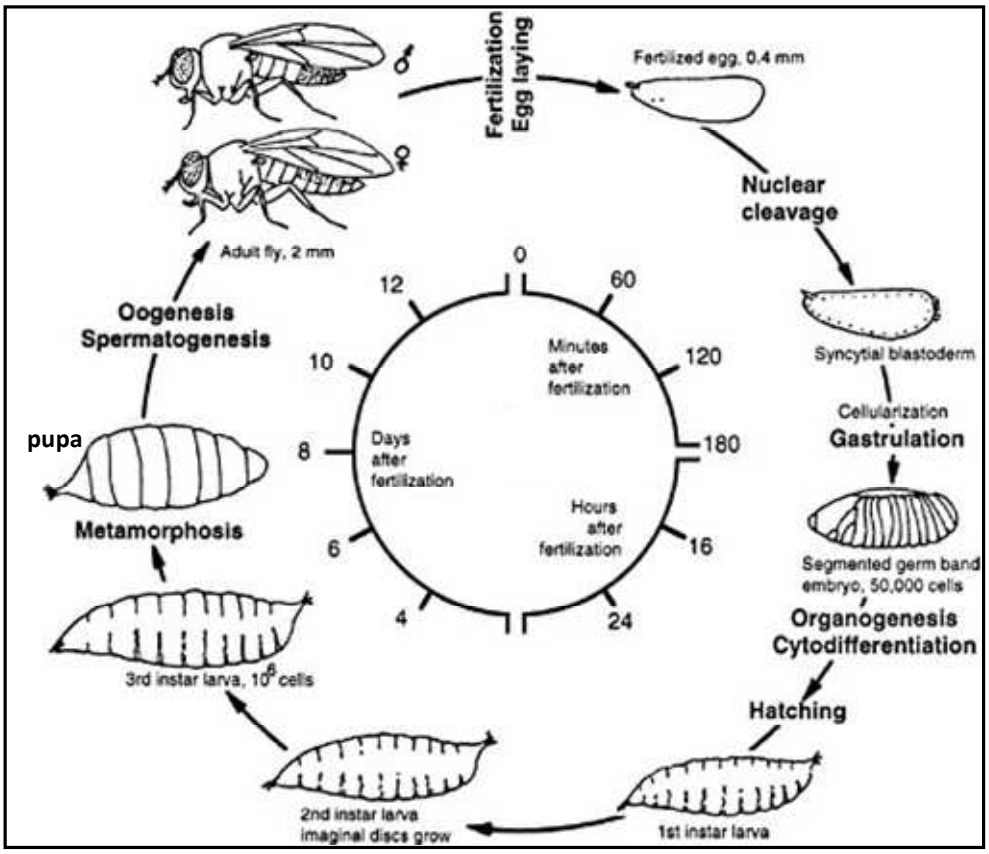

Figure 10. Life cycle of *Drosophila melanogaster*. One day after fertilization the larva hatches. First, second, and third instar are larval stages, each of them ending with a molt. In the pupal stage most of the larval tissues are destroyed and replaced by adult tissues derived from the imaginal discs that were growing in the larva. Times are indicative for the life cycle of flies maintained at 25°C; modified from[141].

Since during evolution arthropods separated from vertebrates more than 600 million years ago[142, 143], *Drosophila* might be supposed to be very different from humans with respect to genetics and cellular pathways. However, comparative analysis of the genome of *Drosophila* and humans revealed striking similarities in the structural composition of individual genes[144] and *Drosophila* quickly became an important tool for genetic, molecular and behavioral studies.

5.1 *Drosophila* as a model organism

Since T.H. Morgan in 1910 demonstrated the chromosome theory of heredity in the fruit fly *Drosophila*, this organism has played an important role in the development of modern biology, in particular in the area of genetics. Today it is one of the most important model organisms in studies of development and differentiation[145], aging[146], cell cycle[147], transcriptional and translational control[148], signaling pathways[149], sensorial perception[150], neurodegenerative diseases[151] and circadian rhythms[152].

Moreover *Drosophila melanogaster* has been one of the first organisms to be sequenced in its entirety[153], and a database with all nuclear and mitochondrial encoded genes is available[154]. The *Drosophila* genome contains a large number of human orthologs, which include conserved molecules and pathways of key cellular processes[155]. These findings quickly made *Drosophila* an important system to model human diseases[156]. Research projects focused on neurodegenerative diseases[157], cancer[158], cardiac pathologies[159], age-associated dysfunction[160] and recently also on mitochondrial diseases[161-163] have emerged.

Compared to higher organisms *Drosophila* offers some attractive features as a model organism; these are especially suited for studying complex biological processes. *Drosophila* is ideally tractable at the genetic, biochemical, molecular and physiological levels. First of all the flies can be easily maintained in large numbers in stocks and populations without specialized instrumentation. *Drosophila* has a short life-cycle resulting in the production of a large number of progeny over a short, 10-day generation period[155]. Other model organisms such as the mouse require a longer, 21-day gestation time and produce a smaller number of progeny. For the purpose of genetic screens, *Drosophila* provides two benefits in that its genome is comprised of

only 4 pairs of chromosomes, as opposed to 16 in the yeast strain *Saccharomyces cerevisiae*, or 23 in humans, thus simplifying genetic inheritance. The second advantage is that mutants can be created quite easily by molecular techniques using P-element transposons[164], site specific recombination to knock-in and knock-out specific genes, or RNA-interference to knock-down gene expression[165]. In recent years many different tools to trigger gene expression or repression have been developed. Furthermore, the use of X-rays and other mutagenic agents makes it possible to generate large collections of mutant stocks. Several key features of *Drosophila*, such as the compound eye, provide unique methods for studying mutational effects by simple visual observation of the resulting phenotype[155]. Thus, *Drosophila* provides an excellent model organism through the compromise between simple cultivation, genetics and phenotypic scoring, while key cellular processes are evolutionary conserved. Also with respect to my PhD project concerning Ca^{2+} transport and permeability transition in mitochondria, *Drosophila* seemed to be an interesting alternative to the mammalian models, usually employed in these studies.

5.2 *Drosophila* cell lines

Despite the numerous advantages which *Drosophila* offers in various research fields, using whole organisms as basic material for experiments has some limits. For example, some mutations can have lethal effects in adults and therefore it becomes impossible to compare mutant with wild type flies. Another disadvantage can be the heterogeneity of the fully differentiated cell-types in the adult flies and thus an uneven response to stimuli. Thus, for some research projects it becomes necessary to isolate specific tissues, cells or organelles which, due to the size of the flies, can be a laborious and time-consuming work which often results in an insufficient yield. This is especially the case when mutations have an impact on growth and viability of the flies, and therefore the number of adults is limited. Thus, in recent years cultured *Drosophila* cell lines emerged as an important tool in different research fields. The cells are in most cases derived from embryonic states, e.g. Schneider (S2) cells[166], composed of a variety of tissue precursors and are therefore undifferentiated. However, also tissue-specific imaginal disc[167] and CNS-derived[168] cell lines have been established. All these cell lines greatly facilitate biochemical studies and resolve the yield problem mentioned above,

since they provide virtually unlimited amounts of homogenous material. With specific respect to the aim of my PhD Thesis, they proved useful to obtain a sufficient amount of mitochondria to perform studies on bioenergetics, Ca^{2+} fluxes and permeability transition. Moreover, especially with new techniques like RNA-interference[169], different mutant cell lines can be generated, bypassing also the lethal effects of some mutations on adult flies. Furthermore *Drosophila* cell lines have been successfully used in heterologous protein expression studies and stable cell lines constitutively or inductively expressing the desired protein could be created[170-172]. For the study of my PhD Thesis I used the cell line $S_2R^{+(173)}$ which is derived from late embryonic stages (20-24h old embryos), and differs from its ancestor (S2) in that it has the ability to adhere to tissue culture dishes. The primary culture was prepared and immortalized by I. Schneider (1972) from enzymatically disaggregated embryos. For detailed information on the exact procedure see[166]. Although *Drosophila* cell lines can be cultured in a similar way as mammalian cell lines, some important differences should be considered[174]. *Drosophila* cells should be grown at 25°C and need no CO_2 buffering, the ideal gas being ordinary air. Moreover, they do not show the phenomenon of "contact inhibition", displayed by mammalian cells. After forming a monolayer on the substrate, *Drosophila* cells continue to proliferate, building more than one layer or growing in suspension.

5.3 *Drosophila* mitochondria in research

As soon as it became obvious that most of the genes implicated in human diseases have at least one fly homolog[175], *Drosophila* became a powerful tool to elucidate the molecular and cellular mechanisms that underlie these disorders. Most research projects concerning mitochondria from *Drosophila* are focused either on the mitochondria-induced mechanisms of aging or on the mitochondrial involvement in neurodegeneration with the aim to model human neurodegenerative disorders, such as Alzheimer's, Parkinson's and Huntington's disease.

Drosophila and aging

The mitochondrial electron transport chain is one of the primary sources of reactive oxygen species (ROS) within cells, as ROS are by-products of respiration. While ROS may have important roles in cell functions such as cell signaling, it has been discovered

that high levels of ROS also cause cellular damage[176]. Since the early fifties it was hypothesized that the accumulation of molecular damage caused by ROS contributes to the functional decline during the aging process[177]. A number of studies in *Drosophila* confirmed an important role for mitochondrial ROS in modulating lifespan. Those studies engineered flies with increased oxidative stress response by the adult-specific overexpression of the mitochondrial Mn-Superoxide Dismutase (MnSOD), which led to an increased lifespan[178]. Another approach to reduce oxidative stress was the reduction of mitochondrial ROS production, which was achieved by the expression of the human uncoupling protein 2 (hUCP2) in adult *Drosophila* neurons, again leading to the extension of lifespan[179]. However, it cannot be excluded that the reduction of ROS increases lifespan indirectly through changes in cell signaling or gene expression. Other studies in *Drosophila* demonstrated age-related decreases in respiratory chain activity and changes in mitochondrial structure[180, 181]. These observations can be explained either by the damaging effect of ROS or by the decline in expression of genes that are important for the electron transport chain with aging[182].

Drosophila and neurodegeneration

Neurodegenerative diseases are a large group of disorders of the nervous system, characterized by the progressive selective loss of neuronal subtypes such as dopaminergic or motor neurons. Mitochondrial abnormalities have been documented in neurodegenerative diseases, including Alzheimer's, Parkinson's, and Huntington's diseases and amyotrophic lateral sclerosis and several studies have demonstrated that mitochondrial impairment plays an important role in the pathogenesis of this group of disorders (for an overview of the major findings in recent years see[183, 184] and[185]). A suitable model organism to study human neurodegenerative diseases should have homologues to the genes mutated in the human disorder and should possess neurobiological cellular processes (such as synapse formation and neuronal communication) and neurobiological bases of behavior (such as sensory perception, aspects of learning and memory formation) that are similar to those found in humans. All of these criteria are fulfilled by *Drosophila*, where two approaches are commonly used. First, the expression of a human disease gene in its wild type or mutant form in a *Drosophila* tissue, usually the eye, and assessment of the corresponding phenotype[186].

Second, loss or gain of function analysis of the *Drosophila* homolog of the human disease gene and assessment of the associated phenotypes[165]. A third possibility is the screen of compounds in the already established *Drosophila* disease model in order to pick out those that ameliorate the phenotype. This approach was successfully used in fly models of adult-onset, age-related neurodegeneration and led to the complete rescue of disease-related phenotypes[187]. Studies in the last two decades brought up reliable *Drosophila* models for Alzheimer's[188, 189], Parkinson's[190, 191] and motor neuron diseases[192], as well as for trinucleotide expansion diseases[193], such as ataxias[194] and Huntington's disease[195].

5.4 Involvement of *Drosophila* mitochondria in apoptosis

In mammalian cells the key step in mitochondrial-induced cell death occurs when the OMM permeabilizes and several apoptogenic proteins, including cyt *c*, Smac/DIABLO, AIF and endoG are released from the mitochondrial IMS[29]. In mammals, the subsequent activation of caspases is dependent on cyt *c*-induced apoptosome formation[196]. The process of MOMP is highly regulated by members of the Bcl-2 family. Like worms and mammals, the *Drosophila* genome encodes at least two Bcl-2 family members[197]. Sequence analysis revealed that *Drosophila* possesses seven members of the caspase family[198], which can be divided into initiator and effector caspases. The essential apoptotic initiator caspase is named Dronc, and like mammalian caspase 2 and 9 it interacts with Dark, the fly homolog of Apaf-1[199]. Consistently, Dronc can function as an initiator caspase to cleave and activate the effector caspase Drice[200].

However, conclusions about apoptotic pathways drawn on the basis of sequence homologies should be taken with caution. Based on sequence, *Drosophila* might be expected to require mitochondrial MOMP and cyt *c* release for caspase activation; yet, unlike Apaf-1 in mammals, Dark does not appear to require cyt *c* to activate Dronc, and several reports have found no indication that cyt *c* is released from *Drosophila* mitochondria during apoptosis[201-203]. However, this is still a debated issue in the fly community since two recent reports showed that cyt *c* translocates to the cytosol in some types of cell death[201, 204]. To date, *Drosophila* cyt *c* has been linked to caspase

activation only during spermatid differentiation[205] and to the proper timing of cell death in the pupal eye[206]. Despite the debated role of cyt *c* it is well accepted that the key players in regulation of the *Drosophila* apoptotic program are **Diap1,** a fly homolog of the mammalian X-linked inhibitor of apoptosis proteins (XIAP) and its antagonists **Reaper, Hid, Grim and Sickle (RHG proteins)**. Diap1 is the key anti-apoptotic protein in *Drosophila* and ensures cell survival by inhibiting caspase activity[207]. Apoptosis is initiated by the binding of RHG proteins to Diap1, inducing its autoubiquitination and proteasome-mediated degradation and resulting in the activation of effector caspases[208]. Furthermore, it was recently found that Reaper and Hid proteins cause mitochondrial fragmentation and release of cyt *c* in both cultured S2 cells and in the developing fly embryo[201].

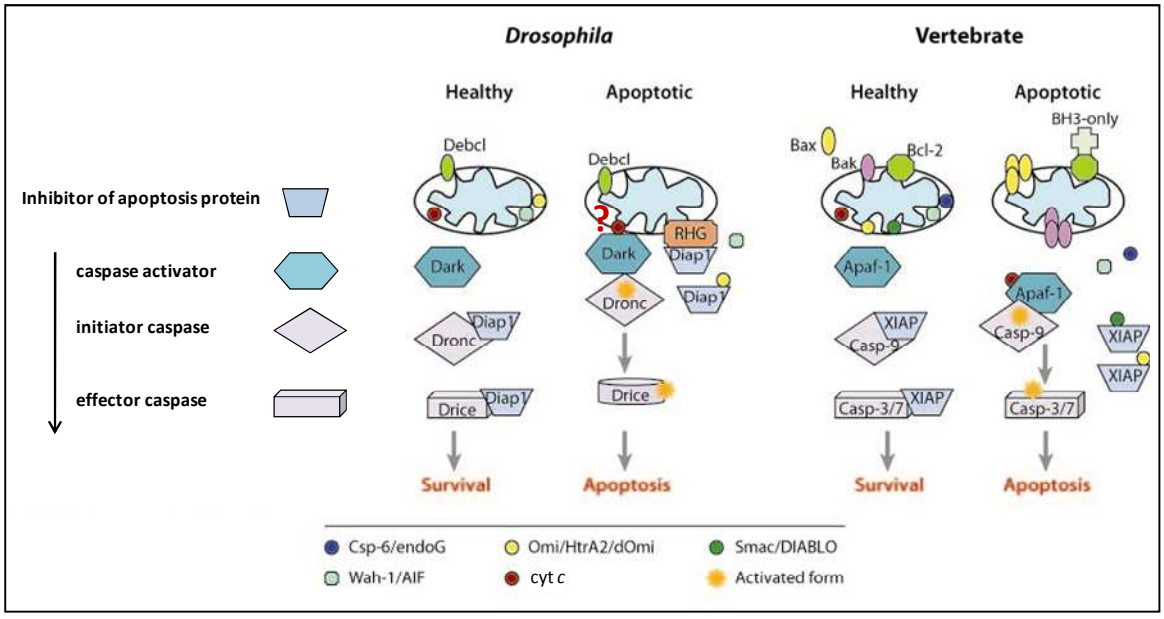

Figure 11. Schematic representation of key proteins in mitochondrial-induced apoptotic pathways in vertebrates and their *Drosophila* homologues. In healthy vertebrate cells, Apaf-1 is auto-inhibited and initiator caspase-9 as well as effector caspases -3 and -7 are inactive due to the binding to X-linked inhibitor of apoptosis protein (XIAP). An apoptotic stimulus leads to the activation of BH3-only proteins which bind to anti-apoptotic Bcl-2 proteins to remove their inhibitory effect or directly induce Bax/Bak channel formation which in turn triggers release of cytochrome *c* (cyt *c*), second mitochondria-derived activator of caspases (Smac)/direct inhibitor of apoptosis binding protein with low pI (Diablo), endonuclease G (endoG), apoptosis inducing factor (AIF), and Omi/HtrA2. Cyt *c* binds to Apaf-1 in the cytosol and thus induces apoptosome formation and activation of downstream caspases. Smac/DIABLO and Omi/HtrA2 bind to XIAP to remove its inhibitory effect.
In *Drosophila*, the initiator caspase Dronc and the effector caspase Drice are ubiquitinated by Diap-1 for proteosomal degradation in healthy cells. Upon apoptotic signals, transcription of genes encoding for the pro-apoptotic proteins Reaper, Hid, Grim and sickle (RHG proteins) is induced, and RHG proteins translocate to mitochondria from where they recruit Diap-1 for interaction. The RHG proteins induce Diap-1 autoubiquitination and proteasomal degradation. Binding of Dark to mitochondria triggers apoptosome formation. dOmi might interact with the *Drosophila* homologue of the vertebrate XIAP, Diap-1 to remove the inhibitory effect of Diap-1 on caspases. Whether cyt *c* is released by *Drosophila* mitochondria during apoptosis is debated. Ortholog proteins in vertebrates and *Drosophila* are labeled in the same shape and color; modified from[209].

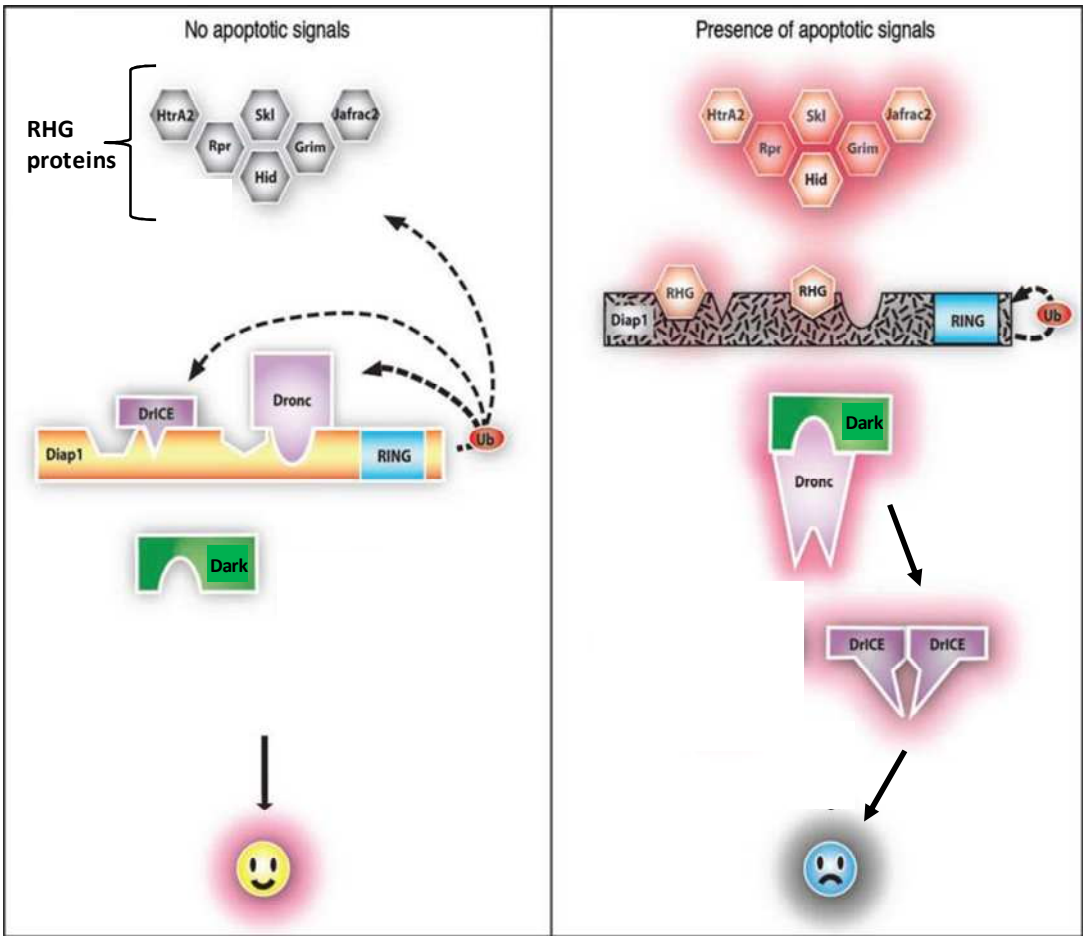

Figure 12. Interaction of the key players in *Drosophila* cell death. In the absence of apoptotic signals, the initiator caspase Dronc and the effector caspase DrICE bind to the *Drosophila* inhibitor of apoptosis protein (Diap1), which ubiquitinates the caspases via its RING domain. Ubiquitylation inactivates the caspases without proteasomal degradation. The RING domain of Diap1 is also capable of ubiquitylating Reaper. In the presence of apoptotic stimuli, the RHG proteins displace the caspases from Diap1 and stimulate auto-ubiquitylation and proteasomal degradation of Diap1. Dronc is free to bind to the caspase activator Dark for apoptosome formation leading to activation of DrICE for cell death induction; modified from[208].

However, the possible lack of MOMP and cyt *c* release in *Drosophila* cell death does not necessarily mean that mitochondria are not important during apoptosis in flies. Indeed, there is strong evidence for mitochondria as a docking site to bring the key players in apoptosis into close proximity. Reaper, Hid and Grim were all found to localize to mitochondria. Hid possesses a hydrophobic C-terminal mitochondrial targeting sequence[210] and seems to recruit the other pro-apoptotic RHG proteins via their GH3 domain, an amphipathic helix conserved between Grim, Reaper and Sickle and essential for their Diap1 degradation and killing activity[211]. It was hypothesized that Reaper may be part of a high-order complex at the OMM to locally regulate Diap1 turnover and caspase activity [212]. The Bcl-2 homologues Debcl and Buffy do not seem to play a pivotal role in developmental cell death in flies as analyzed in either single or double knockout

flies[213]. Surprisingly, the fly Bcl-2 homologues are able to induce cell death in mammalian cells[214]. Taken together, these results suggest that Bcl-2 proteins in *Drosophila* can potentially induce apoptosis, and that flies can bypass the need of Bcl-2 proteins by another regulatory strategy, i.e. transcriptional control of the potent Diap1 inhibitors Reaper, Hid, Grim and Sickle. Thus, *Drosophila* does not require the control of Bcl-2 proteins to regulate MOMP and the release of IAP antagonist (such as Smac and Omi), as is the case in mammals[209].

It is not known whether additional cell death pathways that depend on mitochondrial Ca^{2+} and oxidative stress are active in *Drosophila*. These pathways in mammals are mediated by the PTP, but whether Ca^{2+} transport- and PTP-dependent IMM permeabilization can also play a role in *Drosophila* was not known. This is the topic of my PhD work.

MATERIALS AND METHODS

I. S_2R^+-cells

I.1 Cell culture

Cells were cultured in Schneider's insect medium (Gibco) supplemented with 10% heat-inactivated fetal bovine serum (culture medium). Culture medium for the transfected S_2R^+pActCypD/pCoPuro cells was supplemented with 8 µg/µl puromycin. Depending on the desired culture size cells were kept in 75cm^2 T flasks or in tissue culture dishes (245x245x25mm). S_2R^+ cells grow as adherent monolayers as well as in suspension. Cells were incubated in a 25°C thermostated room and split every three or four days at 1:5 to 1:10 dilutions.

I.2 Cell permeabilization

Cells were detached with a sterile cell scraper, centrifuged at 200 x *g* for 10 min and washed twice with Dulbecco's phosphate buffered saline (PBS) without Ca^{2+} and Mg^{2+}, pH 7.4 (Euroclone). The resulting pellet was resuspended in 130 mM KCl, 10 mM MOPS-Tris, pH 7.4 (KCl medium) containing 150 µM digitonin and 1 mM EGTA-Tris and incubated for 20 min on ice (6 x 10^7 cells x ml^{-1}). Cells were then diluted 1:5 in KCl medium containing 10 µM EGTA-Tris and centrifuged at 200 x *g* in a refrigerated centrifuge (4°C) for 6 min. The final pellet was resuspended in KCl medium containing 10 µM EGTA-Tris at 4 x 10^8 cells x ml^{-1} and kept on ice.

I.3 Subcellular fractionation

Cell membranes were lysed by hypotonic shock in a medium containing 10 mM Tris-HCl, pH 6.7, 10 mM KCl, 150 µM $MgCl_2$ supplemented with protease and phosphatase inhibitor cocktails (Sigma) for 30 min on ice, followed by further disruption of the cell membranes using a 26 G x ½" syringe (Artsana). Hypotonic shock was stopped by the addition of sucrose at a final concentration of 250 mM and differential centrifugation was performed for subcellular fractionation. Lysates were centrifuged three times at 2,200 x *g* for 10 min at 4°C to remove nuclei and cell debris. The supernatant was centrifuged another three times at 8,200 x *g* for 10 min at 4°C to separate mitochondria from the cytoplasm.

I.4 Stable Transfection

Two million cells were plated in each well of a 6-well tissue culture plate in 2 ml culture medium per well. Cells were incubated for 5 h at room temperature (RT) for attachment and then transfected with the Effectene® Transfection Reagent kit (Qiagen). Selection vector (pCoPuro) and expression vector (pActCypD) were used in a 1:20 ratio. PCoPuro (0.3 µg) and pActCypD (6 µg) were mixed with 50.4 µl Enhancer and 543.4 µl EC-Buffer and incubated for 5 min at RT, followed by the addition of 60 µl Effectene. The mixture was incubated for 15 min at RT and then added drop-wise to the cells. After 3d the medium was removed and culture medium containing 8 µg/ml puromycin (selection medium) was added. Cells were maintained in selection medium and split to culture flasks when they reached confluence. The whole selection process took about three weeks.

II. Mitochondrial bioenergetics

II.1 Measurement of mitochondrial respiration

Rates of mitochondrial respiration were measured using a Clark-type oxygen electrode (Yellow Springs Instruments, OH, USA) equipped with magnetic stirring and thermostatic control maintained at 25°C, and additions were made through a syringe port in the frosted glass stopper sealing the chamber. Initial O_2 concentration in the 2 ml chamber at 25°C is 520 natoms O_2/ml at air saturation. Intact S_2R^+ cells were incubated in Hank's Balanced Salt Solution (HBSS) supplemented with 5 mM Pi-Tris, pH 7.4 while digitonin-permeabilized cells were incubated in 130 mM KCl, 10 mM MOPS-Tris, 5 mM Pi-Tris, 10 µM EGTA, pH 7.4. In both cases 2 x 10^7 cells were incubated in 2 ml of medium, followed by the addition of a respiratory substrate (10 mM glucose in the case of intact cells and 5 mM succinate-Tris in the case of permeabilized cells). Further additions were made as indicated in the figure legends. Addition of ADP allows oxidative phosphorylation to proceed, dissipating some of the protonmotive force and thereby stimulating electron transport (state 3 respiration). The rate of O_2 consumption after the addition of the F_OF_1 ATP synthase inhibitor oligomycin (state 4 respiration) is an indicator of how coupled mitochondrial respiration is to ATP synthesis and the ratio between state 3/state 4 is called respiratory control ratio. Addition of an uncoupler

(protonophore) fully dissipates the protonmotive force and stimulates O_2 consumption maximally (uncoupled respiration). When the O_2 concentration falls to zero, respiration ceases. O_2 consumption was calculated according to the slope of the registered graph, and plotted as ng atoms $O_2 \times min^{-1} \times mg^{-1}$, or $cells^{-1}$.

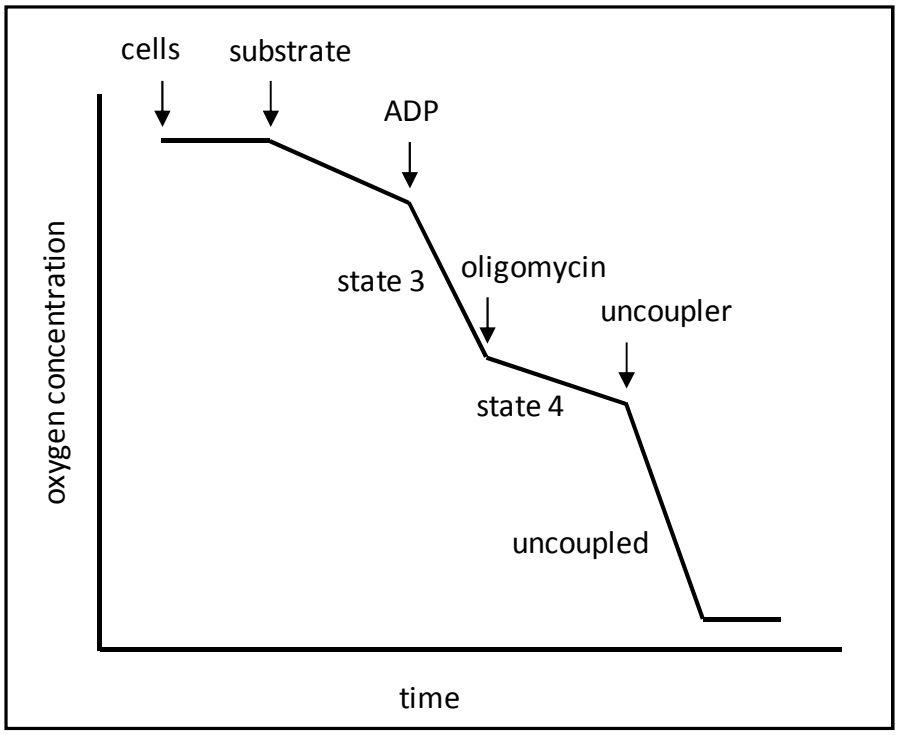

Figure 13. Schematic representation of a polarographic Clark type oxygen electrode trace. Shown are effects of respiratory substrates, ADP, oligomycin and uncouplers on the oxygen consumption rate in coupled mitochondria. State 3 = ADP-stimulated coupled respiration, state 4 = basal respiration in the absence of ADP or in the presence of oligomycin, that is a specific inhibitor of the F_OF_1 ATP synthase, uncoupled respiration = stimulated respiration due to a proton leak of the inner mitochondrial membrane induced e.g. by an uncoupler (protonophore).

II.2 Measurement of mitochondrial membrane potential

Mitochondrial membrane potential ($\Delta\Psi_m$) was measured using a Perkin-Elmer spectrofluorometer and evaluated based on the uptake of the positively charged fluorescent probe $Rhodamine_{123}$, which accumulates in energized mitochondria because of their inside negative $\Delta\Psi_m$. The intensity of the registered fluorescence corresponds to the concentration of the probe in the medium, because under the chosen experimental conditions intramitochondrial fluorescence of $Rhodamine_{123}$ is quenched. Thus, the higher $\Delta\Psi_m$, the lower the fluorescence of $Rhodamine_{123}$. Two

milliliters of assay medium (130 mM KCl, 10 mM MOPS-Tris, 5 mM Pi-Tris, 10 µM EGTA, 0.15 µM Rhodamine$_{123}$, pH 7.4) were added to the cuvette. The fluorescence of Rhodamine$_{123}$ was monitored at the excitation and emission wavelengths of 503 and 523 nm, respectively, with the slit width set at 2.5 nm. After a short incubation to reach stabilization of the signal, 2 x 10^7 permeabilized S_2R^+ cells were added to the cuvette. Further additions were as indicated in the figure legends.

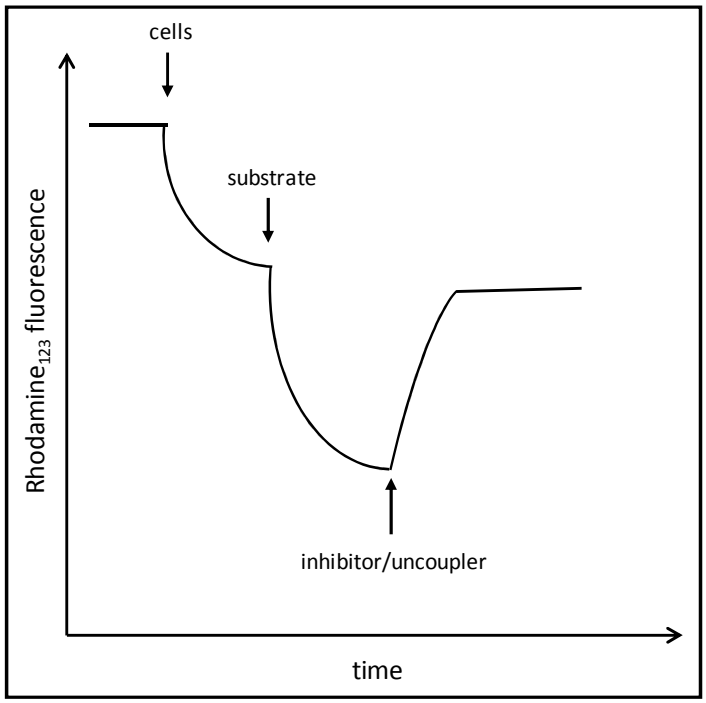

Figure 14. Evaluation of mitochondrial membrane potential ($\Delta\Psi_m$) based on Rhodamine$_{123}$ fluorescence. Shown is a scheme illustrating a typical trace recorded at a fluorimeter.

III. Mitochondrial Ca^{2+} transport and permeability transition

III.1 Measurement of mitochondrial Ca^{2+} fluxes and Ca^{2+} retention capacity

The mitochondrial CRC-assay was used to assess opening of the *Drosophila* Ca^{2+}-induced Ca^{2+} release channel in permeabilized S_2R^+ cells. The Ca^{2+} threshold needed to open the channel can be determined by adding Ca^{2+}-pulses of known concentrations at short intervals. Opening of the Ca^{2+}-induced Ca^{2+} release channel is marked by a sudden release of the accumulated Ca^{2+}. Extramitochondrial Ca^{2+} was measured with Calcium Green 5N (Molecular Probes) using either a Perkin-Elmer LS50B spectrofluorometer

equipped with magnetic stirring (excitation and emission wavelengths of 505 and 535 nm, respectively) or a Fluoroskan Ascent FL (Thermo Electron Corp.) equipped with a plate shaker (excitation and emission wavelengths of 485 and 538 nm, respectively with a 10-nm bandpass filter). The incubation medium contained 130 mM KCl or 250 mM sucrose, 10 mM MOPS-Tris, 5 mM succinate-Tris, 10 µM EGTA, 2 µM rotenone, 0.5 µM Calcium Green 5N, pH 7.4 and Pi-Tris as indicated in the figure legends. Permeabilized cells (2×10^7 in a final volume of 2 ml in the Perkin-Elmer spectrofluorometer and 2×10^6 in a final volume of 0.2 ml in the Fluoroskan) were used. Further additions were made as indicated in the figure legends.

Calcium Green 5N is a Ca^{2+}-sensitive dye, not permeable to the mitochondrial inner membrane. Therefore, adding a Ca^{2+}-pulse to the cell suspension leads to a peak in Calcium Green 5N fluorescence, followed by an immediate decrease of the latter when Ca^{2+} is taken up by mitochondria. When a threshold-concentration of matrix Ca^{2+} is reached, the Ca^{2+}-induced Ca^{2+} release channel opens, which leads to a release of Ca^{2+} out of the mitochondria and thus to a quick increase in Calcium Green 5N fluorescence.

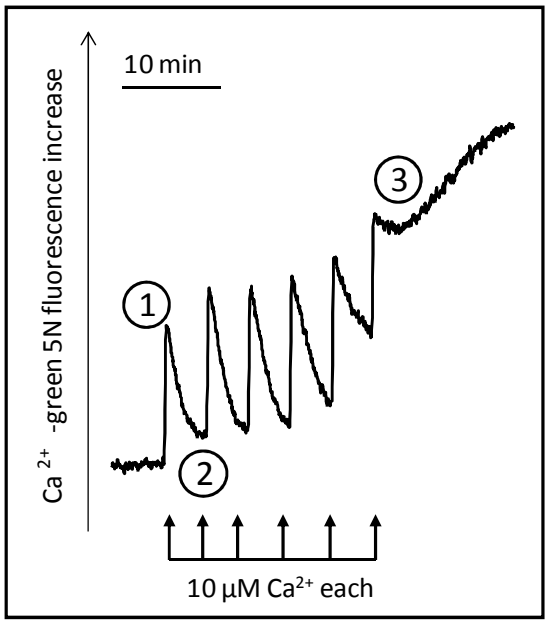

Figure 15. Calcium Retention Capacity (CRC) assay. Extramitochondrial Ca^{2+} is measured fluorimetrically by the Ca^{2+}-sensitive dye Calcium Green 5N. Addition of a Ca^{2+} pulse to the mitochondria or permeabilized cells leads to increase in fluorescence (1) followed by an immediate decrease of the latter when Ca^{2+} is taken up by mitochondria (2). When a threshold concentration of Ca^{2+} accumulated in the matrix is reached, the Ca^{2+}-induced Ca^{2+} release channel opens leading to a quick increase in fluorescence (3).

III.2 Light scattering

The light scattering technique is based on the correlation between mitochondrial matrix volume and the optical density of the mitochondrial suspension. Intact mitochondria scatter light at 540-nm wavelength. An increase in matrix volume due to mitochondrial swelling leads to a decrease in light scattering. Light scattering at 90° was monitored with a Perkin-Elmer LS50B spectrofluorimeter at 540 nm with a 5.5 nm slit width. Twenty million permeabilized cells in a final volume of 2 ml were incubated in a medium containing 130 mM KCl, 10 mM MOPS-Tris, 5 mM succinate-Tris, 10 µM EGTA, 2 µM rotenone, pH 7.4 and Pi-Tris as indicated in the figure legends.

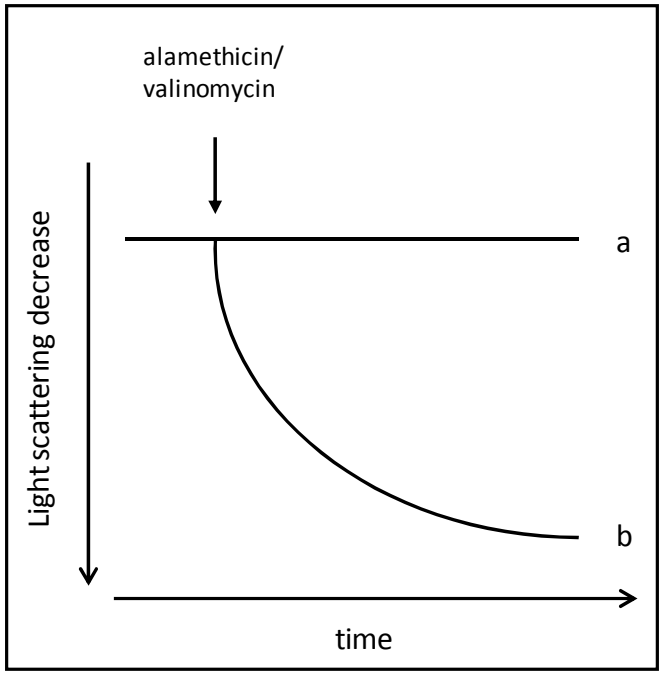

Figure 16. Schematic representation of the light scattering technique as indicator of mitochondrial volume changes. Addition of alamethicin (a pore-forming peptide) or valinomycin (a K^+-ionophore) to a mitochondrial or permeabilized cell suspension leads to a decrease in light scattering indicating mitochondrial swelling (b), (a) = control trace without any additions.

IV. Epifluorescence microscopy

IV.1 Fluorescent staining of S_2R^+ cell mitochondria

Energization of mitochondria in both intact and permeabilized S_2R^+ cells was analyzed based on accumulation of the potentiometric probe tetramethyl rhodamine methyl ester (TMRM, Molecular Probes), that accumulates in mitochondria based on their inside-negative $\Delta\Psi_m$. Three days before the experiments cells were seeded onto

sterilized 24-mm round glass coverslips at 2 x 10^6 cells per well in 2 ml culture medium. On the day of experiment cells were washed once with PBS and incubated for 20 min at RT with 1 ml of serum-free Schneider's medium supplemented with 1 µg/ml Cyclosporin H (CsH) and 10 nM TMRM. CsH is an inhibitor of the plasma membrane multidrug resistance pumps that does not affect the PTP of mammals and allows an appropriate loading with the probe by preventing its extrusion at the plasma membrane[215, 216]. Images were acquired with an Olympus IX71/IX51 inverted microscope equipped with a xenon light source (75 W) for epifluorescence illumination, and with a 12-bit digital cooled CCD camera (Micromax). For detection of TMRM fluorescence, 568 ± 25-nm bandpass excitation and 585-nm longpass emission filter settings were used.

IV.2 Immunofluorescence

One day before the experiments stably transfected S_2R^+pActCypD cells were seeded on sterilized 13-mm round glass coverslips in a 24-well tissue culture plate at 2 x 10^5 cells per well in 0.5 ml of culture medium. On the day of experiment cells were washed once with PBS and incubated for 20 min at RT with 0.5 ml of serum-free Schneider's medium supplemented with 1 µg/ml CsH and 100 nM Mitotracker® Red CMXRos (Molecular Probes) for mitochondrial staining. After another washing step with PBS, cells were fixed with 4% paraformaldehyde for 20 min at RT. Cells were washed again with PBS, permeabilized with 50 mM NH_4Cl in PBS + 0.1% Triton for 5 min at RT, washed again and blocked with PBS containing 3% goat serum for 1h at RT. Monoclonal anti-HA (clone HA-7, Sigma) diluted 1:100 in PBS with 2% goat serum was added to the cells and incubated over night at 4°C. On the next day cells were washed 3 times with PBS and the immunoreaction was revealed with FITC-conjugated anti-mouse IgG (Fab-specific, Sigma) at a working dilution of 1:500 in PBS with 2% goat serum for 45 min at RT. After another three washings in PBS coverslips were mounted with Mowiol and examined with an Olympus epifluorescence microscope at 60x magnification.

V. Electron microscopy

S_2R^+ cells were washed with PBS and fixed in 2.5% glutaraldehyde in 0.1 M K^+ phosphate buffer pH 7.4 for 2 h at 4°C. After washing with 0.15 M K^+ phosphate buffer pH 7.0 cells were finally embedded in 2% gelatin as previously described[217]. Gelatin-embedded samples were post-fixed with 1% osmium tetroxide in cacodylate buffer 0.1 M, pH 7.4, and embedded in Epon812 resin, sectioned and stained following standard procedures[218]. Ultrathin sections were observed with a Philips EM400 transmission electron microscope operating at 100 Kv.

VI. SDS-PAGE and Western Blotting

VI.1 Sample preparation

Cells were pelleted at 3,000 x *g* and mitochondria at 8,200 x *g* at 4°C and resuspended in a lysis buffer (LB) containing 150 mM NaCl, 20 mM Tris, pH 7.4, 5 mM EDTA-Tris, 10% Glycerol, 1% Triton X-100, supplemented with protease and phosphatase inhibitor cocktails (Sigma), and kept on ice for 20 min. Lysates were then centrifuged at 18,000 x *g* for 25 min at 4°C to remove insoluble materials. The supernatants were solubilized in Laemmli gel sample buffer containing 10% sodium dodecyl sulfate (SDS), 250 mM Tris, pH 6.8, 50% glycerol, 12.5% ß-mercaptoethanol and 0.02% bromophenol blue. Cytoplasmic fractions and post-cellular supernatants were concentrated by adding five volumes -20°C acetone to one volume of sample. Samples were kept overnight at -20° and finally centrifuged at 18,000 x *g* for 30 min at 4°C. The pellets were resuspended in 20% methanol, centrifuged again at 18,000 x *g* for 15 min at 4°C and finally solubilized in Laemmli gel sample buffer.

VI.2 SDS-PAGE

All samples to be run on the SDS-PAGE were previously solubilized in Laemmli gel sample buffer and denatured by boiling for 5 min. Samples were then loaded and separated electrophoretically in a 15% polyacrylamide gel.

VI.3 Western Blotting

Separated proteins were transferred electrophoretically to nitrocellulose membranes in a buffer containing 0.5 M glycine, 0.4 M Tris and 20% methanol at 4°C using a Mini Trans-Blot system (Bio-Rad). The membrane was then saturated for 1 h in PBS containing 3% nonfat dry milk and 0.02% Tween to avoid non-specific protein binding. Saturated membranes were incubated with a primary antibody overnight at 4°C. The next day membranes were washed three times in PBS/ 0.02% Tween for 5 min each and incubated with a secondary horseradish peroxidase-conjugated antibody (anti-mouse, anti-rabbit or anti-goat, depending on the source of the primary antibody) in PBS containing 3% nonfat dry milk and 0.02% Tween for 1 h and 30 min at RT. After another three washings, the antibody protein binding was revealed by the ECL (Enhanced ChemiLuminescence; Milipore) kit.

antibody	source	company	dilution
anti-cytochrome *c*	mouse monoclonal	BD Pharmingen	1:500
anti-OxPhos complex IV subunit I	mouse monoclonal	Invitrogen	1:500
anti-TOM20	rabbit polyclonal	Santa Cruz Biotechnology	1:300-1:500
anti-HA	mouse monoclonal	Sigma	1:1000
anti-Cyp-D	mouse monoclonal	Calbiochem	1:1000-1:3000
anti-actin	goat polyclonal	Santa Cruz Biotechnology	1:1000
anti-caspase3	rabbit polyclonal	Cell Signalling	1:1000

Table 1. List of all primary antibodies for Western Blotting used in this work.

VII. Plasmids and constructs

VII.1 Cloning of human Cyp-D cDNA into a *Drosophila* expression vector

Total RNA was extracted from the human osteosarcoma cell line HQB17 with TRIzol® Reagent (Invitrogen) according to the manufacturer's protocol. cDNA was synthesized using SuperScript™ II Reverse Transcriptase (Invitrogen), following the manufacturer's instructions. A construct of human Cyp-D cDNA carrying a mitochondrial targeting sequence (MTS) from *Drosophila* Hsp60 (a mitochondrial matrix protein) at its 5' end and an HA-tag at its 3' end was created by polymerase chain reaction (PCR) using a forward primer carrying the MTS and a reverse primer carrying the HA-tag. Exchange of the human MTS for a *Drosophila* MTS was meant to assure proper localization of the heterologous protein in the mitochondrial matrix upon translation in the *Drosophila* cell line, and the attachment of the nonapeptide HA (YPYDVPDYA) at the C-terminus was aimed to facilitate the detection of the heterologous protein by Western Blot or Immunofluorescence analysis. Long primers K_MTSCYPD_FWD and S_HACYPD_REV were used for generation of the MTS_CypD_HA construct from human cDNA by PCR. The second shorter primer pair (K_MTS_FWD and S_HA_REV) was used for screening of proper insertion in the vector by colony PCR, as described below.

name	sequence
K_MTSCYPD_FWD	*ctGGTACC*ATGTTCCGTTTGCCAGTTTCGCTTGCTCGCTCCTCCA TTAGCCGCCAGTTGGCCATGCGCGGCTATGCCAAGGATGTGTG CAGCAAGGGCTCCGGCGACCCG
S_HACYPD_REV	*ccGAGCTC*TTAAGCGTAATCTGGAACATCGTATGGGTAGCTCAA CTGGCCACAGTCTGTGATG
K_MTS_FWD	*ctGGTACC*ATGTTCCGTTTGCCAGTTTCGCTTG
S_HA_REV	*ccGAGCTC*TTAAGCGTAATCTGGAACATCGTATG

Table 2. Primers used for generation of a cDNA MTS-CypD-HA construct. Forward (FWD) and reverse (REV) primer contain cleavage sites for the restriction enzymes KpnI GGTACC and SacI GAGCTC (in red).

PCRs were performed in a 50 µl reaction mixture containing:

- 100 ng cDNA
- 25 µl 2x Phusion® High-Fidelity Master Mix with HF Buffer (Finnzymes)
- 10 µM primer K_MTSCYPD_FWD
- 10 µM primer S_HACYPD_REV

cycle step	temperature	time	cycles
denaturation	98°C	5 min	1
denaturation annealing extension	98°C 60°C 72°C	30 sec 30 sec 1 min	30
final extension	72°C	10 min	1

Table 3. PCR amplification protocol for generation of a cDNA MTS-CypD-HA construct.

A further incubation step at 72°C for 10 min was performed with GoTaq® DNA polymerase (Promega) to add an adenine (A)-overhang at the 3' end of the PCR product.

MTS Hsp60 *Drosophila*
HA Tag
human Cyp-D cDNA

ATGTTCCGTTTGCCAGTTTCGCTTGCTCGCTCCTCCATTAGCCGCCAGTTGGCCATGC
GCGGCTATGCCAAGGATGTGTGCAGCAAGGGCTCCGGCGACCCGTCCTCTTCCTCCTCCTCCGGGA
ACCCGCTCGTGTACCTGGACGTGGACGCCAACGGGAAGCCGCTCGGCCGCGTGGTGCTGGAGCTGA
AGGCAGATGTCGTCCCAAAGACAGCTGAGAACTTCAGAGCCCTGTGCACTGGTGAGAAGGGCTTCG
GCTACAAAGGCTCCACCTTCCACAGGGTGATCCCTTCCTTCATGTGCCAGGCGGGCGACTTCACCA
ACCACAATGGCACAGGCGGGAAGTCCATCTACGGAAGCCGCTTTCCTGACGAGAACTTTACACTGA
AGCACGTGGGGCCAGGTGTCCTGTCCATGGCTAATGCTGGTCCTAACACCAACGGCTCCCAGTTCT
TCATCTGCACCATAAAGACAGACTGGTTGGATGGCAAGCATGTTGTGTTCGGTCACGTCAAAGAGG
GCATGGACGTCGTGAAGAAAATAGAATCTTTCGGCTCTAAGAGTGGGAGGACATCCAAGAAGATTG
TCATCACAGACTGTGGCCAGTTGAGC**TACCCATACGATGTTCCAGATTACGCTTAA**

Figure 17. cDNA sequence of the MTS-CypD-HA construct. The mitochondrial targeting sequence (MTS) of the human Cyp-D sequence was exchanged for an MTS of *Drosophila* Hsp60 (a mitochondrial matrix protein; cyan) in order to assure proper mitochondrial localization of the heterologous protein in *Drosophila*. The sequence encoding for an HA-tag (pink) was attached to the 3' end of the human Cyp-D cDNA sequence (yellow) in order to facilitate detection of the protein. Restriction enzyme sites attached to the 3' and 5' ends are not shown.

The obtained 654 bp PCR product was ligated into the pGEM®-T vector (Promega) according to the manufacturer's instructions and the resulting vector was used to transform One Shot TOP10 *E. coli* cells (Invitrogen).

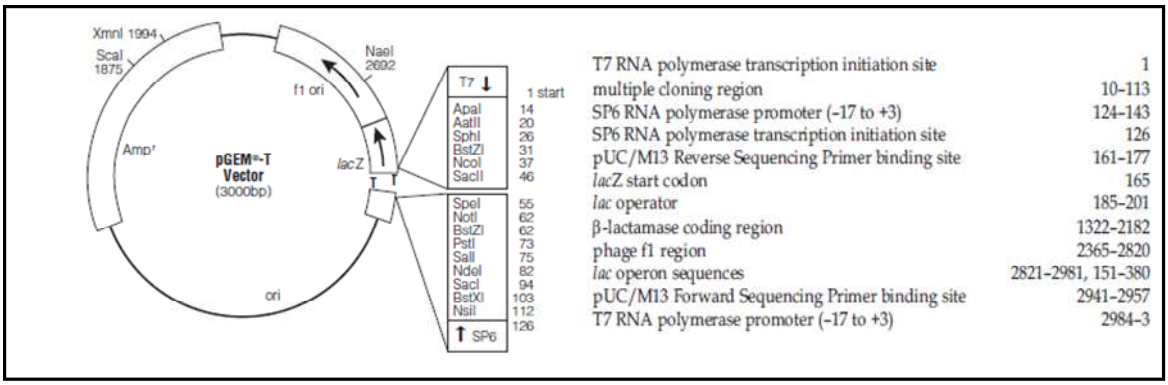

Figure 18. pGEM®-T vector map and sequence reference points.

Positive clones were detected by β-galactosidase screening and colony PCR. Furthermore, all the constructs were fully sequenced to assess the in-frame insertion of the cDNA and to control for unwanted mutations (BMR Genomics).

The 50 µl reaction mixture for colony PCR contained:

- 3 µl bacterial suspension grown overnight from a single colony
- 5 µl 10x PCR buffer
- 10 µM primer K_MTS_FWD
- 10 µM primer S_HA_REV
- 25 mM $MgCl_2$
- 10 mM dNTPs (10 mM each dATP, dTTP, dGTP, dCTP)
- 2.5 u GoTaq® DNA polymerase (Promega)

cycle step	temperature	time	cycles
denaturation	95°C	10 min	1
denaturation annealing extension	95°C 58°C 72°C	45 sec 45 sec 1 min	30
final extension	72°C	10 min	1

Table 4. Colony PCR amplification protocol for detection of MTS-CypD-HA-positive clones.

Using conventional restriction enzyme digestion techniques, the MTS_CypD_HA sequence was extracted with SacI from the pGEM®-T vector (SacI cuts at the 3′ end of the MTS_CypD_HA insert as well as upstream the 5′ end in the multiple cloning site of the pGEM®-T vector) and ligated into the pAct *Drosophila* transformation vector, which was linearized with the same restriction enzyme. The resulting pActCypD vector contains the MTS_CypD_HA construct under the control of the *Drosophila* actin 5C promoter, which drives constitutive expression of the heterologous protein. Positive clones were detected with colony PCR, as described above. The vector was purified by Miniprep and sequenced again in order to screen for plasmids containing the MTS_CypD_HA construct inserted in the right direction.

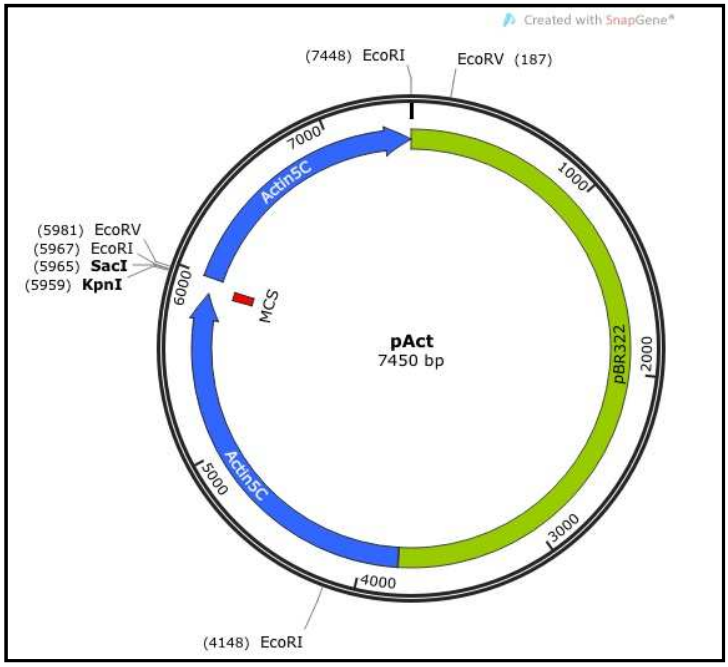

Figure 19. pAct vector map.

The expression vector pActCypD was co-transfected with the selection vector pCoPuro (Addgene plasmid 17533, coding for puromycin-resistance) into *Drosophila* S_2R^+ cells, in order to generate a stable polyclonal cell population, constitutively expressing human Cyp-D. Transfection procedure and selection process were performed as described above.

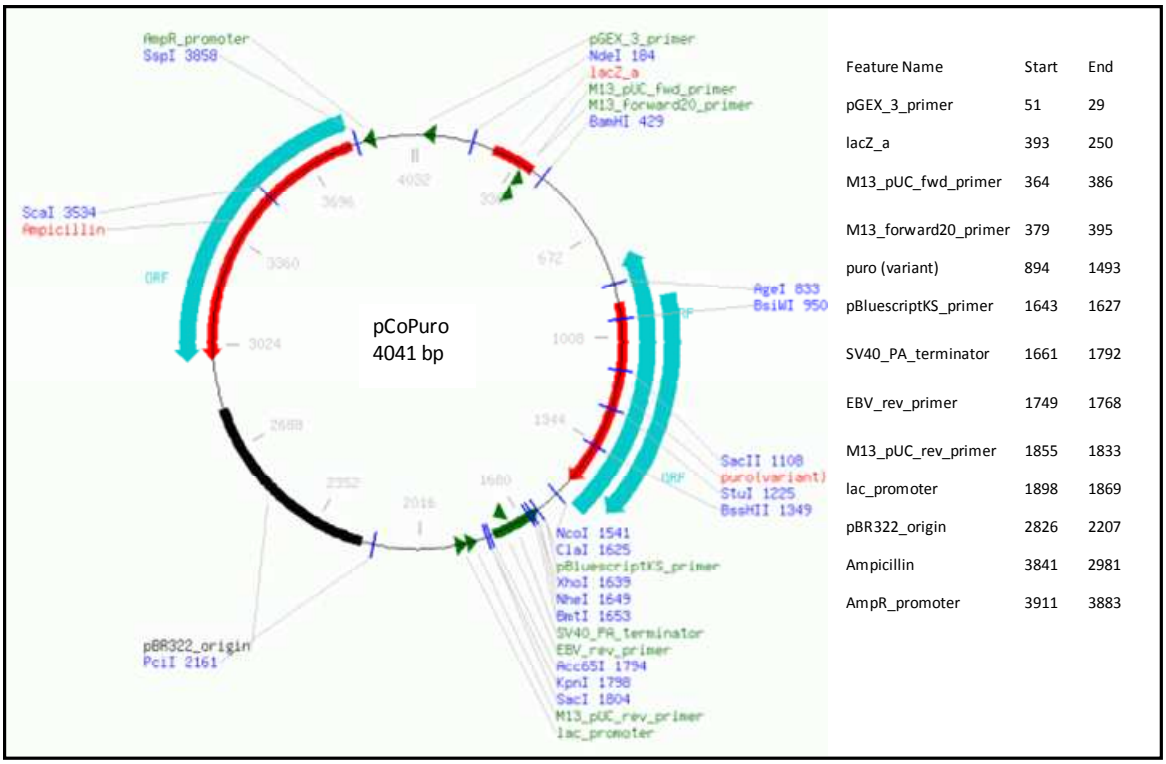

Feature Name	Start	End
pGEX_3_primer	51	29
lacZ_a	393	250
M13_pUC_fwd_primer	364	386
M13_forward20_primer	379	395
puro (variant)	894	1493
pBluescriptKS_primer	1643	1627
SV40_PA_terminator	1661	1792
EBV_rev_primer	1749	1768
M13_pUC_rev_primer	1855	1833
lac_promoter	1898	1869
pBR322_origin	2826	2207
Ampicillin	3841	2981
AmpR_promoter	3911	3883

Figure 20. pCoPuro vector map and sequence reference points.

RESULTS

Part I: Properties of a Selective Ca^{2+}-induced Ca^{2+} Release Channel in Mitochondria of *Drosophila melanogaster*

Mitochondria are key players in cellular Ca^{2+} homeostasis and are thereby involved in a wide field of physiological processes such as buffering of cytoplasmic Ca^{2+} signals, excitation-contraction coupling and induction of cell death. Indeed, the mitochondrial proton electrochemical gradient $\Delta\tilde{\mu}H$ is used not only to synthesize ATP but also to accumulate cations into the mitochondrial matrix. Ca^{2+} uptake into respiring mitochondria is mediated by the mitochondrial Ca^{2+} uniporter (MCU), localized in the inner mitochondrial membrane (IMM), while exchangers (Ca^{2+} for Na^+ and/or H^+) are responsible for Ca^{2+} efflux. However, mitochondria are exposed to the danger of Ca^{2+} overload when matrix Ca^{2+} load exceeds the capacity of IMM exchangers and thus, an additional Ca^{2+} efflux pathway may exist in mitochondria through opening of the permeability transition pore (PTP). The mitochondrial permeability transition (PT) describes a process of Ca^{2+}-dependent, tightly regulated increase in the permeability of the IMM due to the opening of a high-conductance channel, the PTP. Prolonged opening of the PTP causes mitochondrial depolarization, loss of ionic homeostasis, depletion of pyridine nucleotides, respiratory inhibition, matrix swelling, release of cytochrome *c* and cell death via apoptosis or necrosis depending on a variety of additional factors, among which cellular ATP and Ca^{2+} levels play a major role. On the other hand, transient openings of the PTP (flickering) may be involved in physiological Ca^{2+} homeostasis. The PTP has been thoroughly characterized based on its sensitivity to a large number of effectors, but its molecular nature remains elusive.

In spite of its importance as a model organism, remarkably little was known about the properties of Ca^{2+} transport in mitochondria of the fruit fly *Drosophila melanogaster*, and on whether these mitochondria can undergo a PT. Thus, we studied the pathways for Ca^{2+} transport in mitochondria in the embryonic *Drosophila* cell line S_2R^+ and identified a selective mitochondrial Ca^{2+}-dependent Ca^{2+} release channel displaying features intermediate between the mammalian PTP and the pore of yeast. The results of this study are illustrated in **Publication 1** and the conclusions are summarized in the final Section of this Thesis.

Publication 1

Supplemental Material can be found at:
http://www.jbc.org/content/suppl/2011/10/07/M111.268375.DC1.html

THE JOURNAL OF BIOLOGICAL CHEMISTRY VOL. 286, NO. 48, pp. 41163–41170, December 2, 2011

Properties of Ca^{2+} Transport in Mitochondria of *Drosophila melanogaster*[*S]

Received for publication, June 9, 2011, and in revised form, September 1, 2011 Published, JBC Papers in Press, October 7, 2011, DOI 10.1074/jbc.M111.268375

Sophia von Stockum[‡1], **Emy Basso**[‡], **Valeria Petronilli**[‡], **Patrizia Sabatelli**[§], **Michael A. Forte**[¶], **and Paolo Bernardi**[‡2]

From the [‡]*Consiglio Nazionale delle Ricerche Institute of Neuroscience and Department of Biomedical Sciences, University of I-35121 Padova, Italy and* [§]*Institute of Molecular Genetics at the Istituto Ortopedico Rizzoli, I-40126 Bologna, Italy, and the* [¶]*Vollum Institute, Oregon Health & Sciences University, Portland, Oregon 97239*

Background: We have studied the properties of Ca^{2+} transport in *Drosophila* mitochondria.
Results: *Drosophila* mitochondria possess Ca^{2+} transport systems matching their mammalian equivalents but have a unique selective Ca^{2+} release channel that does not mediate swelling.
Conclusion: The *Drosophila* Ca^{2+} release channel is involved in Ca^{2+} homeostasis rather than cell death.
Significance: This channel may represent the missing link between the permeability transition pore of yeast and mammals.

We have studied the pathways for Ca^{2+} transport in mitochondria of the fruit fly *Drosophila melanogaster*. We demonstrate the presence of ruthenium red (RR)-sensitive Ca^{2+} uptake, of RR-insensitive Ca^{2+} release, and of Na^+-stimulated Ca^{2+} release in energized mitochondria, which match well characterized Ca^{2+} transport pathways of mammalian mitochondria. Following larger matrix Ca^{2+} loading *Drosophila* mitochondria underwent spontaneous RR-insensitive Ca^{2+} release, an event that in mammals is due to opening of the permeability transition pore (PTP). Like the PTP of mammals, *Drosophila* Ca^{2+}-induced Ca^{2+} release could be triggered by uncoupler, diamide, and *N*-ethylmaleimide, indicating the existence of regulatory voltage- and redox-sensitive sites and was inhibited by tetracaine. Unlike PTP-mediated Ca^{2+} release in mammals, however, it was (i) insensitive to cyclosporin A, ubiquinone 0, and ADP; (ii) inhibited by P_i, as is the PTP of yeast mitochondria; and (iii) not accompanied by matrix swelling and cytochrome *c* release even in KCl-based medium. We conclude that *Drosophila* mitochondria possess a selective Ca^{2+} release channel with features intermediate between the PTP of yeast and mammals.

Mitochondria play a pivotal role in cellular Ca^{2+} homeostasis and thereby participate in the orchestration of a diverse range of cellular activities. Indeed, the mitochondrial proton electrochemical gradient is used not only to synthesize ATP but also to accumulate cations into the mitochondrial matrix (1–4). Consequently, when local cytoplasmic free Ca^{2+} levels rise, mitochondria rapidly accumulate cytoplasmic Ca^{2+} and then gradually release it as normal cytoplasmic levels are restored, amplifying and sustaining signals arising from elevation of cytoplasmic Ca^{2+}, as well as protecting cells and neurons against transient elevation in intracellular Ca^{2+} during periods of hyperactivity (1, 5, 6). As a result, the mechanisms controlling cellular and mitochondrial Ca^{2+} homeostasis, metabolism, and bioenergetics must function as a tightly integrated system within the overall cellular Ca^{2+} homeostatic network (2, 7–9).

The pathways responsible for mitochondrial Ca^{2+} uptake and release have been intensely studied on a functional level for >50 years. In energized mitochondria, the Ca^{2+} uniporter mediates Ca^{2+} uptake across the inner mitochondrial membrane, whereas exchangers (Ca^{2+} for Na^+ and/or H^+) are responsible for Ca^{2+} efflux (9–13). However, when the mitochondrial Ca^{2+} load exceeds the capacity of inner membrane exchangers, an additional pathway for Ca^{2+} efflux from mitochondria may exist through opening of the permeability transition pore (PTP).[3]

The mitochondrial permeability transition (PT) describes a process of Ca^{2+}-dependent, tightly regulated increase in the permeability of the inner mitochondrial membrane due to the opening of a high-conductance channel, the PTP (10). PTP opening causes collapse of the mitochondrial membrane potential ($\Delta\psi$) and Ca^{2+} release through the pore itself, an event that for short "open" times may indeed be involved in physiological Ca^{2+} homeostasis (14, 15), as recently shown in mouse hearts (16) and adult neurons (17) consistent with a role of the PTP in cell signaling (18). Prolonged opening of the PTP, on the other hand, causes stable depolarization, loss of ionic homeostasis, depletion of pyridine nucleotides, respiratory inhibition, matrix swelling, release of cytochrome *c*, and cell death via apoptosis or necrosis depending on a variety of additional factors, among which cellular ATP and Ca^{2+} levels play a major role (19).

* This work was supported, in whole or in part, by National Institutes of Health Grant GM069883. This work was also supported in part by grants from the Fondazione Cariparo and the University of Padova Progetti di Eccellenza Models of Mitochondrial Diseases.
[S] The on-line version of this article (available at http://www.jbc.org) contains supplemental Figs. 1–3.
[1] This work was submitted to partially fulfill the requirements for a PhD in Cell Biology at the University of Padova.
[2] To whom correspondence should be addressed: Dept. of Biomedical Sciences, University of Padova, Viale Giuseppe Colombo 3, I-35121 Padova, Italy. Fax: 39-049-827-6361; E-mail: bernardi@bio.unipd.it.

[3] The abbreviations used are: PTP, permeability transition pore; CRC, Ca^{2+} retention capacity; $\Delta\psi$, inner membrane potential difference; FCCP, carbonylcyanide-*p*-trifluoromethoxyphenylhydrazone; NEM, *N*-ethylmaleimide; OMM, outer mitochondrial membrane; RR, ruthenium red; TMRM, tetramethylrhodamine methyl ester.

Together with matrix Ca^{2+}, P_i is an essential inducer of PTP opening in mammals (19), whereas P_i exerts an inhibitory action on the yeast permeability pathways triggered by ATP and energization (20–24; see Ref. 25 for a recent review). In mammals, the PTP can be desensitized by submicromolar concentrations of the immunosuppressant drug cyclosporin A (26–28) via an interaction with its matrix receptor cyclophilin D (29). Our recent discovery that the inhibitory effect of cyclosporin A and of cyclophilin D ablation on the pore requires P_i (30) opens new scenarios. Indeed, this observation may bridge the gap between the pore of yeast and mammals, which we have hypothesized to be much closer than previously thought (31; see Ref. 32 for a review of earlier literature).

Despite its importance as a model organism, the characteristics of mitochondrial Ca^{2+} transport have been little studied in *Drosophila melanogaster*. The present study demonstrates that *Drosophila* mitochondria possess Ca^{2+} transport systems that are very close to those of mammals and that they can undergo a ruthenium red (RR)-insensitive Ca^{2+}-induced Ca^{2+} release through a selective channel that is insensitive to cyclosporin A and inhibited by P_i, and whose general features may be intermediate between the properties of the PTP of yeast and that of mammals.

EXPERIMENTAL PROCEDURES

Cell Cultures—S_2R^+ cells (33) were cultured in Schneider's insect medium supplemented with 10% heat-inactivated FBS and kept in 75-cm^2 T flasks or in tissue culture dishes (245 × 245 × 25 mm) at 25 °C.

Cell Permeabilization—Cells were detached with a sterile cell scraper, centrifuged at 200 × *g* for 10 min, and washed twice with Dulbecco's PBS without Ca^{2+} and Mg^{2+}, pH 7.4 (Euroclone). The resulting pellet was resuspended in 130 mM KCl, 10 mM MOPS-Tris, pH 7.4 (KCl medium), containing 150 μM digitonin and 1 mM EGTA-Tris and incubated for 20 min on ice (6×10^7 cells × ml^{-1}). Cells were then diluted 1:5 in KCl medium containing 10 μM EGTA-Tris and centrifuged at 200 × *g* in a refrigerated centrifuge (4 °C) for 6 min. The final pellet was resuspended in KCl medium containing 10 μM EGTA-Tris at 4×10^8 cells × ml^{-1} and kept on ice.

Fluorescent Staining of S_2R^+ Cell Mitochondria—In the experiments of Fig. 1*A* energization of mitochondria in both intact and permeabilized S_2R^+ cells was analyzed based on accumulation of the potentiometric probe tetramethyl rhodamine methyl ester (TMRM, Molecular Probes). Three days before the experiments, cells were seeded onto sterilized 24-mm round glass coverslips at 2×10^6 cells per well in 2 ml of Schneider's medium supplemented with 10% FBS. On the day of experiment, cells were washed once with PBS and incubated for 20 min at room temperature with 1 ml of serum-free Schneider's medium supplemented with 1 μg/ml cyclosporin H and 10 nM TMRM. Cyclosporin H is an inhibitor of the plasma membrane multidrug resistance pumps and allows an appropriate loading with the probe by preventing its extrusion at the plasma membrane (34). Images were acquired with an Olympus IX71/IX51 inverted microscope equipped with a xenon light source (75 watts) for epifluorescence illumination and with a 12-bit digital cooled CCD camera (Micromax). For detection of TMRM fluorescence, 568 ± 25-nm bandpass excitation and 585-nm long pass emission filter settings were used.

In the experiments of Fig. 1*C*, mitochondrial membrane potential was measured using a Perkin-Elmer LS50B spectrofluorometer and evaluated based on the fluorescence quenching of Rhodamine 123. Two milliliters of 130 mM KCl, 10 mM MOPS-Tris, 5 mM Pi-Tris, 10 μM EGTA, 0.15 μM Rhodamine 123, pH 7.4, were added to the cuvette. The fluorescence of Rhodamine 123 was monitored at the excitation and emission wavelengths of 503 and 523 nm, respectively, with the slit width set at 2.5 nm. After a short incubation to reach stabilization of the signal, 2×10^7 permeabilized S_2R^+ cells were added to the cuvette. Further additions were as indicated in the figure legends.

Electron Microscopy—S_2R^+ cells were washed with PBS and fixed in 2.5% glutaraldehyde in 0.1 M potassium phosphate buffer, pH 7.4, for 2 h at 4 °C. After washing with 0.15 M potassium phosphate buffer, pH 7.0, cells were finally embedded in 2% gelatin as described previously (35). Gelatin-embedded samples were post-fixed with 1% osmium tetroxide in cacodylate buffer 0.1 M, pH 7.4, and embedded in Epon812 resin, sectioned, and stained following standard procedures (36). Ultrathin sections were observed with a Philips EM400 transmission electron microscope operating at 100 kV.

Mitochondrial Respiration—Rates of mitochondrial respiration were measured using a Clark-type oxygen electrode equipped with magnetic stirring and thermostatic control maintained at 25 °C, and additions were made through a syringe port in the frosted glass stopper sealing the chamber. Intact S_2R^+ cells were incubated in Hank's balanced salt solution supplemented with 10 mM glucose and 5 mM P_i-Tris, pH 7.4, whereas digitonin-permeabilized cells (see above) were incubated in 130 mM KCl, 10 mM MOPS-Tris, 5 mM P_i-Tris, 5 mM succinate-Tris, 10 μM EGTA, pH 7.4. In both cases, 2×10^7 cells in 2 ml were used, and further additions are specified in the figure legends.

Light Scattering and Mitochondrial Ca^{2+} Fluxes—Light scattering at 90° was monitored with a PerkinElmer LS50B spectrofluorimeter at 540 nm with a 5.5-nm slit width. Extramitochondrial Ca^{2+} was measured with Calcium Green 5N (Molecular Probes) using either the PerkinElmer LS50B spectrofluorometer equipped with magnetic stirring (excitation and emission wavelengths of 505 and 535 nm, respectively) or a Fluoroskan Ascent FL (Thermo Electron Corp.) equipped with a plate shaker (excitation and emission wavelengths of 485 and 538 nm, respectively with a 10-nm band pass filter). The incubation medium contained 130 mM KCl, 10 mM MOPS-Tris, 5 mM succinate-Tris, 10 μM EGTA, 2 μM rotenone, pH 7.4, and P_i-Tris as indicated in the figure legends. In the Ca^{2+} measurements, 0.5 μM Calcium-Green 5N was also added. Permeabilized cells (2×10^7 in a final volume of 2 ml in the PerkinElmer spectrofluorometer and 2×10^6 in a final volume of 0.2 ml in the Fluoroskan) were used. Further additions were made as indicated in the figure legends.

Western Blotting—Cell suspensions were centrifuged at 3000 × *g* at 4 °C. Proteins from the supernatants were precipitated in acetone at −20 °C and centrifuged for 30 min at

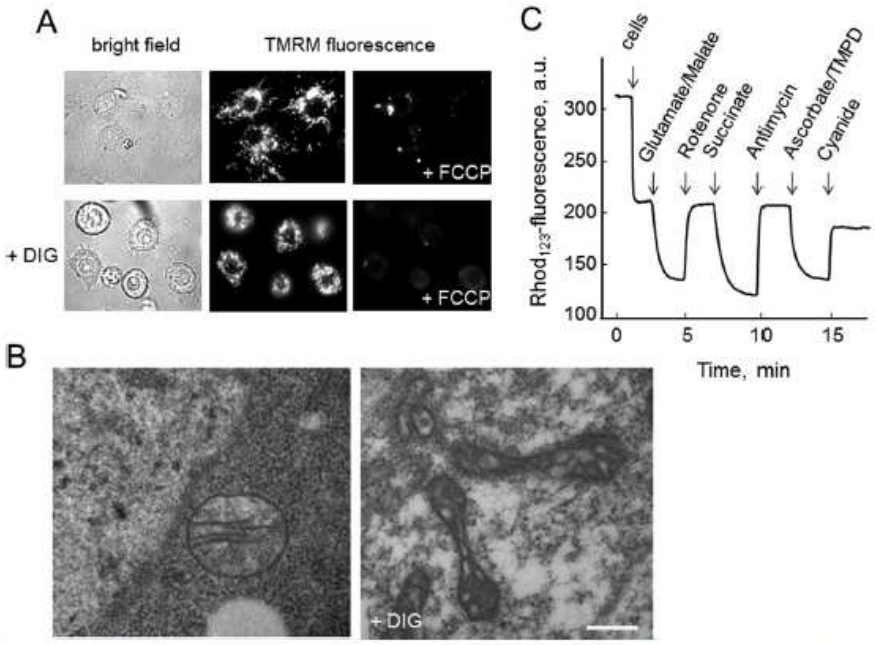

FIGURE 1. **Evaluation of mitochondrial energization and membrane potential in intact and permeabilized *Drosophila* S_2R^+ cells.** *A*, cells were seeded on glass coverslips, loaded with 10 nM TMRM as described under "Experimental Procedures," and observed under bright field conditions or for TMRM fluorescence before and after the addition of 4 μM FCCP either without further additions (*upper row*) or after permeabilization with 30 μM digitonin (+*DIG*, *lower row*). *B*, ultrastructural analysis of untreated (*left panel*) and digitonin-permeabilized (*right panel*, *DIG*) S_2R^+ cells; *bar*, 300 nm for both panels. *C*, cells were digitonized as described under "Experimental Procedures" and incubated in 130 mM KCl, 10 mM MOPS-Tris, 10 μM EGTA, and 0.15 μM Rhodamine 123 ($Rhod_{123}$), pH 7.4. Further additions were 5 mM glutamate-Tris plus 2.5 mM malate-Tris, 2 μM rotenone, 5 mM succinate-Tris, 0.1 μg/ml antimycin A, 5 mM ascorbate-Tris plus 100 μM tetramethyl-*p*-phenylene diamine (*TMPD*) and 2 mM KCN. *a.u.*, arbitrary units.

18,000 × *g* at 4 °C. Pellets were washed twice in 20% methanol and finally solubilized in Laemmli gel sample buffer. Cell pellets were lysed in a buffer containing 150 mM NaCl, 20 mM Tris, pH 7.4, 5 mM EDTA-Tris, 10% glycerol, 1% Triton X-100, and supplemented with protease and phosphatase inhibitor cocktails (Sigma), and kept on ice for 20 min. Suspensions were then centrifuged at 18,000 × *g* for 25 min at 4 °C to remove insoluble materials. The supernatants were solubilized in Laemmli gel sample buffer. Samples were separated by 15% SDS-PAGE and transferred electrophoretically to nitrocellulose membranes using a Mini Trans-Blot system (Bio-Rad). Western blotting was performed in PBS containing 3% nonfat dry milk with monoclonal mouse anti-cytochrome *c* (BD Biosciences), monoclonal mouse anti-OxPhos complex IV subunit I (Invitrogen), or rabbit polyclonal anti-TOM20 (Santa Cruz Biotechnology) antibodies.

Reagents and Statistics—All chemicals were of the highest purity commercially available. Reported results are typical of at least three replicates for each condition, and error bars refer to the S.D.

RESULTS

We initially isolated mitochondria from *Drosophila* flight muscles after dissection of the thoraces to prevent contamination from the yeast on which *Drosophila* feeds and that may be present in the abdomen. Despite our great efforts mitochondria were of poor quality, as judged from the respiratory control ratios (results not shown). An additional problem we encountered was that the low yield of these preparations did not allow a reproducible analysis of the Ca^{2+} transport properties of mitochondria. Thus, we characterized mitochondrial function in intact S_2R^+ *Drosophila* cells and then used digitonin permeabilization to access mitochondria *in situ*, an approach that we have successfully applied to mammalian cells (37) and to cells from 6-h-old embryos from *Danio rerio* (zebrafish) (38).

Mitochondria in both intact and permeabilized S_2R^+ cells were energized, as shown by fluorescence images after the addition of the potentiometric probe TMRM (Fig. 1*A*). Mitochondria appeared as bright bodies, and fluorescence was lost upon addition of an uncoupler (Fig. 1*A*). Ultrastructural analysis of intact S_2R^+ cells revealed round-shaped mitochondria with thin cristae aligned in parallel rows (Fig. 1*B*, *left panel* illustrates a typical example), which is strikingly similar to the morphology of mammalian mitochondria *in situ* and to the "orthodox" configuration of Hackenbrock (39). After digitonin treatment, most cells showed evidence of permeabilization as reflected by a change in the electron density of the cytoplasm and loss of chromatin definition (results not shown), but the overall morphology of organelles was retained (Fig. 1*B*, *right panel*). Mitochondria, however, now displayed a "condensed" configuration very similar to that of isolated mammalian mitochondria (39), which is characterized by an electron-dense matrix and evident and well preserved cristae and outer membrane (Fig. 1*B*, *right panel*).

Digitonin-permeabilized cells are accessible to substrates, and this allows the study of their response to energization. Mitochondria readily developed a membrane potential (as

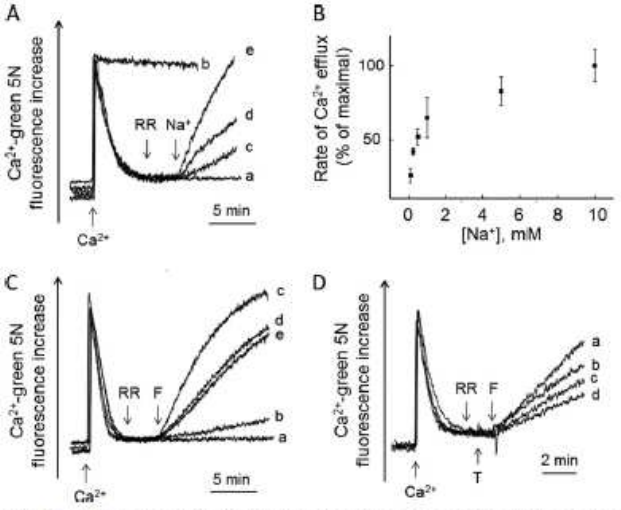

FIGURE 2. **Mitochondrial Ca^{2+} transport in permeabilized *Drosophila* S_2R^+ cells.** Digitonin-permeabilized S_2R^+ cells were incubated in 130 mM KCl, 10 mM MOPS-Tris, 5 mM P_i-Tris, 5 mM succinate-Tris, 10 μM EGTA, 2 μM rotenone, and 0.5 μM Calcium Green 5N, pH 7.4. *A*, in *trace b* only, the incubation medium was supplemented with 0.2 μM RR; where indicated, 25 μM Ca^{2+} with no further additions (*trace a*) or followed by 0.2 μM RR and by 0.1 mM (*trace c*), 1 mM (*trace d*), or 10 mM NaCl (*trace e*). *B*, rate of Na^+-induced Ca^{2+} release obtained in protocols such as those depicted in *A* as a function of the added Na^+ concentration; values were normalized to the rate observed after the addition of 10 mM NaCl (taken as maximal), and *error bars* report the S.D. of triplicate experiments. *C*, in *trace e* only, the medium was supplemented with 1 μg/ml cyclosporin A; where indicated, 25 μM Ca^{2+} was added followed by the addition of 0.2 μM RR and/or 0.5 μM FCCP where indicated by *arrows* as follows: no addition after the Ca^{2+} pulse (*a*), RR only (*b*), FCCP only (*c*), and RR and FCCP (*d* and *e*). *D*, where indicated, 25 μM Ca^{2+} pulse, 0.2 μM RR, 0.5 mM (*b*), 1 mM (*c*), or 2 mM (*d*) tetracaine and 0.5 μM FCCP. *Trace a* was obtained after the addition of RR and FCCP without tetracaine.

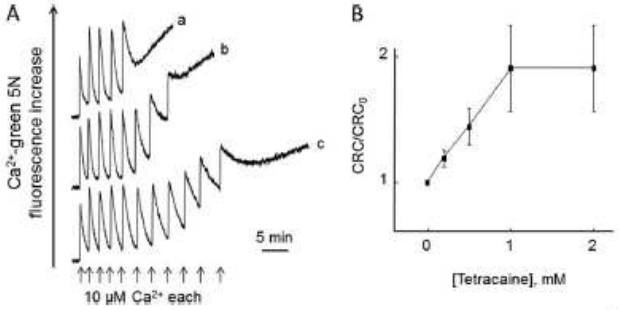

FIGURE 3. **Effect of tetracaine on CRC of permeabilized *Drosophila* S_2R^+ cells.** Experimental conditions were as described in the legend to Fig. 2, except that the concentration of P_i was 1 mM. *A*, extramitochondrial Ca^{2+} was monitored, and CRC was determined by stepwise addition of 10 μM Ca^{2+} pulses (*arrows*) in the absence of further additions (*trace a*) or in the presence of 0.5 or 1 mM tetracaine (*traces b* and *c*, respectively). *B*, The amount of Ca^{2+} accumulated prior to onset of Ca^{2+}-induced Ca^{2+} release in presence of the stated concentrations of tetracaine was normalized to that obtained in absence of tetracaine (CRC_0).

judged on the basis of fluorescence quenching of Rhodamine 123) upon addition of the complex I substrates glutamate and malate (Fig. 1*C*). The sequential addition of rotenone, succinate, antimycin A, ascorbate plus tetramethyl-*p*-phenylene diamine, and finally cyanide caused the expected repolarization-depolarization cycles that indicate functioning of all respiratory complexes (Fig. 1*C*).

Intact S_2R^+ cells displayed a good respiratory activity that was largely inhibited by oligomycin, indicating that a prevalent fraction of oxygen uptake was devoted to ATP synthesis. Basal respiration could be stimulated >5-fold by the addition of the uncoupler carbonyl cyanide *p*-trifluoromethoxyphenylhydrazone (FCCP), indicating a good reserve capacity of the respiratory chain (supplemental Fig. 1*A*). In addition, permeabilized cells displayed a good phosphorylation capacity after energization with succinate (supplemental Fig. 1*B*), and we used these conditions to study the properties of mitochondrial Ca^{2+} transport.

Energized mitochondria readily took up and retained a Ca^{2+} pulse of 25 μM (Fig. 2*A*, *trace a*), in a process that was fully inhibited by pretreatment with RR (Fig. 2*A*, *trace b*), the inhibitor of the mitochondrial Ca^{2+} uniporter (40, 41) in mammals (42–44). After accumulation of Ca^{2+} and addition of RR, Ca^{2+} efflux could be stimulated by Na^+ (Fig. 2*A*, *traces c–e*) in the range 0.1–10 mM, with a concentration dependence (Fig. 2*B*) that is very similar to the Na^+-Ca^{2+} antiporter of mammalian mitochondria (45–48), recently identified as NCLX (49).

Addition of RR alone after Ca^{2+} uptake was followed by a slow process of Ca^{2+} release (Fig. 2*C*, *trace b*), which suggests the existence of a Na^+-insensitive Ca^{2+} release pathway as also found in mammalian mitochondria (10). Addition of FCCP after accumulation of Ca^{2+} caused a fast process of Ca^{2+} release (Fig. 2*C*, *trace c*), which was only partly inhibited by RR (Fig. 2*C*, *trace d*) without any additional inhibitory effect of cyclosporin A (Fig. 2*C*, *trace e*). These experiments suggest the presence of a voltage-dependent Ca^{2+} release pathway (the RR-insensitive fraction of FCCP-induced Ca^{2+} release) resembling the PTP of mammalian mitochondria except for its lack of sensitivity to cyclosporin A (50, 51). We screened additional compounds for potential inhibition of RR-insensitive, FCCP-induced Ca^{2+} release, and we found a concentration-dependent inhibition by tetracaine (Fig. 2*D*, *traces b–d*), which also inhibits the PTP of mammalian mitochondria (52, 53).

We next studied the Ca^{2+} retention capacity (CRC) of *Drosophila* mitochondria by adding a train of Ca^{2+} pulses to permeabilized cells (Fig. 3). Ca^{2+} uptake was followed by spontaneous Ca^{2+} release (Fig. 3*A*, *trace a*), which was accompanied by mitochondrial depolarization (results not shown) and delayed by tetracaine (Fig. 3*A*, *traces b* and *c*), which considerably increased the CRC (Fig. 3*B*). Note that the rate of Ca^{2+} uptake was not affected by tetracaine, indicating that the Ca^{2+} uniporter is not inhibited by this drug.

The CRC was strikingly affected by P_i, in the sense that the threshold Ca^{2+} load required for onset of Ca^{2+} release increased at increasing concentrations of P_i (Fig. 4). The rate of spontaneous Ca^{2+} release decreased at increased P_i concentrations despite the larger matrix Ca^{2+} load (Fig. 4*A*). The half-maximal effect of P_i was seen at ~1 mM, which is similar to that required for inhibition by P_i of the PTP of yeast (23, 54) and of the PTP of mammals in cyclophilin D null mitochondria and in wild-type mitochondria treated with cyclosporin A (30).

We also tested the effect on the CRC of Ub0, a cyclophilin D-independent inhibitor of the mammalian pore (55, 56) and of the combination of ADP plus oligomycin, which is very effective at desensitizing the PTP to Ca^{2+} (57). No changes of CRC were observed with any of these PTP inhibitors, irrespective of whether the P_i concentration was 1 or 5 mM (supplemental Fig. 2).

Mitochondrial Ca^{2+}-induced Ca^{2+} release could be induced by the dithiol oxidant diamide (Fig. 5*A*) in a process that was prevented by dithiothreitol (Fig. 5*B*). Ca^{2+} release could also be induced by *N*-ethylmaleimide (NEM) (Fig. 6) after a lag phase that decreased as the concentration of NEM was increased (Fig. 6*B*) in the same range causing PTP opening in mammalian mitochondria (58).

We assessed mitochondrial volume changes in mitochondria subjected to an appropriate Ca^{2+} load sufficient to cause spontaneous Ca^{2+} release at 0.1 mM P_i. Parallel readings of Ca^{2+} fluxes (Fig. 7*A*) and of light scattering at 540 nm (a sensitive measure of mitochondrial volume changes, Fig. 7*B*) revealed that after the small light scattering increase (matrix volume contraction) accompanying Ca^{2+} uptake no matrix swelling (which should manifest itself as a decreased light scattering) could be detected after the onset of Ca^{2+} release (Fig. 7*B*). It should be noted that mitochondria in permeabilized S_2R^+ cells can undergo swelling upon addition of the pore-forming peptide alamethicin, which also caused rapid release of residual matrix Ca^{2+} (Fig. 7), or of the selective K^+ ionophore valinomycin (supplemental Fig. 3). Mitochondrial Ca^{2+}-dependent Ca^{2+} release was not accompanied by cytochrome *c* release, which was instead readily elicited by the addition of alamethicin (Fig. 7*C*). This result is particularly striking because our experiments were carried out in KCl-based medium, which promotes ready cytochrome *c* removal if the outer membrane breaks following osmotic swelling of mammalian mitochondria (59). Electron microscopy fully confirmed that the condensed mitochondrial morphology was totally unaffected by a load of Ca^{2+} able to induce full Ca^{2+} release (compare the *left* and *middle panels* of Fig. 7*D*). This is a unique feature compared with the swelling response of mitochondria from all sources tested so far under similar conditions (19). On the other hand, mitochondrial swelling was readily detected after the addition of alamethicin (Fig. 7*D*, *right panel*).

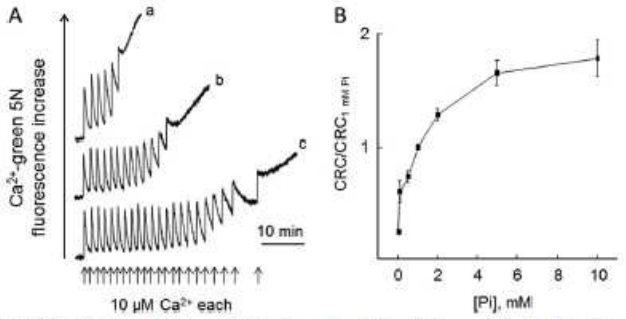

FIGURE 4. **Effect of P_i on CRC of permeabilized *Drosophila* S_2R^+ cells.** Experimental conditions were as described in the legend to Fig. 2, except that the concentration of P_i in *A* was 0.1, 1, or 5 mM (*traces a*, *b*, and *c*, respectively) or as indicated on the *abscissa* in *B*, where the CRC was normalized to the one obtained in the presence of 1 mM P_i ($CRC_{1\ mM\ Pi}$).

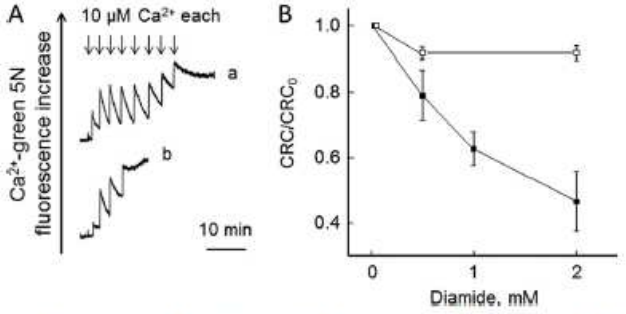

FIGURE 5. **Effect of diamide on CRC of permeabilized *Drosophila* S_2R^+ cells.** Experimental conditions were as in Fig. 2, except that the concentration of P_i was 1 mM. *A*, where indicated, 10 μM Ca^{2+} pulses (*arrows*) were added in the absence (*trace a*) or presence of 2 mM diamide (*trace b*). *B*, the CRC in presence of the stated concentrations of diamide alone (*closed symbols*) or after treatment with 1 mM dithiothreitol 1 min after diamide (*open symbols*) was normalized to that obtained in absence of diamide (CRC_0).

DISCUSSION

In this work, we have characterized the pathways for Ca^{2+} transport in mitochondria from digitonin-permeabilized *Drosophila* S_2R^+ cells. These cells were originally derived from late embryonic stages (20–24 h), and selection was made based on the ability to adhere to tissue culture dishes (60). According to Schneider (60), they represent a variety of tissue precursors, and we assume that they are representative of *Drosophila*, although a full characterization of the Ca^{2+} release channel will have to await its molecular definition.

We have found that mitochondria of S_2R^+ cells possess the classical pathways found in mammalian mitochondria, *i.e.* (i) the RR-sensitive Ca^{2+} uniporter, which has been characterized by electrophysiology (12) and recently identified at the molecular level in mammals (40, 41). The existence in the *Drosophila*

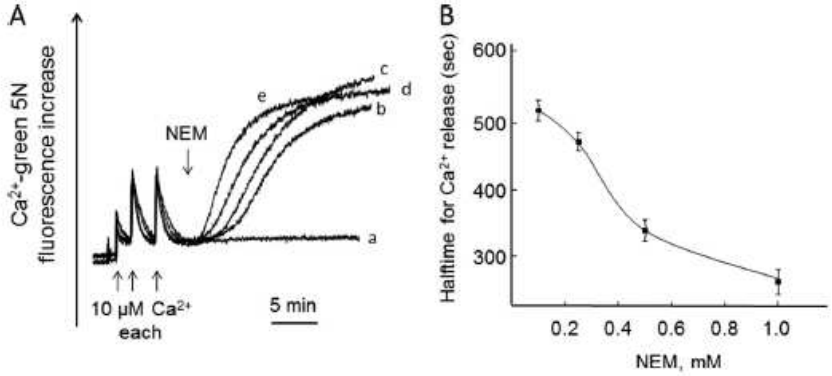

FIGURE 6. **Effect of NEM on Ca^{2+} retention of permeabilized *Drosophila* S_2R^+ cells.** Experimental conditions were as in Fig. 5. *A*, three 10 μM Ca^{2+} pulses were added followed by 0.05 (*trace a*), 0.1 (*trace b*), 0.25 (*trace c*), 0.5 (*trace d*), or 1 mM NEM (*trace e*). *B*, half-time required for Ca^{2+} release was calculated for experiments like those depicted in *A*.

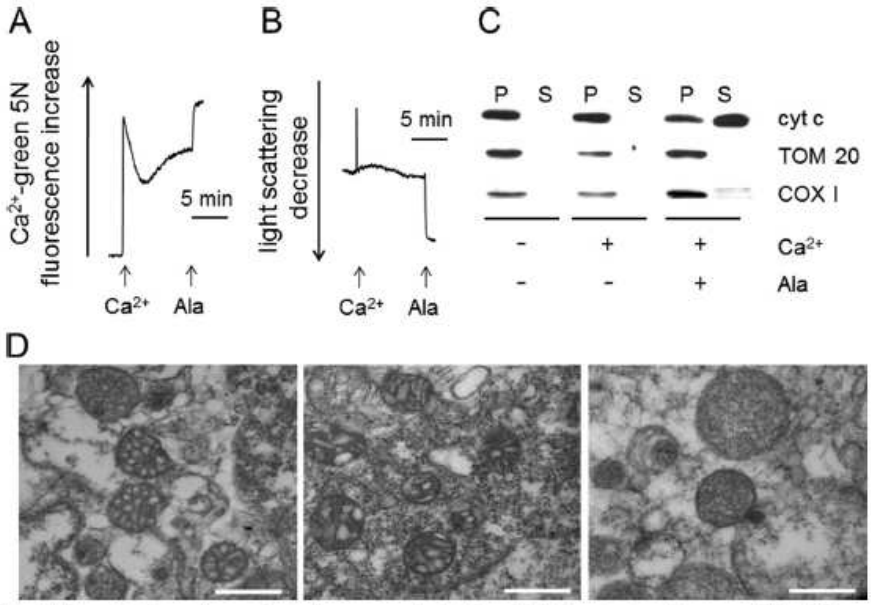

FIGURE 7. **Effect of Ca^{2+} on light scattering, release of cytochrome *c* and mitochondrial ultrastructure in permeabilized *Drosophila* S_2R^+ cells.** Experimental conditions were as described in the legend to Fig. 2, except that the concentration of P_i was 0.1 mM and calcium Green 5N was omitted in the experiments of *B*. *A* and *B*, where indicated, 40 μM Ca^{2+} and 3 μM alamethicin were added. *C*, permeabilized cells were centrifuged before the addition of Ca^{2+}, after addition of 40 μM Ca^{2+} or after addition of 40 μM Ca^{2+} and 3 μM alamethicin (as indicated by + and − symbols); pellets (*P*) and supernatants (*S*) were subjected to SDS-PAGE, transfer, and subsequent Western blotting with specific antibodies against cytochrome (*cyt*) *c*, TOM 20, and cytochrome oxidase (*COX*) subunit I. *D*, permeabilized cells were fixed and processed for electron microscopy before the addition of Ca^{2+} (*left panel*), after addition of 40 μM Ca^{2+} (*middle panel*) or after addition of 40 μM Ca^{2+} and 3 μM alamethicin (*right panel*); *bar*, 200 nm.

genome of close orthologs of the mitochondrial Ca^{2+} uniporter (40, 41) and of the previously identified MICU1 (61) (CG18769 and CG4495, respectively) predicts the existence of a mitochondrial Ca^{2+} uniporter in keeping with our findings. (ii) The Na^+-Ca^{2+} antiporter recently identified as NCLX (49), whose ortholog also exists in *Drosophila* (CG14744) and is the likely mediator of the Na^+-dependent Ca^{2+} release defined here. (iii) The putative H^+-Ca^{2+} antiporter mediating Ca^{2+} release at high membrane potential, which can be unmasked by the addition of RR (10). Notably, it recently has been proposed that LETM1 (and its *Drosophila* ortholog CG4589) mediates H^+-Ca^{2+} exchange by catalyzing RR-sensitive Ca^{2+} uptake in mitochondria (62). However, this contrasts with the well established role of LETM1 as a K^+-H^+ antiporter (63–66) and with the fact, confirmed here, that the putative H^+-Ca^{2+} antiporter is insensitive to RR. (iv) A tetracaine-sensitive, RR-insensitive release pathway that opens in response to matrix Ca^{2+} loading or to depolarization and mediates Ca^{2+} release. The tetracaine-sensitive pathway, which displays unique features that appear to be intermediate between those of the PTP of yeast and mammals (31), is the main focus of the present manuscript.

Disequilibrium between Distribution of Ca^{2+} and Its Electrochemical Gradient—Ca^{2+} uptake is an electrophoretic process driven by the Ca^{2+} electrochemical gradient, $\Delta\tilde{\mu}Ca$.

$$\Delta\tilde{\mu}Ca = zF\Delta\psi + RT\ln[Ca^{2+}]_i/[Ca^{2+}]_o \qquad \text{(Eq. 1)}$$

In respiring mitochondria, the inside-negative $\Delta\psi$ favors uptake of Ca^{2+} (67, 68); and with a $\Delta\psi$ of −180 mV, the Ca^{2+} accumulation ratio at equilibrium (*i.e.* at $\Delta\tilde{\mu}Ca = 0$) should be 10^6 (69). This is never reached because at resting cytosolic Ca^{2+} levels, the rate of Ca^{2+} uptake is comparable with that of the efflux pathways, and Ca^{2+} distribution is governed by a kinetic steady state rather than by the thermodynamic equilibrium (69, 70). The activity of the mitochondrial Ca^{2+} uniporter and of the antiporters indeed creates a Ca^{2+} cycle across the inner membrane, whose energy requirement is very low (71) because the combined maximal rate of the efflux pathways is ~20 nmol $Ca^{2+} \times mg^{-1}$ protein $\times$ min^{-1} (10). On the other hand, because the V_{max} of the uniporter is ~1400 nmol $Ca^{2+} \times mg^{-1}$ protein $\times$ min^{-1}, and its activity increases sharply with the increase of extramitochondrial [Ca^{2+}] (72), this arrangement exposes mitochondria to the hazards of Ca^{2+} overload when cytosolic [Ca^{2+}] increases. We have argued that the PTP may serve the purpose of providing mitochondria with a fast Ca^{2+} release channel (10, 14). This hypothesis is consistent with the effects of cyclosporin A on Ca^{2+} distribution in rat ventricular cardiomyocytes (73), with a PTP activating response to the combined action of two physiological stimuli increasing cytosolic [Ca^{2+}] without detrimental effects on cell survival (17), and with the demonstration that cyclophilin D ablation causes mitochondrial Ca^{2+} overload *in vivo*, which, in turn, increases the propensity to heart failure after transaortic constriction, overexpression of Ca^{2+}/calmodulin-dependent protein kinase IIδc or swimming exercise (16; see Ref. 75 for discussion).

Properties of Drosophila Ca^{2+}-induced Ca^{2+} Release—The properties of the *Drosophila* Ca^{2+} release system described here appear to be intermediate between those of the PTP of mammals and yeast. Like the mammalian pore, *Drosophila* Ca^{2+} release is inhibited by tetracaine (52) and opens in response to matrix Ca^{2+} loading (76), inner membrane depo-

larization (77), thiol oxidation (78), and treatment with relatively high concentrations of NEM (58); like the yeast PTP (and at variance from the mammalian pore), it is inhibited by P_i (22, 23) and insensitive to cyclosporin A (23). The latter observations may be strictly related. P_i is a classical inducer of the mammalian PTP, yet P_i is essential for PTP inhibition by cyclosporin A and cyclophilin D ablation (30), suggesting that cyclophilin D masks an inhibitory site for P_i (79). It is interesting to note that a *Drosophila* mitochondrial cyclophilin has not been found and that even *Drosophila* Cyp1-PA, which according to the primary sequence, has a high probability of import into mitochondria, could not be found in the organelle after tagging with GFP and expression in S_2R^+ and KC cells.[4] It is tempting to speculate that lack of mitochondrial cyclophilin leaves the P_i inhibitory site unhindered and that the PTP-stimulating ability of P_i has developed after the evolutionary divergence of *Drosophila* and vertebrates.

At the onset of Ca^{2+}-dependent Ca^{2+} release, *Drosophila* mitochondria undergo depolarization, suggesting that the putative channel is also permeable to H^+. On the other hand, no matrix swelling is observed in KCl-based medium, indicating that the channel is not permeable to K^+ (and Cl^-), despite the fact that the hydrated radius of Ca^{2+} is larger than that of K^+. Lack of swelling, which was confirmed by lack of cytochrome *c* release and by ultrastructural analysis, is not due to peculiar features of *Drosophila* mitochondria because matrix swelling and cytochrome *c* release readily followed the addition of the K^+ ionophore valinomycin or of the pore-forming peptide alamethicin. We conclude that the putative Ca^{2+} release channel of *Drosophila* mitochondria is also permeable to H^+. This is an essential feature because the Ca^{2+} diffusion potential created by efflux through a Ca^{2+}-selective channel would otherwise oppose Ca^{2+} release (10).

Mitochondrial Ca^{2+}-dependent Ca^{2+} Release as Mediator of Cell Death in Drosophila?—Available evidence points to persistent activation of the PTP as a prime mediator of apoptotic or necrotic cell death in a variety of situations (19). Indeed, unregulated opening of the PTP and ensuing mitochondrial and cellular dysfunction may be responsible for the pathology that characterizes a variety of human diseases (19). Although many of the proteins important for apoptosis in mammalian cells are conserved in *Drosophila*, the role that mitochondria play in cell death in this organism remains controversial (74, 80). The apparent absence of a regulatory role for a mitochondrial cyclophilin in the function of the "*Drosophila* PTP" prevents an investigation based on the effects of cyclosporin A in cells. However, our functional studies pave the way for the application of the sophisticated genetic strategies available in *Drosophila* to define the molecular nature of the channel and its role in pathophysiology of Ca^{2+} homeostasis.

REFERENCES

1. Friel, D. D. (2000) *Cell Calcium* **28,** 307–316
2. Giacomello, M., Drago, I., Pizzo, P., and Pozzan, T. (2007) *Cell Death Differ.* **14,** 1267–1274
3. Csordás, G., and Hajnóczky, G. (2009) *Biochim. Biophys. Acta* **1787,** 1352–1362
4. Rizzuto, R., Marchi, S., Bonora, M., Aguiari, P., Bononi, A., De Stefani, D., Giorgi, C., Leo, S., Rimessi, A., Siviero, R., Zecchini, E., and Pinton, P. (2009) *Biochim. Biophys. Acta* **1787,** 1342–1351
5. Kann, O., and Kovács, R. (2007) *Am. J. Physiol. Cell Physiol.* **292,** C641–657
6. Nicholls, D. G. (2009) *Biochim. Biophys. Acta* **1787,** 1416–1424
7. Rizzuto, R., Bernardi, P., and Pozzan, T. (2000) *J. Physiol. Lond.* **529,** 37–47
8. Rizzuto, R., and Pozzan, T. (2003) *Nat. Genet.* **34,** 135–141
9. Szabadkai, G., and Duchen, M. R. (2008) *Physiology* **23,** 84–94
10. Bernardi, P. (1999) *Physiol. Rev.* **79,** 1127–1155
11. Gunter, T. E., and Gunter, K. K. (2001) *IUBMB Life* **52,** 197–204
12. Kirichok, Y., Krapivinsky, G., and Clapham, D. E. (2004) *Nature* **427,** 360–364
13. Gunter, T. E., and Sheu, S. S. (2009) *Biochim. Biophys. Acta* **1787,** 1291–1308
14. Bernardi, P., and Petronilli, V. (1996) *J. Bioenerg. Biomembr.* **28,** 131–138
15. Ichas, F., Jouaville, L. S., and Mazat, J. P. (1997) *Cell* **89,** 1145–1153
16. Elrod, J. W., Wong, R., Mishra, S., Vagnozzi, R. J., Sakthievel, B., Goonasekera, S. A., Karch, J., Gabel, S., Farber, J., Force, T., Brown, J. H., Murphy, E., and Molkentin, J. D. (2010) *J. Clin. Invest.* **120,** 3680–3687
17. Barsukova, A., Komarov, A., Hajnóczky, G., Bernardi, P., Bourdette, D., and Forte, M. (2011) *Eur. J. Neurosci.* **33,** 831–842
18. Rasola, A., Sciacovelli, M., Pantic, B., and Bernardi, P. (2010) *FEBS Lett.* **584,** 1989–1996
19. Bernardi, P., Krauskopf, A., Basso, E., Petronilli, V., Blachly-Dyson, E., Di Lisa, F., and Forte, M. A. (2006) *FEBS J.* **273,** 2077–2099
20. Prieto, S., Bouillaud, F., Ricquier, D., and Rial, E. (1992) *Eur. J. Biochem.* **208,** 487–491
21. Guérin, B., Bunoust, O., Rouqueys, V., and Rigoulet, M. (1994) *J. Biol. Chem.* **269,** 25406–25410
22. Prieto, S., Bouillaud, F., and Rial, E. (1996) *Arch. Biochem. Biophys.* **334,** 43–49
23. Jung, D. W., Bradshaw, P. C., and Pfeiffer, D. R. (1997) *J. Biol. Chem.* **272,** 21104–21112
24. Roucou, X., Manon, S., and Guérin, M. (1997) *Biochim. Biophys. Acta* **1324,** 120–132
25. Uribe-Carvajal, S., Luévano-Martínez, L. A., Guerrero-Castillo, S., Cabrera-Orefice, A., Corona-de-la-Peña, N. A., and Gutiérrez-Aguilar, M. (2011) *Mitochondrion* **11,** 382–390
26. Fournier, N., Ducet, G., and Crevat, A. (1987) *J. Bioenerg. Biomembr.* **19,** 297–303
27. Crompton, M., Ellinger, H., and Costi, A. (1988) *Biochem. J.* **255,** 357–360
28. Broekemeier, K. M., Klocek, C. K., and Pfeiffer, D. R. (1998) *Biochemistry* **37,** 13059–13065
29. Halestrap, A. P., and Davidson, A. M. (1990) *Biochem. J.* **268,** 153–160
30. Basso, E., Petronilli, V., Forte, M. A., and Bernardi, P. (2008) *J. Biol. Chem.* **283,** 26307–26311
31. Azzolin, L., von Stockum, S., Basso, E., Petronilli, V., Forte, M. A., and Bernardi, P. (2010) *FEBS Lett.* **584,** 2504–2509
32. Manon, S., Roucou, X., Guérin, M., Rigoulet, M., and Guérin, B. (1998) *J. Bioenerg. Biomembr.* **30,** 419–429
33. Yanagawa, S., Lee, J. S., and Ishimoto, A. (1998) *J. Biol. Chem.* **273,** 32353–32359
34. Bernardi, P., Scorrano, L., Colonna, R., Petronilli, V., and Di Lisa, F. (1999) *Eur. J. Biochem.* **264,** 687–701
35. Taupin, P. (2008) *Eur. J. Histochem.* **52,** 135–139
36. Angelin, A., Tiepolo, T., Sabatelli, P., Grumati, P., Bergamin, N., Golfieri, C., Mattioli, E., Gualandi, F., Ferlini, A., Merlini, L., Maraldi, N. M., Bonaldo, P., and Bernardi, P. (2007) *Proc. Natl. Acad. Sci. U.S.A.* **104,** 991–996
37. Chiara, F., Castellaro, D., Marin, O., Petronilli, V., Brusilow, W. S., Juhaszova, M., Sollott, S. J., Forte, M., Bernardi, P., and Rasola, A. (2008) *PLoS One* **3,** e1852
38. Azzolin, L., Basso, E., Argenton, F., and Bernardi, P. (2010) *Biochim. Biophys. Acta* **1797,** 1775–1779
39. Hackenbrock, C. R. (1966) *J. Cell Biol.* **30,** 269–297
40. De Stefani, D., Raffaello, A., Teardo, E., Szabó, I., and Rizzuto, R. (2011) *Nature* **476,** 336–340

[4] K. R. Jones and M. A. Forte, unpublished results.

Mitochondrial Ca^{2+} Transport in Drosophila

41. Baughman, J. M., Perocchi, F., Girgis, H. S., Plovanich, M., Belcher-Timme, C. A., Sancak, Y., Bao, X. R., Strittmatter, L., Goldberger, O., Bogorad, R. L., Koteliansky, V., and Mootha, V. K. (2011) *Nature* **476,** 341–345
42. Moore, C. L. (1971) *Biochem. Biophys. Res. Commun.* **42,** 298–305
43. Carafoli, E., and Sacktor, B. (1972) *Biochem. Biophys. Res. Commun.* **49,** 1498–1503
44. Vasington, F. D., Gazzotti, P., Tiozzo, R., and Carafoli, E. (1972) *Biochim. Biophys. Acta* **256,** 43–54
45. Carafoli, E., Tiozzo, R., Lugli, G., Crovetti, F., and Kratzing, C. (1974) *J. Mol. Cell Cardiol.* **6,** 361–371
46. Crompton, M., Capano, M., and Carafoli, E. (1976) *Eur. J. Biochem.* **69,** 453–462
47. Crompton, M., Künzi, M., and Carafoli, E. (1977) *Eur. J. Biochem.* **79,** 549–558
48. Crompton, M., Moser, R., Lüdi, H., and Carafoli, E. (1978) *Eur. J. Biochem.* **82,** 25–31
49. Palty, R., Silverman, W. F., Hershfinkel, M., Caporale, T., Sensi, S. L., Parnis, J., Nolte, C., Fishman, D., Shoshan-Barmatz, V., Herrmann, S., Khananshvili, D., and Sekler, I. (2010) *Proc. Natl. Acad. Sci. U.S.A.* **107,** 436–441
50. Broekemeier, K. M., Dempsey, M. E., and Pfeiffer, D. R. (1989) *J. Biol. Chem.* **264,** 7826–7830
51. Petronilli, V., Cola, C., and Bernardi, P. (1993) *J. Biol. Chem.* **268,** 1011–1016
52. Dawson, A. P., Selwyn, M. J., and Fulton, D. V. (1979) *Nature* **277,** 484–486
53. Broekemeier, K. M., Schmid, P. C., Schmid, H. H., and Pfeiffer, D. R. (1985) *J. Biol. Chem.* **260,** 105–113
54. Yamada, A., Yamamoto, T., Yoshimura, Y., Gouda, S., Kawashima, S., Yamazaki, N., Yamashita, K., Kataoka, M., Nagata, T., Terada, H., Pfeiffer, D. R., and Shinohara, Y. (2009) *Biochim. Biophys. Acta* **1787,** 1486–1491
55. Cesura, A. M., Pinard, E., Schubenel, R., Goetschy, V., Friedlein, A., Langen, H., Polcic, P., Forte, M. A., Bernardi, P., and Kemp, J. A. (2003) *J. Biol. Chem.* **278,** 49812–49818
56. Krauskopf, A., Eriksson, O., Craigen, W. J., Forte, M. A., and Bernardi, P. (2006) *Biochim. Biophys. Acta* **1757,** 590–595
57. Novgorodov, S. A., Gudz, T. I., Milgrom, Y. M., and Brierley, G. P. (1992) *J. Biol. Chem.* **267,** 16274–16282
58. Pfeiffer, D. R., Schmid, P. C., Beatrice, M. C., and Schmid, H. H. (1979) *J. Biol. Chem.* **254,** 11485–11494
59. Jacobs, E. E., and Sanadi, D. R. (1960) *J. Biol. Chem.* **235,** 531–534
60. Schneider, I. (1972) *J. Embryol. Exp. Morphol.* **27,** 353–365
61. Perocchi, F., Gohil, V. M., Girgis, H. S., Bao, X. R., McCombs, J. E., Palmer, A. E., and Mootha, V. K. (2010) *Nature* **467,** 291–296
62. Jiang, D., Zhao, L., and Clapham, D. E. (2009) *Science* **326,** 144–147
63. Nowikovsky, K., Froschauer, E. M., Zsurka, G., Samaj, J., Reipert, S., Kolisek, M., Wiesenberger, G., and Schweyen, R. J. (2004) *J. Biol. Chem.* **279,** 30307–30315
64. Nowikovsky, K., Reipert, S., Devenish, R. J., and Schweyen, R. J. (2007) *Cell Death Differ.* **14,** 1647–1656
65. Dimmer, K. S., Navoni, F., Casarin, A., Trevisson, E., Endele, S., Winterpacht, A., Salviati, L., and Scorrano, L. (2008) *Hum. Mol. Genet.* **17,** 201–214
66. McQuibban, A. G., Joza, N., Megighian, A., Scorzeto, M., Zanini, D., Reipert, S., Richter, C., Schweyen, R. J., and Nowikovsky, K. (2010) *Hum. Mol. Genet.* **19,** 987–1000
67. Scarpa, A., and Azzone, G. F. (1970) *Eur. J. Biochem.* **12,** 328–335
68. Wingrove, D. E., Amatruda, J. M., and Gunter, T. E. (1984) *J. Biol. Chem.* **259,** 9390–9394
69. Azzone, G. F., Pozzan, T., Massari, S., Bragadin, M., and Dell'Antone, P. (1977) *FEBS Lett.* **78,** 21–24
70. Nicholls, D. G. (1978) *Biochem. J.* **176,** 463–474
71. Stucki, J. W., and Ineichen, E. A. (1974) *Eur. J. Biochem.* **48,** 365–375
72. Bragadin, M., Pozzan, T., and Azzone, G. F. (1979) *Biochemistry* **18,** 5972–5978
73. Altschuld, R. A., Hohl, C. M., Castillo, L. C., Garleb, A. A., Starling, R. C., and Brierley, G. P. (1992) *Am. J. Physiol.* **262,** H1699–1704
74. Wang, C., and Youle, R. J. (2009) *Annu. Rev. Genet.* **43,** 95–118
75. Di Lisa, F., Carpi, A., Giorgio, V., and Bernardi, P. (2011) *Biochim. Biophys. Acta* **1813,** 1316–1322
76. Hunter, D. R., Haworth, R. A., and Southard, J. H. (1976) *J. Biol. Chem.* **251,** 5069–5077
77. Bernardi, P. (1992) *J. Biol. Chem.* **267,** 8834–8839
78. Petronilli, V., Costantini, P., Scorrano, L., Colonna, R., Passamonti, S., and Bernardi, P. (1994) *J. Biol. Chem.* **269,** 16638–16642
79. Giorgio, V., Soriano, M. E., Basso, E., Bisetto, E., Lippe, G., Forte, M. A., and Bernardi, P. (2010) *Biochim. Biophys. Acta* **1797,** 1113–1118
80. Krieser, R. J., and White, K. (2009) *Apoptosis* **14,** 961–968

Supplemental Material for

Properties of Ca^{2+} Transport in Mitochondria of *Drosophila melanogaster*

Sophia von Stockum, Emy Basso, Valeria Petronilli, Patrizia Sabatelli, Michael A. Forte, Paolo Bernardi

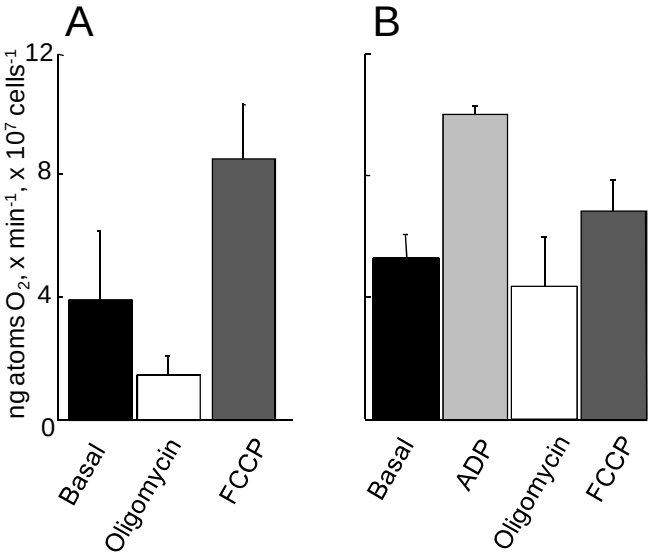

Supplementary Figure 1. **Oxygen consumption rates in intact and permeabilized *Drosophila* S_2R^+ cells.** *A*, cells were incubated in Hank's balanced salt solution supplemented with 10 mM glucose and 5 mM Pi-Tris, pH 7.4 and respiration recorded with a Clark-type oxygen electrode under basal conditions, after the addition of 1 µg/ml oligomycin followed by that of 50 nM FCCP. *B*, digitonin-permeabilized cells were incubated in 130 mM KCl, 10 mM MOPS-Tris, 5 mM succinate-Tris, 5 mM Pi-Tris and 10 µM EGTA-Tris, pH 7.4 and basal respiration measured, followed by the addition of 0.1 mM ADP, 1 µg/ml oligomycin and 50 nM FCCP. Respiratory rates are average ± SD from three independent experiments.

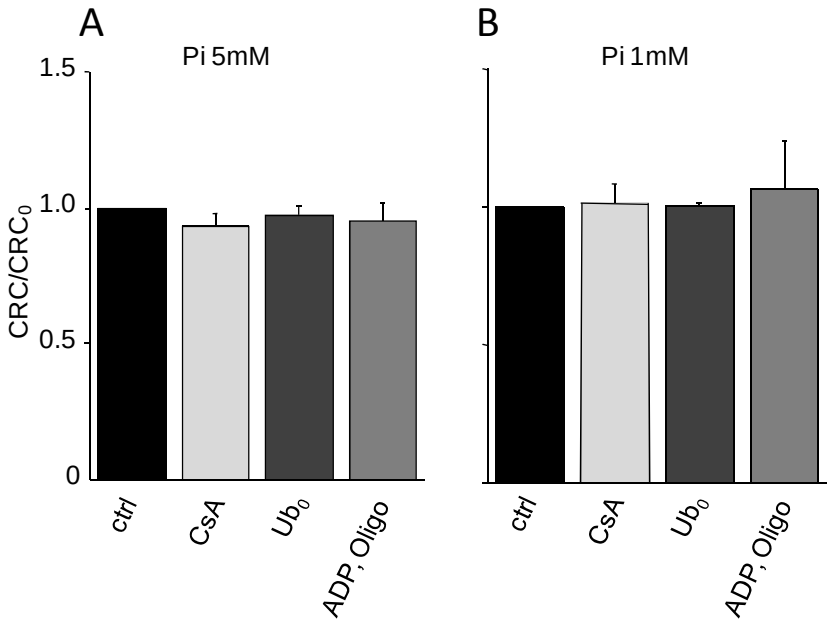

Supplementary Figure 2. Effect of CsA, Ub_0, ADP and oligomycin on CRC of permeabilized *Drosophila* S_2R^+ cells. Experimental conditions were as in Fig. 2 except that the concentration of Pi was 5 mM (*A*) or 1 mM (*B*). The CRC was determined in protocols identical to those shown in Fig. 4 in the absence of further additions (ctrl), or in the presence of 2 µg/ml CsA, 5 µM Ub0 or 0.1 mM ADP plus 1µg/ml oligomycin (Oligo). CRC values are normalized to those observed in absence of additions other than Ca2+ (CRC0). Experiments were performed in triplicate and reported values are average ± SD.

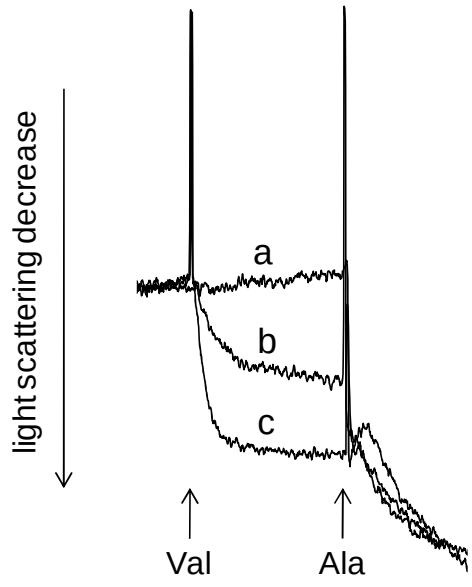

Supplementary Figure 3. Effect of valinomycin and alamethicin on light scattering in permeabilized *Drosophila* S_2R^+ cells. Experimental conditions were as in Fig. 2, and 90° light scattering changes were measured at 540 nm. Where indicated 150 nM (*trace b*) or 1 µM (*trace c*) valinomycin (Val) and 3 µM alamethicin (Ala) were added. *Trace a*, no valinomycin. The figure shows representative traces from three independent experiments.

Part II: Expression of Human Cyclophilin D in *Drosophila melanogaster* Cells – Impact on Regulation of the *Drosophila* Mitochondrial Ca^{2+} Release Channel

A key modulator of the mammalian permeability transition pore (PTP) is Cyclophilin D (Cyp-D), a mitochondrial peptidyl-prolyl-cis-trans isomerase (PPIase) that in mice is encoded by the *Ppif* gene and that plays an important role in protein folding. Cyp-D can be selectively inhibited by the immunosuppressant drug Cyclosporin A (CsA) and genetic Cyp-D ablation (or treatment with CsA) remarkably desensitizes the PTP in that its opening requires about twice the Ca^{2+} load necessary to open the PTP in ctrl mitochondria. Recently, it was shown that the desensitizing effect of Cyp-D ablation or CsA treatment on the pore is only seen in the presence of Pi, but not when the latter is replaced by its analogues arsenate or vanadate. These results suggest that when Cyp-D does not bind to the PTP (because of genetic ablation or of the binding to CsA) Pi can bind to an inhibitory site on the pore thereby delaying pore opening[68].

The *Drosophila* genome encodes for fourteen different Cyclophilins. However, according to sequence analysis[219] and GFP-tagging (unpublished results) there is no *Drosophila* Cyclophilin with a predicted mitochondrial localization. As described in **Part I**, the *Drosophila* Ca^{2+}-induced Ca^{2+} release channel has some similar characteristics to the mammalian PTP, but possesses also some unique features in that it is insensitive to CsA, selective to Ca^{2+} and H^+ and inhibited by Pi. Another striking difference between the pore of *Drosophila* and that of mammals is the lack of mitochondrial swelling and cytochrome *c* release during the opening of the channel. Taken together, these results suggest that the PTP is a phenomenon conserved throughout evolution, although it is regulated in different manners in different species. In this second part of the study, we investigated if the lack of sensitivity of the *Drosophila* channel to CsA is due to a lacking mitochondrial Cyclophilin and what the evolutionary role of Cyp-D is in pore regulation. Thus, we stably expressed a human Cyp-D construct in the *Drosophila* embryonic cell line S_2R^+ in order to investigate the impact of the heterologous protein on regulation of the *Drosophila* Ca^{2+}-induced Ca^{2+} release channel.

In order to express the human Cyp-D protein in S_2R^+ cells, we cloned a construct of human Cyp-D cDNA carrying a *Drosophila* MTS at its 5′ end and an HA-tag at its 3′ end in the *Drosophila* expression vector pAct, that drives constitutive expression of the heterologous protein.

Exchange of the human MTS for a *Drosophila* MTS was meant to assure proper localization of Cyp-D in the mitochondrial matrix upon translation in the *Drosophila* cell line, and the attachment of an HA-tag at the C-terminus was aimed at facilitating the detection of the heterologous protein by Western Blot or Immunofluorescence analysis. Cells were transfected with the expression vector pActCypD and the selection vector pCoPuro (encoding for puromycin-resistance) in a 20:1 ratio in order to minimize the occurrence of cells containing the selection but not the expression vector. A careful titration of puromycin was performed in order to define the proper concentration able to kill non-transfected ctrl cells but not puromycin-resistant pActCypD/pCoPuro cells. Puromycin-resistant cells were selected over three weeks to obtain a stable polyclonal cell population.

First, we wanted to analyze if and to what extend the transfected cells express human Cyp-D. Therefore we performed Western Blot analysis of total cell lysates and subcellular fractions, showing that S_2R^+ pActCypD-HA cells express the heterologous Cyp-D in a comparable amount to a human osteosarcoma cell line (SAOS) expressing the endogenous form (Figure 21 A) and that heterologous Cyp-D is mostly localized in the mitochondria (Figure 21 B). The faint band of Cyp-D in the cytoplasmic fraction could be due to the very high expression of the heterologous protein under the control of the actin 5C promoter. Mitochondrial localization of human Cyp-D in S_2R^+ cells was confirmed by Immunofluorescence analysis (Figure 21 C).

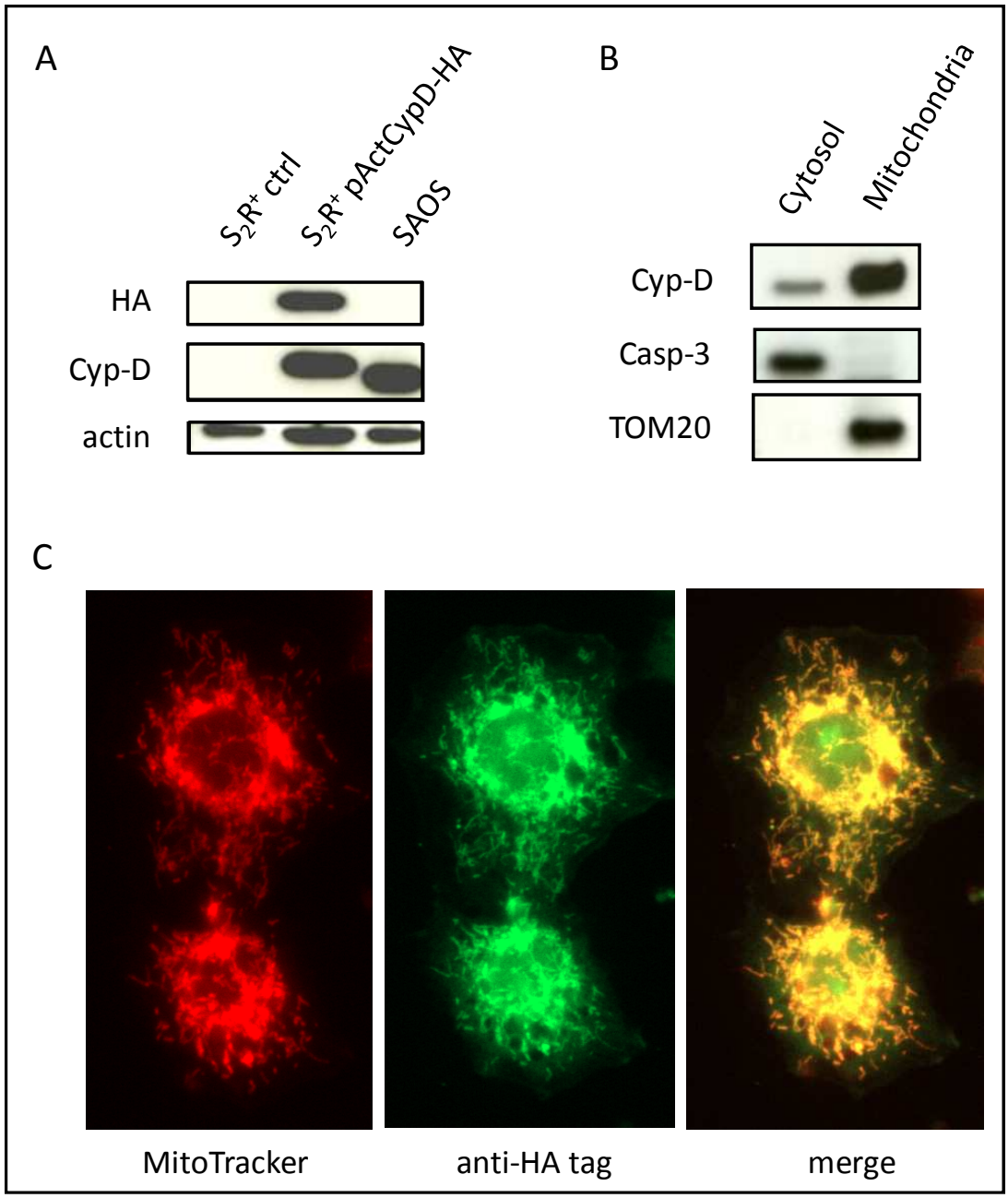

Figure 21. Expression level and subcellular localization of human Cyclophilin D expressed in *Drosophila* S_2R^+ cells. (A) Western Blot analysis of total cell lysates from non-transfected S_2R^+ cells (S_2R^+ ctrl), S_2R^+ cells stably transfected with pAct-CypD and pCoPuro vectors (S_2R^+pActCyp-D-HA) and human osteosarcoma cells (SAOS). Immunoblotting was performed with antibodies against Cyp-D, HA-tag and actin as internal loading control. The slight difference in molecular weight between the heterologously and the endogenously expressed Cyp-D is due to the HA-tag. (B) Western Blot analysis of cytosolic and mitochondrial fractions from S_2R^+pActCyp-D-HA showing the subcellular localization of Cyp-D. Antibodies against caspase-3 (Casp-3) and translocase of outer membrane 20 (TOM20) were used as markers for cytosol and mitochondria, respectively and were meant to address the purity of subcellular fractions. (C) Subcellular localization of Cyp-D in S_2R^+pActCyp-D-HA addressed by Immunofluorescence. Mitochondria were stained with Mitotracker Red CMXRos (red fluorescence) and cells were incubated with a specific antibody against the HA-tag attached to Cyp-D, followed by incubation with FITC-conjugated anti-mouse IgG (green fluorescence). The right panel shows the merged image from red and green fluorescence.

In order to address the impact of human Cyp-D on the *Drosophila* Ca^{2+}-induced Ca^{2+} release channel we studied the CRC in cells co-transfected with the expression vector pActCypD and the selection vector pCoPuro compared to ctrl cells transfected exclusively with the pCoPuro vector. Cyp-D expression strikingly reduced the CRC in pActCypD/pCoPuro cells compared to ctrl cells irrespective of the Pi concentration (Figure 22 A, panels a and a'). CsA was not able to prevent the inducing effect of Cyp-D on the *Drosophila* Ca^{2+}-induced Ca^{2+} release channel (Figure 22 A, panels b and b') and was ineffective in ctrl cells, as shown in **Part I**. We believe that Cyp-D acts specifically on the Ca^{2+} release channel since the potent PTP inhibitor rotenone[73] restored the CRC in Cyp-D-expressing cells, which became able to accumulate Ca^{2+} in a comparable amount to ctrl cells (Figure 22 A, panels c and c'). Figure 22 A shows an extreme case in which Cyp-D expression led to immediate opening of the *Drosophila* Ca^{2+}-induced Ca^{2+} release channel and prevented any Ca^{2+} uptake by mitochondria. Figure 22 B shows ratios of CRCs in the absence or presence of Cyp-D (in the latter case of course only experiments where some Ca^{2+} uptake took place were considered). The lack of sensitivity to CsA might be due to a very high affinity of the human Cyp-D for the *Drosophila* pore and/or to the high abundance of the overexpressed Cyp-D, which may require higher CsA concentrations for displacement from the Ca^{2+} release channel, an issue that will be addressed in the future.

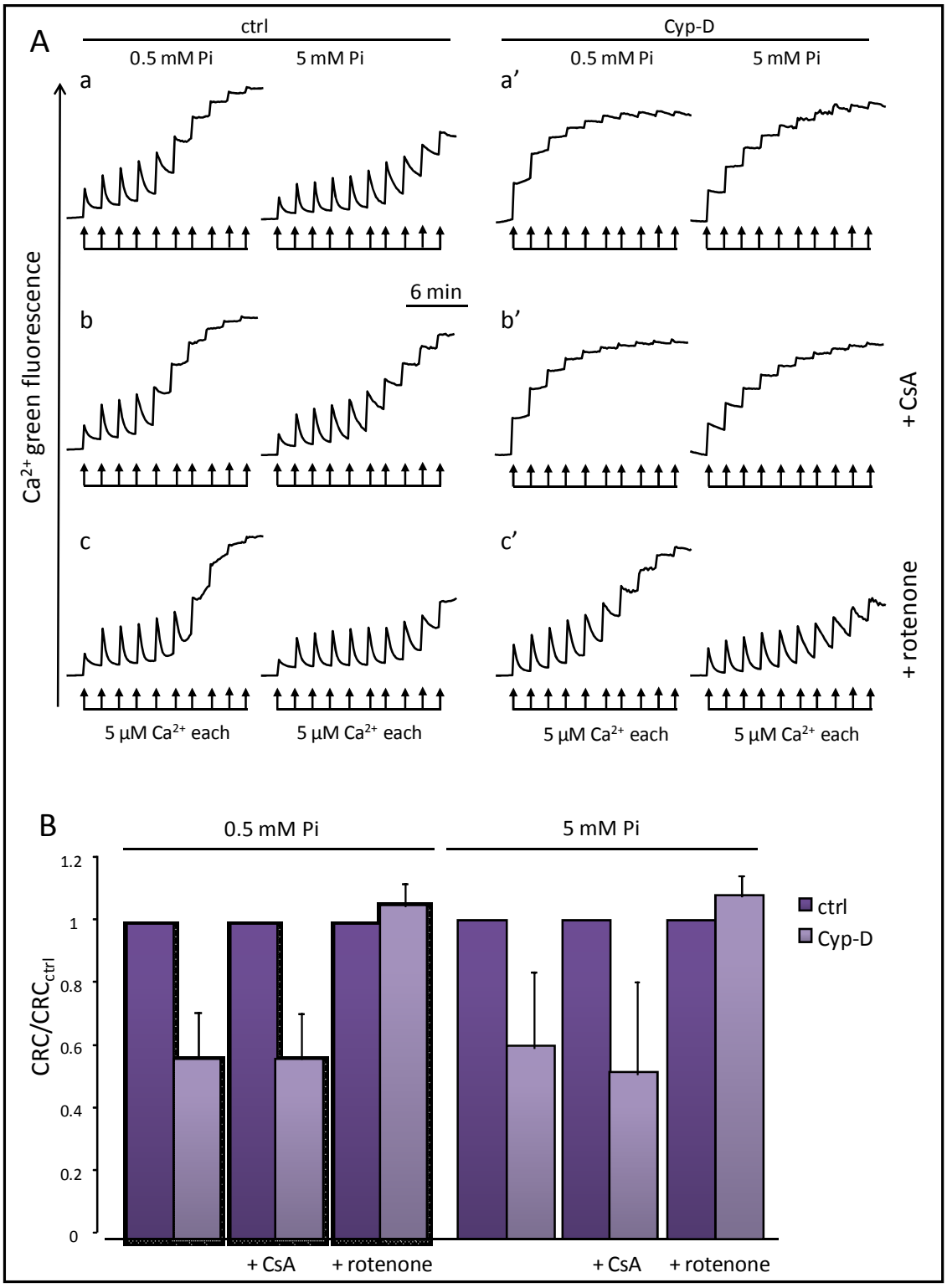

Figure 22. Effect of human Cyp-D on mitochondrial Ca^{2+} retention capacity (CRC) in permeabilized *Drosophila* S_2R^+ cells. (A) Digitonin-permeabilized S_2R^+ cells transfected either with pActCypD expression vector and pCoPuro selection vector (Cyp-D, panels a'-c') or only with the selection vector (ctrl, panels a-c) were incubated in 250 mM sucrose, 10 mM MOPS-Tris, 5 mM succinate-Tris, 10 µM EGTA, 0.5 µM Calcium Green 5N, pH 7.4 and Pi-Tris, as shown in the figure. In panels b and b' the medium was supplemented with 0.8 µM CsA and in panels c and c' with 2 µM rotenone. Extramitochondrial Ca^{2+} was monitored, and CRC was determined by stepwise addition of 5 µM Ca^{2+} pulses. (B) The amount of Ca^{2+} accumulated prior to onset of Ca^{2+}-induced Ca^{2+} release without further additions, in the presence of 2 µM rotenone (+ rotenone) or 0.8 µM CsA (+ CsA) was normalized to that obtained in the ctrl cells. Note that only the values where some Ca^{2+} uptake could be observed were included in this graph. Error bars report the standard deviation of three different experiments.

CONCLUSIONS

In this study we characterized Ca^{2+} transport mechanisms in one of the most popular and widely used model organism, *Drosophila melanogaster*. In particular we identified a novel mitochondrial Ca^{2+}-dependent Ca^{2+} release channel in a digitonin-permeabilized embryonic *Drosophila* cell model, displaying features intermediate between the mammalian PTP and the pore of yeast. Like the mammalian PTP, *Drosophila* Ca^{2+} release is inhibited by tetracaine and opens in response to matrix Ca^{2+} loading, inner membrane depolarization, thiol oxidation, and treatment with relatively high concentrations of NEM. Like the yeast pore (and at variance from the mammalian PTP), the *Drosophila* channel is inhibited by Pi and insensitive to CsA. A striking difference between the pore of *Drosophila* and that of mammals is its selectivity to Ca^{2+} and H^+ and the lack of mitochondrial swelling and cyt *c* release during the opening of the channel. Available evidence points to persistent activation of the PTP as a prime mediator of apoptotic and necrotic cell death in mammals. As described in Chapter 5.4, permeabilization of mitochondrial membranes might not be required to induce the *Drosophila* apoptotic pathways and cyt *c* seems to be dispensable for activation of down-stream caspases. However, it is unknown if Ca^{2+}-mediated cell death pathways do exist in *Drosophila* cells. Our results indicate that the *Drosophila* Ca^{2+}-induced Ca^{2+} release channel might be more involved into Ca^{2+} homeostasis than into cell death induction due to the fact that its opening does not cause morphological changes and membrane permeabilization in mitochondria. However, this issue can now be addressed based on the results of the second part of this study, in which we were able to express human Cyp-D in *Drosophila* S_2R^+ cells. The heterologous protein was properly targeted to the mitochondria and decreased the Ca^{2+} retention capacity of Cyp-D-expressing cells in a rotenone-sensitive but CsA-insensitive manner. If the Cyp-D in *Drosophila* cells changes selectivity, size and properties of the Ca^{2+}-induced Ca^{2+} release channel can now be addressed. It will be particularly interesting to investigate if Cyp-D induces the swelling of mitochondria undergoing Ca^{2+} release, and if mitochondria do now release cyt *c*. This could shed further light on the evolution of the PTP and mitochondria-mediated cell death pathways in the animal kingdom. Furthermore, we can benefit from the sophisticated genetic strategies that *Drosophila* provides to define the molecular nature of the PTP and its role in pathophysiology of Ca^{2+} homeostasis.

REFERENCES

1. Tovar, J. *et al*. Mitochondrial remnant organelles of Giardia function in iron-sulphur protein maturation. *Nature* **426**, 172-176 (2003).

2. Williams, B. A. P., Hirt, R. P., Lucocq, J. M. & Embley, T. M. A mitochondrial remnant in the microsporidian Trachipleistophora hominis. *Nature* **418**, 865-869 (2002).

3. McBride, H. M., Neuspiel, M. & Wasiak, S. Mitochondria: more than just a powerhouse. *Current Biology* **16**, R551-R560 (2006).

4. Youle, R. J. & Van Der Bliek, A. M. Mitochondrial fission, fusion, and stress. *Science* **337**, 1062-1065 (2012).

5. Liu, X. & Hajnóczky, G. Ca2+-dependent regulation of mitochondrial dynamics by the Miro-Milton complex. *International Journal of Biochemistry and Cell Biology* **41**, 1972-1976 (2009).

6. http://www.origin-of-mitochondria.net.

7. http://molpath.ucsd.edu/.

8. Nass, M. M. & Nass, S. Intramitochondrial fibers with DNA characteristics. I. Fixation and electron staining reactions. *J. Cell Biol.* **19**, 593-611 (1963).

9. http://www.wadsworth.org/rvbc/cryo.html.

10. Mitchell, P. Chemiosmotic coupling in oxidative and photosynthetic phosphorylation. *Biol.Rev.Camb.Philos.Soc.* **41**, 445-502 (1966).

11. Abrahams, J. P., Leslie, A. G. W., Lutter, R. & Walker, J. E. Structure at 2.8 A resolution of F1-ATPase from bovine heart mitochondria. *Nature* **370**, 621-628 (1994).

12. Wittig, I. & Schägger, H. Structural organization of mitochondrial ATP synthase. *Biochim. Biophys. Acta* **1777**, 592 (2008).

13. Collinson, I. R., Skehel, J. M., Fearnley, I. M., Runswick, M. J. & Walker, J. E. The F1FO-ATPase complex from bovine heart mitochondria: the molar ratio of the subunits in the stalk region linking the F1 and FO domains. *Biochemistry* **35**, 12640-12646 (1996).

14. Noji, H., Yasuda, R., Yoshida, M. & Kinosita, K. Direct observation of the rotation of F1-ATPase. *Nature* **386**, 299-302 (1997).

15. Walker, J. E. & Dickson, V. K. The peripheral stalk of the mitochondrial ATP synthase. *Biochim. Biophys. Acta* **1757**, 286 (2006).

16. Cabezon, E., Montgomery, M. G., Leslie, A. G. W. & Walker, J. E. The structure of bovine F1-ATPase in complex with its regulatory protein IF1. *Nat. Struct. Biol.* **10**, 744-750 (2003).

17. Green, D. W. & Grover, G. J. The IF(1) inhibitor protein of the mitochondrial F(1)F(0)-ATPase. *Biochim. Biophys. Acta* **1458**, 343-355 (2000).

18. Symersky, J., Osowski, D., Walters, D. E. & Mueller, D. M. Oligomycin frames a common drug-binding site in the ATP synthase. *Proceedings of the National Academy of Sciences* **109**, 13961-13965 (2012).

19. Granata, S. *et al*. Mitochondrial dysregulation and oxidative stress in patients with chronic kidney disease. *BMC Genomics* **10** (2009).

20. Kerr, J. F., Wyllie, A. H. & Currie, A. R. Apoptosis: a basic biological phenomenon with wide-ranging implications in tissue kinetics. *Br. J. Cancer* **26**, 239-257 (1972).

21. Wu, W., Liu, P. & Li, J. Necroptosis: An emerging form of programmed cell death. *Crit. Rev. Oncol.* **82**, 249-258 (2012).

22. Li, J. & Yuan, J. Caspases in apoptosis and beyond. *Oncogene* **27**, 6194-6206 (2008).

23. Fischer, U., Jänicke, R. & Schulze-Osthoff, K. Many cuts to ruin: a comprehensive update of caspase substrates. *Cell Death & Differentiation* **10**, 76-100 (2003).

24. Li, H., Zhu, H., Xu, C. & Yuan, J. Cleavage of BID by caspase 8 mediates the mitochondrial damage in the Fas pathway of apoptosis. *Cell* **94**, 491-502 (1998).

25. Katz, C. *et al*. Molecular basis of the interaction between proapoptotic truncated BID (tBID) protein and mitochondrial carrier homologue 2 (MTCH2) protein: key players in mitochondrial death pathway. *J. Biol. Chem.* **287**, 15016-15023 (2012).

26. Riedl, S. J. & Salvesen, G. S. The apoptosome: signalling platform of cell death. *Nature Reviews Molecular Cell Biology* **8**, 405-413 (2007).

27. Joza, N. *et al*. Essential role of the mitochondrial apoptosis-inducing factor in programmed cell death. *Nature* **410**, 549-554 (2001).

28. Hotchkiss, R. S., Strasser, A., McDunn, J. E. & Swanson, P. E. Cell death. *N. Engl. J. Med.* **361**, 1570-1583 (2009).

29. Danial, N. N. & Korsmeyer, S. J. Cell death: critical control points. *Cell* **116**, 205-219 (2004).

30. Soriano, M. E. & Scorrano, L. Traveling Bax and forth from mitochondria to control apoptosis. *Cell* **145**, 15-17 (2011).

31. Wei, M. C. *et al*. tBID, a membrane-targeted death ligand, oligomerizes BAK to release cytochrome c. *Genes Dev.* **14**, 2060-2071 (2000).

32. Martinou, J. C. & Youle, R. J. Mitochondria in apoptosis: Bcl-2 family members and mitochondrial dynamics. *Developmental cell* **21**, 92-101 (2011).

33. Rizzuto, R., Duchen, M. R. & Pozzan, T. Flirting in little space: the ER/mitochondria Ca2+ liaison. *Science Signalling* **2004**, re1 (2004).

34. DeLuca, H. & Engstrom, G. Calcium uptake by rat kidney mitochondria. *Proc. Natl. Acad. Sci. U. S. A.* **47**, 1744 (1961).

35. Rizzuto, R. *et al*. Close contacts with the endoplasmic reticulum as determinants of mitochondrial Ca2+ responses. *Science* **280**, 1763-1766 (1998).

36. Rizzuto, R., Bernardi, P. & Pozzan, T. Mitochondria as all-round players of the calcium game. *J. Physiol. (Lond.)* **529**, 37-47 (2004).

37. Kirichok, Y., Krapivinsky, G. & Clapham, D. E. The mitochondrial calcium uniporter is a highly selective ion channel. *Nature* **427**, 360-364 (2004).

38. De Stefani, D., Raffaello, A., Teardo, E., Szabò, I. & Rizzuto, R. A forty-kilodalton protein of the inner membrane is the mitochondrial calcium uniporter. *Nature* **476**, 336-340 (2011).

39. Baughman, J. M. *et al*. Integrative genomics identifies MCU as an essential component of the mitochondrial calcium uniporter. *Nature* **476**, 341-345 (2011).

40. Nicholls, D. G. Mitochondrial calcium function and dysfunction in the central nervous system. *Biochimica et Biophysica Acta (BBA)-Bioenergetics* **1787**, 1416-1424 (2009).

41. Azzone, G., Pozzan, T., Massari, S., Bragadin, M. & Dell'Antone, P. H /site ratio and steady state distribution of divalent cations in mitochondria. *FEBS Lett.* **78**, 21 (1977).

42. Nicholls, D. G. The regulation of extramitochondrial free calcium ion concentration by rat liver mitochondria. *Biochem. J.* **176**, 463 (1978).

43. Bernardi, P. & Pietrobon, D. On the nature of Pi-induced, Mg2+-prevented Ca2+ release in rat liver mitochondria. *FEBS Lett.* **139**, 9-12 (1982).

44. Mitchell, P. Keilin's respiratory chain concept and its chemiosmotic consequences. *Science* **206**, 1148-1159 (1979).

45. Kristian, T., Pivovarova, N. B., Fiskum, G. & Andrews, S. B. Calcium-induced precipitate formation in brain mitochondria: composition, calcium capacity, and retention. *J. Neurochem.* **102**, 1346-1356 (2007).

46. Palty, R. *et al*. NCLX is an essential component of mitochondrial Na+/Ca2+ exchange. *Proc. Natl. Acad. Sci. U. S. A.* **107**, 436-441 (2010).

47. Pfeiffer, D. R., Gunter, T. E., Eliseev, R., Broekemeier, K. M. & Gunter, K. K. Release of Ca2+ from mitochondria via the saturable mechanisms and the permeability transition. *IUBMB Life* **52**, 205-212 (2008).

48. Drago, I., Pizzo, P. & Pozzan, T. After half a century mitochondrial calcium in-and efflux machineries reveal themselves. *EMBO J.* **30**, 4119-4125 (2011).

49. Bragadin, M., Pozzan, T. & Azzone, G. F. Kinetics of calcium (2+) ion carrier in rat liver mitochondria. *Biochemistry (N. Y.)* **18**, 5972-5978 (1979).

50. Bernardi, P. Mitochondrial transport of cations: channels, exchangers, and permeability transition. *Physiol. Rev.* **79**, 1127-1155 (1999).

51. Bernardi, P. & Petronilli, V. The permeability transition pore as a mitochondrial calcium release channel: a critical appraisal. *J. Bioenerg. Biomembr.* **28**, 131-138 (1996).

52. Rasola, A., Sciacovelli, M., Pantic, B. & Bernardi, P. Signal transduction to the permeability transition pore. *FEBS Lett.* **584**, 1989-1996 (2010).

53. Bernardi, P. *et al*. The mitochondrial permeability transition from in vitro artifact to disease target. *FEBS Journal* **273**, 2077-2099 (2006).

54. Kung, G., Konstantinidis, K. & Kitsis, R. N. Programmed necrosis, not apoptosis, in the heart. *Circ. Res.* **108**, 1017-1036 (2011).

55. Nicolli, A., Petronilli, V. & Bernardi, P. Modulation of the mitochondrial cyclosporin A-sensitive permeability transition pore by matrix pH. Evidence that the pore open-closed probability is regulated by reversible histidine protonation. *Biochemistry (N. Y.)* **32**, 4461-4465 (1993).

56. Bernardi, P. Modulation of the mitochondrial cyclosporin A-sensitive permeability transition pore by the proton electrochemical gradient. Evidence that the pore can be opened by membrane depolarization. *J. Biol. Chem.* **267**, 8834-8839 (1992).

57. Lê Quôc, K. & Lê Quôc, D. Involvement of the ADP/ATP carrier in calcium-induced perturbations of the mitochondrial inner membrane permeability: importance of the orientation of the nucleotide binding site. *Arch. Biochem. Biophys.* **265**, 249 (1988).

58. Hunter, D. R. & Haworth, R. A. The Ca2+-induced membrane transition in mitochondria. I. The protective mechanisms. *Arch. Biochem. Biophys.* **195**, 453-459 (1979).

59. Halestrap, A. & Davidson, A. Inhibition of Ca2(+)-induced large-amplitude swelling of liver and heart mitochondria by cyclosporin is probably caused by the inhibitor binding to mitochondrial-matrix peptidyl-prolyl cis-trans isomerase and preventing it interacting with the adenine nucleotide translocase. *Biochem. J.* **268**, 153-160 (1990).

60. Fontaine, E., Eriksson, O., Ichas, F. & Bernardi, P. Regulation of the permeability transition pore in skeletal muscle mitochondria. *J. Biol. Chem.* **273**, 12662-12668 (1998).

61. Walter, L. *et al*. Three classes of ubiquinone analogs regulate the mitochondrial permeability transition pore through a common site. *J. Biol. Chem.* **275**, 29521-29527 (2000).

62. Costantini, P., Chernyak, B. V., Petronilli, V. & Bernardi, P. Modulation of the mitochondrial permeability transition pore by pyridine nucleotides and dithiol oxidation at two separate sites. *J. Biol. Chem.* **271**, 6746-6751 (1996).

63. Chernyak, B. V. & Bernardi, P. The mitochondrial permeability transition pore is modulated by oxidative agents through both pyridine nucleotides and glutathione at two separate sites. *European Journal of Biochemistry* **238**, 623-630 (2004).

64. Kowaltowski, A. J., Vercesi, A. E. & Castilho, R. F. Mitochondrial membrane protein thiol reactivity with N-ethylmaleimide or mersalyl is modified by Ca2+: correlation with mitochondrial permeability transition. *Biochim. Biophys. Acta* **1318**, 395-402 (1997).

65. Petronilli, V. *et al*. The voltage sensor of the mitochondrial permeability transition pore is tuned by the oxidation-reduction state of vicinal thiols. Increase of the gating potential by oxidants and its reversal by reducing agents. *J. Biol. Chem.* **269**, 16638-16642 (1994).

66. Costantini, P., Chernyak, B. V., Petronilli, V. & Bernardi, P. Selective inhibition of the mitochondrial permeability transition pore at the oxidation-reduction sensitive dithiol by monobromobimane. *FEBS Lett.* **362**, 239 (1995).

67. Seidlmayer, L. K., Gomez-Garcia, M. R., Blatter, L. A., Pavlov, E. & Dedkova, E. N. Inorganic polyphosphate is a potent activator of the mitochondrial permeability transition pore in cardiac myocytes. *J. Gen. Physiol.* **139**, 321-331 (2012).

68. Basso, E., Petronilli, V., Forte, M. A. & Bernardi, P. Phosphate is essential for inhibition of the mitochondrial permeability transition pore by cyclosporin A and by cyclophilin D ablation. *J. Biol. Chem.* **283**, 26307-26311 (2008).

69. Giorgio, V. *et al*. Cyclophilin D in mitochondrial pathophysiology. *Biochimica et Biophysica Acta (BBA)-Bioenergetics* **1797**, 1113-1118 (2010).

70. Broekemeier, K., Dempsey, M. & Pfeiffer, D. Cyclosporin A is a potent inhibitor of the inner membrane permeability transition in liver mitochondria. *J. Biol. Chem.* **264**, 7826-7830 (1989).

71. Scorrano, L., Nicolli, A., Basso, E. & Petronilli, V. P. Two modes of activation of the permeability transition pore: the role of mitochondrial cyclophilin. *Mol. Cell. Biochem.* **174**, 181-184 (1997).

72. Nicolli, A., Basso, E., Petronilli, V., Wenger, R. M. & Bernardi, P. Interactions of cyclophilin with the mitochondrial inner membrane and regulation of the permeability transition pore, a cyclosporin A-sensitive channel. *J. Biol. Chem.* **271**, 2185-2192 (1996).

73. Li, B. *et al*. Inhibition of complex I regulates the mitochondrial permeability transition through a phosphate-sensitive inhibitory site masked by cyclophilin D. *Biochimica et Biophysica Acta (BBA)-Bioenergetics* (2012).

74. Rasola, A. & Bernardi, P. The mitochondrial permeability transition pore and its involvement in cell death and in disease pathogenesis. *Apoptosis* **12**, 815-833 (2007).

75. Szabó, I. & Zoratti, M. The mitochondrial permeability transition pore may comprise VDAC molecules. I. Binary structure and voltage dependence of the pore. *FEBS Lett.* **330**, 201 (1993).

76. Szabó, I., De Pinto, V. & Zoratti, M. The mitochondrial permeability transition pore may comprise VDAC molecules. II. The electrophysiological properties of VDAC are compatible with those of the mitochondrial megachannel. *FEBS Lett.* **330**, 206 (1993).

77. Gincel, D., Zaid, H. & Shoshan-Barmatz, V. Calcium binding and translocation by the voltage-dependent anion channel: a possible regulatory mechanism in mitochondrial function. *Biochem. J.* **358**, 147 (2001).

78. Zizi, M., Forte, M., Blachly-Dyson, E. & Colombini, M. NADH regulates the gating of VDAC, the mitochondrial outer membrane channel. *J. Biol. Chem.* **269**, 1614-1616 (1994).

79. Gincel, D. & Shoshan-Barmatz, V. Glutamate interacts with VDAC and modulates opening of the mitochondrial permeability transition pore. *J. Bioenerg. Biomembr.* **36**, 179-186 (2004).

80. Pastorino, J. G. & Hoek, J. B. Hexokinase II: the integration of energy metabolism and control of apoptosis. *Curr. Med. Chem.* **10**, 1535-1551 (2003).

81. Xu, X., Decker, W., Sampson, M., Craigen, W. & Colombini, M. Mouse VDAC isoforms expressed in yeast: channel properties and their roles in mitochondrial outer membrane permeability. *J. Membr. Biol.* **170**, 89-102 (1999).

82. Krauskopf, A., Eriksson, O., Craigen, W. J., Forte, M. A. & Bernardi, P. Properties of the permeability transition in VDAC1(-/-) mitochondria. *Biochim. Biophys. Acta* **1757**, 590-595 (2006).

83. Baines, C. P., Kaiser, R. A., Sheiko, T., Craigen, W. J. & Molkentin, J. D. Voltage-dependent anion channels are dispensable for mitochondrial-dependent cell death. *Nat. Cell Biol.* **9**, 550-555 (2007).

84. Haworth, R. A. & Hunter, D. R. M. Control of the mitochondrial permeability transition pore by high-affinity ADP binding at the ADP/ATP translocase in permeabilized mitochondria. *J. Bioenerg. Biomembr.* **32**, 91-96 (2000).

85. Kokoszka, J. E. *et al*. The ADP/ATP translocator is not essential for the mitochondrial permeability transition pore. *Nature* **427**, 461-465 (2004).

86. Fontaine, E., Ichas, F. & Bernardi, P. A ubiquinone-binding site regulates the mitochondrial permeability transition pore. *J. Biol. Chem.* **273**, 25734-25740 (1998).

87. Cesura, A. M. *et al*. The voltage-dependent anion channel is the target for a new class of inhibitors of the mitochondrial permeability transition pore. *J. Biol. Chem.* **278**, 49812-49818 (2003).

88. Leung, A. W. C., Varanyuwatana, P. & Halestrap, A. P. The mitochondrial phosphate carrier interacts with cyclophilin D and may play a key role in the permeability transition. *J. Biol. Chem.* **283**, 26312-26323 (2008).

89. Varanyuwatana, P. & Halestrap, A. P. The roles of phosphate and the phosphate carrier in the mitochondrial permeability transition pore. *Mitochondrion* **12**, 120-125 (2012).

90. Connern, C. P. & Halestrap, A. P. Recruitment of mitochondrial cyclophilin to the mitochondrial inner membrane under conditions of oxidative stress that enhance the opening of a calcium-sensitive non-specific channel. *Biochem. J.* **302**, 321 (1994).

91. Baines, C. P. *et al*. Loss of cyclophilin D reveals a critical role for mitochondrial permeability transition in cell death. *Nature* **434**, 658-662 (2005).

92. Reutenauer, J., Dorchies, O., Patthey-Vuadens, O., Vuagniaux, G. & Ruegg, U. Investigation of Debio 025, a cyclophilin inhibitor, in the dystrophic mdx mouse, a model for Duchenne muscular dystrophy. *Br. J. Pharmacol.* **155**, 574-584 (2009).

93. Sharpe, J. C., Arnoult, D. & Youle, R. J. Control of mitochondrial permeability by Bcl-2 family members. *Biochimica et Biophysica Acta (BBA)-Molecular Cell Research* **1644**, 107-113 (2004).

94. O'Gorman, E. *et al*. The role of creatine kinase in inhibition of mitochondrial permeability transition. *FEBS Lett.* **414**, 253 (1997).

95. Mathupala, S., Ko, Y. & Pedersen, P. Hexokinase II: cancer's double-edged sword acting as both facilitator and gatekeeper of malignancy when bound to mitochondria. *Oncogene* **25**, 4777-4786 (2006).

96. Robey, R. & Hay, N. Mitochondrial hexokinases, novel mediators of the antiapoptotic effects of growth factors and Akt. *Oncogene* **25**, 4683-4696 (2006).

97. Šileikytė, J. *et al*. Regulation of the inner membrane mitochondrial permeability transition by the outer membrane translocator protein (peripheral benzodiazepine receptor). *J. Biol. Chem.* **286**, 1046-1053 (2011).

98. Altschuld, R. A. *et al*. Cyclosporin inhibits mitochondrial calcium efflux in isolated adult rat ventricular cardiomyocytes. *American Journal of Physiology - Heart and Circulatory Physiology* **262**, H1699-H1704 (1992).

99. Eriksson, O., Pollesello, P. & Geimonen, E. Regulation of total mitochondrial Ca 2+ in perfused liver is independent of the permeability transition pore. *American Journal of Physiology - Cell Physiology* **276**, C1297-C1302 (1999).

100. Elrod, J. W. *et al*. Cyclophilin D controls mitochondrial pore - dependent Ca2+ exchange, metabolic flexibility, and propensity for heart failure in mice. *J. Clin. Invest.* **120**, 3680-3687 (2010).

101. Barsukova, A. *et al*. Activation of the mitochondrial permeability transition pore modulates Ca 2+ responses to physiological stimuli in adult neurons. *Eur. J. Neurosci.* **33**, 831-842 (2011).

102. Schinzel, A. C. *et al*. Cyclophilin D is a component of mitochondrial permeability transition and mediates neuronal cell death after focal cerebral ischemia. *Proc. Natl. Acad. Sci. U. S. A.* **102**, 12005-12010 (2005).

103. Du, H. *et al*. Cyclophilin D deficiency attenuates mitochondrial and neuronal perturbation and ameliorates learning and memory in Alzheimer's disease. *Nat. Med.* **14**, 1097-1105 (2008).

104. Wang, X. *et al*. Developmental shift of cyclophilin D contribution to hypoxic-ischemic brain injury. *The Journal of Neuroscience* **29**, 2588-2596 (2009).

105. Guérin, B., Bunoust, O., Rouqueys, V. & Rigoulet, M. ATP-induced unspecific channel in yeast mitochondria. *J. Biol. Chem.* **269**, 25406-25410 (1994).

106. Jung, D. W., Bradshaw, P. C. & Pfeiffer, D. R. Properties of a cyclosporin-insensitive permeability transition pore in yeast mitochondria. *J. Biol. Chem.* **272**, 21104 (1997).

107. Manon, S., Roucou, X., Guerin, M., Rigoulet, M. & Guérin, B. Minireview: Characterization of the yeast mitochondria unselective channel: a counterpart to the mammalian permeability transition pore? *J. Bioenerg. Biomembr.* **30**, 419-429 (1998).

108. Pérez-Vázquez, V., Saavedra-Molina, A. & Uribe, S. In Saccharomyces cerevisiae, cations control the fate of the energy derived from oxidative metabolism through the opening and closing of the yeast mitochondrial unselective channel. *J. Bioenerg. Biomembr.* **35**, 231-241 (2003).

109. Yamada, A. *et al*. Ca2+-induced permeability transition can be observed even in yeast mitochondria under optimized experimental conditions. *Biochim. Biophys. Acta* **1787**, 1486-1491 (2009).

110. Fortes, F., Castilho, R. F., Catisti, R., Carnieri, E. G. S. & Vercesi, A. E. Ca2+ induces a cyclosporin A-insensitive permeability transition pore in isolated potato tuber mitochondria mediated by reactive oxygen species. *J. Bioenerg. Biomembr.* **33**, 43-51 (2001).

111. Arpagaus, S., Rawyler, A. & Braendle, R. Occurrence and characteristics of the mitochondrial permeability transition in plants. *J. Biol. Chem.* **277**, 1780-1787 (2002).

112. Curtis, M. J. & Wolpert, T. J. The oat mitochondrial permeability transition and its implication in victorin binding and induced cell death. *The Plant Journal* **29**, 295-312 (2003).

113. Virolainen, E., Blokhina, O. & Fagerstedt, K. Ca2+ -induced high amplitude swelling and cytochrome c release from wheat (Triticum aestivum l.) mitochondria under anoxic stress. *Annals of Botany* **90**, 509-516 (2002).

114. Lin, J., Wang, Y. & Wang, G. Salt stress-induced programmed cell death in tobacco protoplasts is mediated by reactive oxygen species and mitochondrial permeability transition pore status. *J. Plant Physiol.* **163**, 731-739 (2006).

115. Toninello, A., Salvi, M. & Colombo, L. The membrane permeability transition in liver mitochondria of the great green goby Zosterisessor ophiocephalus (Pallas). *J. Exp. Biol.* **203**, 3425-3434 (2000).

116. Azzolin, L., Basso, E., Argenton, F. & Bernardi, P. Mitochondrial Ca2+ transport and permeability transition in zebrafish (Danio rerio). *Biochim. Biophys. Acta* **1797**, 1775-1779 (2010).

117. Hanada, H. *et al*. Cyclosporin A inhibits thyroid hormone-induced shortening of the tadpole tail through membrane permeability transition. *Comparative Biochemistry and Physiology Part B: Biochemistry and Molecular Biology* **135**, 473-483 (2003).

118. Savina, M. V., Emelyanova, L. V. & Belyaeva, E. A. Bioenergetic parameters of lamprey and frog liver mitochondria during metabolic depression and activity. *Comparative Biochemistry and Physiology Part B: Biochemistry and Molecular Biology* **145**, 296-305 (2006).

119. Azzolin, L. *et al*. The mitochondrial permeability transition from yeast to mammals. *FEBS Lett.* **584**, 2504-2509 (2010).

120. Nichols, B., Rigoulet, M. & Denton, R. Comparison of the effects of Ca2+ , adenine nucleotides and pH on the kinetic properties of mitochondrial NAD (+)-isocitrate dehydrogenase and oxoglutarate dehydrogenase from the yeast Saccharomyces cerevisiae and rat heart. *Biochem. J.* **303**, 461 (1994).

121. Manon, S. & Guérin, M. Evidence for three different electrophoretic pathways in yeast mitochondria: ion specificity and inhibitor sensitivity. *J. Bioenerg. Biomembr.* **25**, 671-678 (1993).

122. Bazhenova, E. N., Deryabina, Y. I., Eriksson, O., Zvyagilskaya, R. A. & Saris, N. E. L. Characterization of a high capacity calcium transport system in mitochondria of the yeast Endomyces magnusii. *J. Biol. Chem.* **273**, 4372-4377 (1998).

123. Bradshaw, P. C., Jung, D. W. & Pfeiffer, D. R. Free fatty acids activate a vigorous Ca2+:2H+ antiport activity in yeast mitochondria. *J. Biol. Chem.* **276**, 40502-40509 (2001).

124. Ballarin, C. & Sorgato, M. C. An electrophysiological study of yeast mitochondria. *J. Biol. Chem.* **270**, 19262-19268 (1995).

125. Matouschek, A., Rospert, S., Schmid, K., Glick, B. S. & Schatz, G. Cyclophilin catalyzes protein folding in yeast mitochondria. *Proc. Natl. Acad. Sci. U. S. A.* **92**, 6319-6323 (1995).

126. Kowaltowski, A. J., Vercesi, A. E., Rhee, S. G. & Netto, L. E. Catalases and thioredoxin peroxidase protect Saccharomyces cerevisiae against Ca(2+)-induced mitochondrial membrane permeabilization and cell death. *FEBS Lett.* **473**, 177-182 (2000).

127. Marks, A. R. Cellular functions of immunophilins. *Physiol. Rev.* **76**, 631-649 (1996).

128. Handschumacher, R. E., Harding, M. W., Rice, J., Drugge, R. J. & Speicher, D. W. Cyclophilin: a specific cytosolic binding protein for cyclosporin A. *Science (New York, NY)* **226**, 544 (1984).

129. Liu, J. *et al*. Calcineurin is a common target of cyclophilin-cyclosporin A and FKBP-FK506 complexes. *Cell* **66**, 807-815 (1991).

130. Kang, B. H. *et al*. Regulation of tumor cell mitochondrial homeostasis by an organelle-specific Hsp90 chaperone network. *Cell* **131**, 257-270 (2007).

131. Giorgio, V. *et al*. Cyclophilin D modulates mitochondrial F0F1-ATP synthase by interacting with the lateral stalk of the complex. *J. Biol. Chem.* **284**, 33982-33988 (2009).

132. Eliseev, R. A. *et al*. Cyclophilin D interacts with Bcl2 and exerts an anti-apoptotic effect. *J. Biol. Chem.* **284**, 9692-9699 (2009).

133. Argaud, L. *et al*. Specific inhibition of the mitochondrial permeability transition prevents lethal reperfusion injury. *J. Mol. Cell. Cardiol.* **38**, 367-374 (2005).

134. Clarke, S. J., McStay, G. P. & Halestrap, A. P. Sanglifehrin A acts as a potent inhibitor of the mitochondrial permeability transition and reperfusion injury of the heart by binding to cyclophilin-D at a different site from cyclosporin A. *J. Biol. Chem.* **277**, 34793-34799 (2002).

135. Gomez, L. *et al*. Inhibition of mitochondrial permeability transition improves functional recovery and reduces mortality following acute myocardial infarction in mice. *American Journal of Physiology-Heart and Circulatory Physiology* **293**, H1654-H1661 (2007).

136. Azzolin, L. *et al*. Antamanide, a derivative of amanita phalloides, is a novel inhibitor of the mitochondrial permeability transition pore. *PloS one* **6**, e16280 (2011).

137. Basso, E. *et al*. Properties of the permeability transition pore in mitochondria devoid of Cyclophilin D. *J. Biol. Chem.* **280**, 18558-18561 (2005).

138. Nakagawa, T. *et al*. Cyclophilin D-dependent mitochondrial permeability transition regulates some necrotic but not apoptotic cell death. *Nature* **434**, 652-658 (2005).

139. Li, Y., Johnson, N., Capano, M., Edwards, M. & Crompton, M. Cyclophilin-D promotes the mitochondrial permeability transition but has opposite effects on apoptosis and necrosis. *Biochem. J.* **383**, 101 (2004).

140. Matas, J. *et al*. Increased expression and intramitochondrial translocation of cyclophilin-D associates with increased vulnerability of the permeability transition pore to stress-induced opening during compensated ventricular hypertrophy. *J. Mol. Cell. Cardiol.* **46**, 420-430 (2009).

141. Wolpert, L. *et al*. Principles of development. 1998. *Current Biology Ltd London*.

142. Adoutte, A. *et al*. The new animal phylogeny: reliability and implications. *Proc. Natl. Acad. Sci. U. S. A.* **97**, 4453-4456 (2000).

143. Peterson, K. J. *et al*. Estimating metazoan divergence times with a molecular clock. *Proc. Natl. Acad. Sci. U. S. A.* **101**, 6536-6541 (2004).

144. Rubin, G. M. *et al*. Comparative genomics of the eukaryotes. *Science* **287**, 2204-2215 (2000).

145. Wunderlich, Z. & DePace, A. H. Modeling transcriptional networks in Drosophila development at multiple scales. *Curr. Opin. Genet. Dev.* **21**, 711-718 (2011).

146. Helfand, S. L. & Rogina, B. Genetics of aging in the fruit fly, Drosophila melanogaster. *Annu. Rev. Genet.* **37**, 329-348 (2003).

147. Song, Y. H. Drosophila melanogaster: a model for the study of DNA damage checkpoint response. *Mol. Cells* **19**, 167-179 (2005).

148. Wilhelm, J. E. & Smibert, C. A. Mechanisms of translational regulation in Drosophila. *Biology of the Cell* **97**, 235-252 (2005).

149. Davies, S. A. Signalling via cGMP: lessons from Drosophila. *Cell. Signal.* **18**, 409-421 (2006).

150. Davis, R. L. Olfactory memory formation in Drosophila: from molecular to systems neuroscience. *Annu. Rev. Neurosci.* **28**, 275-302 (2005).

151. Hirth, F. Drosophila melanogaster in the study of human neurodegeneration. *CNS & neurological disorders drug targets* **9**, 504 (2010).

152. Hardin, P. E. The circadian timekeeping system of Drosophila. *Curr. Biol.* **15**, R714-22 (2005).

153. Adams, M. D. *et al*. The genome sequence of Drosophila melanogaster. *Science* **287**, 2185-2195 (2000).

154. www.flybase.net.

155. St Johnston, D. The art and design of genetic screens: Drosophila melanogaster. *Nature Reviews Genetics* **3**, 176-188 (2002).

156. Pandey, U. B. & Nichols, C. D. Human disease models in Drosophila melanogaster and the role of the fly in therapeutic drug discovery. *Pharmacol. Rev.* **63**, 411-436 (2011).

157. Bilen, J. & Bonini, N. M. Drosophila as a model for human neurodegenerative disease. *Annu. Rev. Genet.* **39**, 153-171 (2005).

158. Woodhouse, E. C. & Liotta, L. A. Drosophila invasive tumors: a model for understanding metastasis. *Cell Cycle* **3**, 37-39 (2004).

159. Wolf, M. J. *et al*. Drosophila as a model for the identification of genes causing adult human heart disease. *Proc. Natl. Acad. Sci. U. S. A.* **103**, 1394-1399 (2006).

160. Saitoe, M., Horiuchi, J., Tamura, T. & Ito, N. Drosophila as a novel animal model for studying the genetics of age-related memory impairment. *Rev. Neurosci.* **16**, 137-150 (2005).

161. Celotto, A. M., Chiu, W. K., Van Voorhies, W. & Palladino, M. J. Modes of metabolic compensation during mitochondrial disease using the Drosophila model of ATP6 dysfunction. *PloS one* **6**, e25823 (2011).

162. Fernández-Ayala, D. J. M., Chen, S., Kemppainen, E., MC O'Dell, K. & Jacobs, H. T. Gene expression in a Drosophila model of mitochondrial disease. *PloS one* **5**, e8549 (2010).

163. Zordan, M. A. *et al*. Post-transcriptional silencing and functional characterization of the Drosophila melanogaster homolog of human Surf1. *Genetics* **172**, 229-241 (2006).

164. Rubin, G. M. & Spradling, A. C. Genetic transformation of Drosophila with transposable element vectors. *Science* **218**, 348-353 (1982).

165. Venken, K. J. T. & Bellen, H. J. Emerging technologies for gene manipulation in Drosophila melanogaster. *Nature Reviews Genetics* **6**, 167-178 (2005).

166. Schneider, I. Cell lines derived from late embryonic stages of Drosophila melanogaster. *J. Embryol. Exp. Morphol.* **27**, 353-365 (1972).

167. Ui, K., Ueda, R. & Miyake, T. Cell lines from imaginal discs of Drosophila melanogaster. *In Vitro Cellular & Developmental Biology-Plant* **23**, 707-711 (1987).

168. Ui, K. *et al*. Newly established cell lines from Drosophila larval CNS express neural specific characteristics. *In Vitro Cellular & Developmental Biology-Animal* **30**, 209-216 (1994).

169. Clemens, J. C. *et al*. Use of double-stranded RNA interference in Drosophila cell lines to dissect signal transduction pathways. *Proceedings of the National Academy of Sciences* **97**, 6499-6503 (2000).

170. Moraes, A. M. *et al*. Drosophila melanogaster S2 cells for expression of heterologous genes: From gene cloning to bioprocess development. *Biotechnol. Adv.* **30**, 613-628 (2012).

171. González, M. *et al*. Generation of stable Drosophila cell lines using multicistronic vectors. *Scientific reports* **1** (2011).

172. Iwaki, T., Figuera, M., Ploplis, V. A. & Castellino, F. J. Rapid selection of Drosophila S2 cells with the puromycin resistance gene. *BioTechniques* **35**, 482-4, 486 (2003).

173. Yanagawa, S., Lee, J. S. & Ishimoto, A. Identification and characterization of a novel line of Drosophila Schneider S2 cells that respond to wingless signaling. *J. Biol. Chem.* **273**, 32353-32359 (1998).

174. Cherbas, L. & Cherbas, P. Drosophila cell culture and transformation. *Cold Spring Harbor Protocols* **2007**, pdb. top6 (2007).

175. Reiter, L. T., Potocki, L., Chien, S., Gribskov, M. & Bier, E. A systematic analysis of human disease-associated gene sequences in Drosophila melanogaster. *Genome Res.* **11**, 1114-1125 (2001).

176. Beckman, K. B. & Ames, B. N. The free radical theory of aging matures. *Physiol. Rev.* **78**, 547-581 (1998).

177. Harman, D. Aging: a theory based on free radical and radiation chemistry. *J. Gerontol.* **11**, 298-300 (1956).

178. Sun, J., Folk, D., Bradley, T. J. & Tower, J. Induced overexpression of mitochondrial Mn-superoxide dismutase extends the life span of adult Drosophila melanogaster. *Genetics* **161**, 661-672 (2002).

179. Fridell, Y. W. C., Sánchez-Blanco, A., Silvia, B. A. & Helfand, S. L. Targeted expression of the human uncoupling protein 2 (hUCP2) to adult neurons extends life span in the fly. *Cell metabolism* **1**, 145-152 (2005).

180. Walker, D. W. & Benzer, S. Mitochondrial “swirls” induced by oxygen stress and in the Drosophila mutant hyperswirl. *Proc. Natl. Acad. Sci. U. S. A.* **101**, 10290-10295 (2004).

181. Oda, Y., Yui, R., Sakamoto, K., Kita, K. & Matsuura, E. T. Age-related changes in the activities of respiratory chain complexes and mitochondrial morphology in Drosophila. *Mitochondrion* **12**, 345-351 (2012).

182. McCarroll, S. A. *et al*. Comparing genomic expression patterns across species identifies shared transcriptional profile in aging. *Nat. Genet.* **36**, 197-204 (2004).

183. Johri, A. & Beal, M. F. Mitochondrial dysfunction in neurodegenerative diseases. *J. Pharmacol. Exp. Ther.* **342**, 619-630 (2012).

184. Filosto, M. *et al*. The role of mitochondria in neurodegenerative diseases. *J. Neurol.* **258**, 1763-1774 (2011).

185. Kwong, J. Q., Beal, M. F. & Manfredi, G. The role of mitochondria in inherited neurodegenerative diseases. *J. Neurochem.* **97**, 1659-1675 (2006).

186. Bonini, N. M. & Fortini, M. E. Human neurodegenerative disease modeling using Drosophila. *Annu. Rev. Neurosci.* **26**, 627-656 (2003).

187. Chang, S. *et al*. Identification of small molecules rescuing fragile X syndrome phenotypes in Drosophila. *Nature chemical biology* **4**, 256-263 (2008).

188. Moloney, A., Sattelle, D. B., Lomas, D. A. & Crowther, D. C. Alzheimer's disease: insights from Drosophila melanogaster models. *Trends Biochem. Sci.* **35**, 228-235 (2010).

189. Iijima-Ando, K. & Iijima, K. Transgenic Drosophila models of Alzheimer’s disease and tauopathies. *Brain Structure and Function* **214**, 245-262 (2010).

190. Muñoz-Soriano, V. & Paricio, N. Drosophila models of Parkinson's disease: discovering relevant pathways and novel therapeutic strategies. *Parkinson's Disease* **2011** (2011).

191. Park, J., Kim, Y. & Chung, J. Mitochondrial dysfunction and Parkinson’s disease genes: insights from Drosophila. *Disease Models & Mechanisms* **2**, 336-340 (2009).

192. Watson, M. R., Lagow, R. D., Xu, K., Zhang, B. & Bonini, N. M. A drosophila model for amyotrophic lateral sclerosis reveals motor neuron damage by human SOD1. *J. Biol. Chem.* **283**, 24972-24981 (2008).

193. Yu, Z. & Bonini, N. M. Modeling human trinucleotide repeat diseases in Drosophila. *Recent advances in the use of drosophila in neurobiology and neurodegeneration* **99**, 191 (2011).

194. Puccio, H. Multicellular models of Friedreich ataxia. *J. Neurol.* **256**, 18-24 (2009).

195. Green, E. W. & Giorgini, F. Choosing and using Drosophila models to characterize modifiers of Huntington's disease. *Biochem. Soc. Trans.* **40**, 739 (2012).

196. Kulikov, A. *et al*. Cytochrome c: the Achilles' heel in apoptosis. *Cellular and Molecular Life Sciences*, 1-11 (2012).

197. Chen, P. & Abrams, J. M. Drosophila apoptosis and Bcl-2 genes: Outliers fly in. *J. Cell Biol.* **148**, 625-628 (2000).

198. Kumar, S. Caspase function in programmed cell death. *Cell Death & Differentiation* **14**, 32-43 (2006).

199. Oberst, A., Bender, C. & Green, D. R. Living with death: the evolution of the mitochondrial pathway of apoptosis in animals. *Cell Death & Differentiation* **15**, 1139-1146 (2008).

200. Hawkins, C. J. *et al*. The Drosophila caspase DRONC cleaves following glutamate or aspartate and is regulated by DIAP1, HID, and GRIM. *J. Biol. Chem.* **275**, 27084-27093 (2000).

201. Abdelwahid, E. *et al*. Mitochondrial disruption in Drosophila apoptosis. *Dev. Cell.* **12**, 793-806 (2007).

202. Dorstyn, L., Mills, K., Lazebnik, Y. & Kumar, S. The two cytochrome c species, DC3 and DC4, are not required for caspase activation and apoptosis in Drosophila cells. *J. Cell Biol.* **167**, 405-410 (2004).

203. Means, J. C., Muro, I. & Clem, R. J. Lack of involvement of mitochondrial factors in caspase activation in a Drosophila cell-free system. *Cell Death & Differentiation* **13**, 1222-1234 (2005).

204. Goyal, G., Fell, B., Sarin, A., Youle, R. J. & Sriram, V. Role of mitochondrial remodeling in programmed cell death in Drosophila melanogaster. *Dev. Cell.* **12**, 807-816 (2007).

205. Arama, E., Agapite, J. & Steller, H. Caspase activity and a specific cytochrome c are required for sperm differentiation in Drosophila. *Dev. Cell.* **4**, 687-697 (2003).

206. Mendes, C. S. *et al*. Cytochrome c-d regulates developmental apoptosis in the Drosophila retina. *EMBO Rep.* **7**, 933-939 (2006).

207. O'Riordan, M. X. D., Bauler, L. D., Scott, F. L. & Duckett, C. S. Inhibitor of apoptosis proteins in eukaryotic evolution and development: a model of thematic conservation. *Developmental cell* **15**, 497-508 (2008).

208. Xu, D. *et al*. Genetic control of programmed cell death (apoptosis) in Drosophila. *Fly* **3**, 78-90 (2009).

209. Wang, C. & Youle, R. J. The role of mitochondria in apoptosis. *Annual Review of Genetics* **43**, 95-118 (2009).

210. Haining, W., Carboy-Newcomb, C., Wei, C. & Steller, H. The proapoptotic function of Drosophila Hid is conserved in mammalian cells. *Proc. Natl. Acad. Sci. U. S. A.* **96**, 4936-4941 (1999).

211. Clavería, C., Caminero, E., Martínez-A, C., Campuzano, S. & Torres, M. GH3, a novel proapoptotic domain in Drosophila Grim, promotes a mitochondrial death pathway. *EMBO J.* **21**, 3327-3336 (2002).

212. Sandu, C., Ryoo, H. D. & Steller, H. Drosophila IAP antagonists form multimeric complexes to promote cell death. *J. Cell Biol.* **190**, 1039-1052 (2010).

213. Sevrioukov, E. A. *et al*. Drosophila Bcl-2 proteins participate in stress-induced apoptosis, but are not required for normal development. *Genesis* **45**, 184-193 (2007).

214. Zhang, H. *et al*. Drosophila pro-apoptotic Bcl-2/Bax homologue reveals evolutionary conservation of cell death mechanisms. *J. Biol. Chem.* **275**, 27303-27306 (2000).

215. Bernardi, P., Scorrano, L., Colonna, R., Petronilli, V. & Di Lisa, F. Mitochondria and cell death. *European Journal of Biochemistry* **264**, 687-701 (2001).

216. Bernardi, P., Scorrano, L., Colonna, R., Petronilli, V. & Di Lisa, F. Mitochondria and cell death. Mechanistic aspects and methodological issues. *Eur. J. Biochem.* **264**, 687-701 (1999).

217. Taupin, P. Processing scarce biological samples for light and transmission electron microscopy. *Eur. J. Histochem.* **52**, 135-139 (2008).

218. Angelin, A. *et al*. Mitochondrial dysfunction in the pathogenesis of Ullrich congenital muscular dystrophy and prospective therapy with cyclosporins. *Proc. Natl. Acad. Sci. U. S. A.* **104**, 991-996 (2007).

219. Pemberton, T. J. & Kay, J. E. Identification and comparative analysis of the peptidyl-prolyl cis/trans isomerase repertoires of H. sapiens, D. melanogaster, C. elegans, S. cerevisiae and Sz. pombe. *Comp. Funct. Genomics* **6**, 277-300 (2005).

APPENDIX

A. Publication 2

FEBS Letters 584 (2010) 2504–2509

ELSEVIER

FEBS Letters

journal homepage: www.FEBSLetters.org

Review

The mitochondrial permeability transition from yeast to mammals

Luca Azzolin [a], Sophia von Stockum [a], Emy Basso [a], Valeria Petronilli [a], Michael A. Forte [b], Paolo Bernardi [a,*]

[a] Department of Biomedical Sciences, CNR Institute of Neuroscience, University of Padova, Italy
[b] Vollum Institute, Oregon Health and Sciences University, Portland, OR, USA

ARTICLE INFO

Article history:
Received 4 March 2010
Revised 1 April 2010
Accepted 9 April 2010
Available online 14 April 2010

Edited by Jan Rydström

Keywords:
Mitochondria
Permeability transition
Calcium
Cyclosporin
Cyclophilin

ABSTRACT

Regulated permeability changes have been detected in mitochondria across species. We review here their key features, with the goal of assessing whether a "permeability transition" similar to that observed in higher eukaryotes is present in other species. The recent discoveries (i) that treatment with cyclosporin A (CsA) unmasks an inhibitory site for inorganic phosphate (Pi) [Basso, E., Petronilli, V., Forte, M.A. and Bernardi, P. (2008) Phosphate is essential for inhibition of the mitochondrial permeability transition pore by cyclosporin A and by cyclophilin D ablation. J. Biol. Chem. 283, 26307–26311], the classical inhibitor of the permeability transition of yeast and (ii) that under proper experimental conditions a matrix Ca^{2+}-dependence can be demonstrated in yeast as well [Yamada, A., Yamamoto, T., Yoshimura, Y., Gouda, S., Kawashima, S., Yamazaki, N., Yamashita, K., Kataoka, M., Nagata, T., Terada, H., Pfeiffer, D.R. and Shinohara Y. (2009) Ca^{2+}-induced permeability transition can be observed even in yeast mitochondria under optimized experimental conditions. Biochim. Biophys. Acta 1787, 1486–1491] suggest that the mitochondrial permeability transition has been conserved during evolution.

1. Introduction

The permeability transition (PT) is an increase of the inner mitochondrial membrane (IMM) permeability mediated by opening of the PT pore (PTP), a putative channel that has been thoroughly characterized functionally but whose molecular nature remains elusive [1]. Long considered an in vitro artifact of little pathophysiological relevance, the role of the PT in disease has been reevaluated in the context of both programmed and accidental cell death [2]. PTP openings of short duration lead to transient depolarization and to rearrangement of the cristae, making more cytochrome *c* available for release even in the absence of outer mitochondrial membrane (OMM) rupture provided that the Bax-Bak pathway had been activated [3]; while long-lasting openings cause permanent depolarization, loss of ionic homeostasis, depletion of matrix pyridine nucleotides, matrix swelling, OMM rupture and triggering of the mitochondrial pathway to apoptosis [4]. Under these conditions mitochondria hydrolyze any ATP available from glycolysis, and thus substantially contribute to energy depletion.

Mitochondrial swelling, its detrimental effects on energy conservation, and the basic features of the process (stimulation by Ca^{2+}, inorganic phosphate (Pi) and fatty acids and inhibition by Mg^{2+}, adenine nucleotides and acidic pH) have been recognized as soon as isolated mitochondria became available for biochemical studies [5–15]. These initial indications were reported before the chemiosmotic theory of energy conservation was proposed [16,17] and generally accepted [18]. How the chemiosmotic theory influenced studies of mitochondrial cation transport and of the PTP has been covered in some detail in previous reviews, to whom the interested Reader is referred for further details [2,19].

The subsequent history of the PTP can be traced to the work of Pfeiffer and co-workers, who proposed that it could play a role in steroidogenesis through a Ca^{2+}-dependent "transformation" of adrenal cortex mitochondria allowing extramitochondrial pyridine nucleotides to gain access to the otherwise impermeable matrix, in keeping with earlier observations [20], and support the 11-β hydroxylation of deoxycorticosterone [21–23]. Through the work of Haworth and Hunter, who coined the term "permeability transition", the basic features of the PTP in heart mitochondria were meticulously characterized, resulting in the key insight that the PT is due to reversible opening of a proteinaceous IMM pore [24–27]. The discovery that the PT can be desensitized by submicromolar concentrations of cyclosporin A (CsA) was a turning point [28–31] because it rekindled interest on the PTP, and provided a

Abbreviations: ANT, adenine nucleotide translocator; CsA, cyclosporin A; CyP, cyclophilin; IMM, inner mitochondrial membrane; NEM, N-ethylmaleimide; OMM, outer mitochondrial membrane; Pi, inorganic phosphate; PT, permeability transition; PTP, permeability transition pore; VDAC, voltage-dependent anion channel; YMUC, yeast mitochondrial unselective channel

* Corresponding author. Address: Department of Biomedical Sciences, University of Padova, Viale Giuseppe Colombo 3, I-35121 Padova, Italy. Fax: +39 049 827 6361.
E-mail address: bernardi@bio.unipd.it (P. Bernardi).

0014-5793/$36.00
doi:10.1016/j.febslet.2010.04.023

pharmacological tool to address its role in cells and organs [32–37] as well as at the single channel level [38–40].

Most classical studies of the PT were carried out in mitochondria obtained from mammals, although permeability changes, most notably those caused by ATP and substrates, have also been studied in yeast [41–55]. In recent years, the growing interest on the PT in cell death has prompted an increasing number of studies in mitochondria from other organisms including plants [56–71], fish [72,73], amphibians [74,75], and the brine shrimp *Artemia franciscana*, a salt- and anoxia-tolerant organism that may represent an exception in that it apparently lacks a PT [76]. Whether the permeability changes observed in mitochondria from these organisms reflect the same molecular events underlying the PT of mammals is not obvious [46]. Here we compare the features of the PT in various organisms in the light of recent mechanistic advances of PTP regulation. We conclude that, with very few exceptions, regulated IMM permeability changes are a conserved feature of mitochondria across species.

2. Cyclophilin and the mechanism of PTP desensitization by cyclosporin A

CsA is a cyclic undecapeptide produced by the fungus *Tolypocladium inflatum*; its ability to prevent the immune response against xenografts [77] has allowed organ transplantation to become a standard surgical practice. This effect of CsA is mediated by two sequential events, (i) the interaction of CsA with cytosolic cyclophilin (CyP) A followed by the formation of a CsA·CyP-A complex; (ii) the binding of this complex to calcineurin, a Ca^{2+}/calmodulin-dependent cytosolic phosphatase that becomes inhibited [78–80]; as a consequence, phospho-NFAT is no longer dephosphorylated and therefore unable to translocate to the nucleus and trigger the IL-2-dependent activation of the immune response against the transplant [78–80].

CyPs are highly conserved, ubiquitous proteins sharing a common domain of about 109 amino acids, the CyP-like domain [81]; they possess peptidyl-prolyl *cis–trans* isomerase (PPIase) activity [82,83], which is inhibited after the binding of CsA [84]. Work with site-directed mutants of CyP-A has allowed the PPIase activity to be separated from CsA binding and calcineurin inhibition [85], and suggested that CyPs perform specific functions through interactions with a limited set of partner proteins rather than serving as general mediators of protein folding [81]. In keeping with this prediction, CyPs are involved in inflammation and vascular dysfunction [86–90], wound healing [91], innate immunity to HIV [92], hepatitis C infection [93], host-parasite interactions [94], tumor biology [95] and, in some species, regulation of the PTP which is mediated by CyP-D, the mitochondrial isoform of the enzyme [96–99]. Genetic ablation of the mouse *Ppif* gene (which encodes for CyP-D) has demonstrated that CyP-D is a unique mitochondrial receptor for CsA, and that it is responsible for modulation of the PTP but not a structural pore component [100–103] (see [104] for a recent review on the pathophysiology of CyP-D).

An important point should be appreciated, i.e. that CsA is *not* a *bona fide* PTP blocker. The inhibitory effect of CsA (and of CyP-D ablation) on the PTP is best described as "desensitization" in that the PTP becomes more resistant to opening after the uptake of Ca^{2+} and Pi in isolated mitochondria, yet opening still takes place for Ca^{2+}–Pi loads that are about twice those required in naïve mitochondria [2]. The mechanism through which CyP-D modulates the PTP has been recently clarified with our discovery that CyP-D ablation (or treatment with CsA) unmasks an inhibitory site for Pi, which is the actual PTP desensitizing agent [105]. It is remarkable that the PT of *Saccharomyces cerevisiae* mitochondria, which is insensitive to CsA in spite of the presence of a mitochondrial CyP, is inhibited by Pi [44]. As should become clear later in the review, we believe that inhibition by Pi is the unifying feature of the PT in all organisms, which allows to fill the gap between "CsA-sensitive" and "CsA-insensitive" PT, and to shed new light on what we regard as an evolutionarily conserved event.

3. The permeability transition in mammals

The PT has been characterized in a large number of tissues, cells and mitochondria of mammalian origin; due to space constraints, here we will only cover the essential regulatory features that allow a comparison to be made with other organisms, while we refer the Reader to previous reviews for a discussion of the pathophysiology of the PTP and its role in cell death [1,2,19,106–113].

Matrix Ca^{2+} is perhaps the single most important factor required for PTP opening. It is difficult to separate the PTP-inducing effects of Ca^{2+} from those of Pi (and possibly of polyphosphate generated in the matrix [114,115]), because the transport of Pi (or of other species able to prevent the buildup of a relevant ΔpH such as acetate or bicarbonate, see discussion in [105]) is required for the uptake of substantial amounts of Ca^{2+}. As discussed in detail elsewhere, matrix Ca^{2+} is best viewed as a permissive factor for PTP opening [2] in the sense that a PT is not observed in the absence of matrix Ca^{2+}, yet Ca^{2+} alone is not sufficient to induce PTP opening. The effect of Ca^{2+} is counteracted by other Me^{2+} ions that are transported by the Ca^{2+} uniporter (such as Sr^{2+} and Mn^{2+}), but the matrix Me^{2+} binding site(s) remain undefined. All divalent cations, including Mg^{2+} and Ca^{2+} itself, instead favor PTP closure through an external Me^{2+} binding site [116]. In the absence of a Ca^{2+} uniporter allowing fast Ca^{2+} uptake in energized mitochondria, it has been hard to assess the importance of matrix Ca^{2+} in *S. cerevisiae*, but recent work with the Ca^{2+} ionophore ETH129 and of proper concentrations of Pi has recently allowed to establish a Ca^{2+}-dependence in this organism as well [52] (see the following paragraph).

As mentioned above, CsA desensitizes the PTP of mammalian mitochondria through an effect on matrix CyP-D. Binding of CsA to CyP-D unmasks an inhibitory site for Pi, which is the actual PTP antagonist [105]. At variance from what is often, and erroneously, stated CsA is not a blocker of the PTP, and a PT can readily occur in the absence of CyP-D and in CsA-treated mitochondria and cells. Another important feature of the mammalian PTP is its modulation by redox effectors, a more oxidized state favoring PTP opening. This effect is conferred by at least three redox-sensitive sites, i.e. (i) a matrix SH site in apparent redox equilibrium with glutathione, which can be blocked by low micromolar concentrations of N-ethylmaleimide (NEM) and monobromobimane but not by impermeant bimanes or β-hydroxybutyrate; (ii) a matrix site in apparent redox equilibrium with pyridine nucleotides, which can be blocked by NEM or β-hydroxybutyrate but not by monobromobimane [117,118]; and (iii) an external thiol that triggers PTP opening after reaction with millimolar concentrations of NEM or low micromolar concentrations of copper-*o*-phenantroline [119]. This complex array of PTP redox-sensitive sites has recently been confirmed by careful studies based on mitochondrial photoirradiation after loading with hematoporphyrin [120].

4. The permeability transition in yeast

Manon and co-workers have published a very useful review of the properties of the "yeast PTP", also called yeast mitochondrial unselective channel (YMUC), and effectively summarized earlier literature on yeast permeability pathways [46]. They have also compared the features of the PTP of yeast and mammals as of 1998, and concluded that even if YMUC presents some functional analogies with mammalian PTP, its regulation is different enough

to consider it a poor model for understanding the PTP of mammals [46]. Several new results, however, suggest that in fact the PTP of yeast and mammals may be closer than previously thought. We shall therefore reconsider the key points raised by Manon et al. in the light of these recent advances.

A first issue concerns the lack of Ca^{2+}-dependence of YMUC even in the presence of the Ca^{2+} ionophore ETH129, which allows electrophoretic matrix Ca^{2+} accumulation in *S. cerevisiae* mitochondria [44]. It was later established that the apparent lack of effect of Ca^{2+} on the PTP of *S. cerevisiae* in the study of Jung et al. [44] was due to the relatively high concentration of Pi (10 mM), which inhibits the yeast permeability pathway induced by ATP and substrates [41,43,44,55]. When addition of the Ca^{2+} ionophore ETH129 was performed in mitochondria incubated with 2 mM rather than 10 mM Pi, a Ca^{2+}-dependence could be readily observed in yeast mitochondria as well [52]. These results match findings where a PT could be caused in *S. cerevisiae* mitochondria at high concentrations of Ca^{2+} provided that the vicinal thiol crosslinker phenylarsine oxide [121] was used to sensitize the pore [47].

A second key point is the lack of sensitivity of the yeast PTP to CsA; as also noted by Manon et al. [46], this adds to a major discrepancy about the effect of Pi, which is an inhibitor of the yeast pore while it is an activator of the PTP in mammals. As we recently showed, however, Pi becomes a PTP inhibitor in mammalian mitochondria after they have been treated with CsA, or after CyP-D has been genetically ablated. We suspect that the yeast mitochondrial cyclophilin CYP3 [122] may not be able to bind the PTP, and thus to hinder the inhibitory site for Pi; as a result, CsA does not affect the yeast PT in spite of its binding to, and inhibition of, CYP3 [122]. As a PT can still occur in mammals in the presence of CsA or after ablation of CyP-D [100–103], we believe that the importance of sensitivity to CsA as a discriminating tool between the PT of mammals and yeast (and of the very occurrence of a PT) may have been overestimated.

A third important point is the presence of a PTP in yeast devoid of the outer membrane voltage-dependent anion channel (VDAC) or of the adenine nucleotide translocator (ANT) [45], which at the time were considered the main candidates as PTP constituents [46]. Subsequent genetic ablation studies have unequivocally shown that neither the ANT [123] nor any VDAC isoform [124] is essential for the PT to occur. We believe that this set of findings removes one of the major hurdles standing between the PTP of yeast and mammals.

Additional points are the lack of effect in yeast of several inducers of the mammalian PTP like carboxyatractylate (inhibitor of the ANT), ligands of the peripheral benzodiazepine receptor, and prooxidants [46]. While differences may certainly exist, some of these may depend on specific experimental conditions. For example the dithiol crosslinker phenylarsine oxide, one of the most powerful sensitizers of the PTP in mammals [121,125,126], was shown to induce the yeast PTP in the presence of relatively high concentrations of Ca^{2+} [47]; the efficacy of oxidants also reflects the activity of antioxidant mechanisms that may be particularly effective in yeast, a unicellular organism that can be exposed to extreme environmental conditions; and osmolarity profoundly affects yeast permeability pathways, which makes comparisons even more difficult given that what is isoosmotic for yeast is hypertonic for mammals [46].

Based on the above considerations, we believe that the yeast and mammalian PT may be the expression of very similar events, although they differ in modulation through mechanisms that will be fully understood only after the molecular nature of the PTP is defined. Hopefully this will also help understand why strain-specific differences exist (mitochondria from *Endomyces magnusii* [127] and *Yarrowia lipolytica* appear to be resistant to the PT [48,51]).

5. The permeability transition in other organisms

Other than in mammals and yeast, occurrence of a PT has been established in plants [56–71], fish [72,73] and amphibians [74,75]. The key features of the PTP, including desensitization by CsA, have been basically conserved in all these organisms although subtle differences may exist, such as the presence of additional effects of CsA on K^+ channels in some plants [56,65]. In the case of fish, the PT has been studied in the great green goby (*Zosterisessor ophiocephalus*) [72] and in the rainbow trout (*Oncorhynchus mykiss*) [73], and has revealed properties that match quite closely those of the pore of mammals. Due to its importance as a model system, we have investigated the occurrence and properties of the mitochondrial PTP in zebrafish (*Danio rerio*). Our results show that zebrafish mitochondria possess a ruthenium red-sensitive Ca^{2+} uniporter, and that they display a Ca^{2+}-sensitive and redox-modulated PT. Occurrence of the PT in situ is modulated by binding of hexokinase like in mammals [128], and it maintains its Pi-dependent sensitivity to CsA (Azzolin et al., unpublished results). All these features make zebrafish a suitable model to study PTP modulation in vivo, to test its occurrence in disease models, and to evaluate its sensitivity to pharmacological treatments.

Another important model organism for which little is known about Ca^{2+} transport and the PT is *Drosophila melanogaster*. Our studies (von Stockum et al., unpublished results) demonstrate that *Drosophila* mitochondria take up Ca^{2+} through a ruthenium red-sensitive mechanism, and display a ruthenium red-insensitive Ca^{2+} release following matrix Ca^{2+} loading. Ca^{2+} release was inhibited by Mg^{2+} (as is the PTP of all species) and Pi (as is the PT of yeast) but was insensitive to Ub0, ADP and CsA (unlike the mammalian PTP). Fourteen CyPs have been identified in *Drosophila*; none of these has an obvious mitochondrial targeting sequence [129], and it remains to be established whether the lack of sensitivity to CsA is due to the absence of a mitochondrial CyP. Ca^{2+}-induced Ca^{2+} release in *Drosophila* mitochondria could be triggered by thiol reactive compounds such as mersalyl at low concentrations (20 μM) and NEM at high concentrations (1–2 mM). Thus, *Drosophila* mitochondria may possess a Ca^{2+}-regulated permeability pathway with features intermediate between the PTP of yeast and that of vertebrates (von Stockum et al., unpublished results).

An interesting study has investigated Ca^{2+} transport in mitochondria from the brine shrimp *A. franciscana*, a crustacean that can tolerate anoxia for years, and also presents a striking resistance to osmotic stress [76]. These mitochondria displayed a high Ca^{2+} transport ability, and accumulated Ca^{2+} loads in excess of 1 μmol × mg protein^{-1} without undergoing a PT, while under similar experimental conditions the PT was readily induced in rat liver mitochondria at the lowest tested load of 0.1 μmol × mg protein^{-1} [76]. *A. franciscana* mitochondria were also resistant to a variety of classical inducers of the mammalian PTP; and resistance to PTP opening could not be ascribed to a lack of mitochondrial CyP, or of any regulators including the ANT and VDAC [76]. Lack of a PT may contribute to the extreme hypoxia tolerance in this species, and assessing the basis for PTP resistance in *A. franciscana* is of obvious interest for future studies on this topic.

6. Conclusions

Table 1 summarizes the key features of the PT in *S. cerevisiae*, *D. melanogaster*, *D. rerio*, potato and mammals. It is apparent that the major discrepancy between *Saccharomyces* and *Drosophila* on one hand and fish, potato and mammals on the other is the sensitivity to CsA. As discussed in the review, however, we feel that this point may have been overestimated; and that inhibition by Pi (in the absence or presence of CsA), regulation by Ca^{2+} and sensitivity to

Table 1
Properties of the permeability transition across species. It summarizes the occurrence of the permeability transition (PT), the presence of a Ca^{2+} uniporter (Unip), the dependence of the PT on matrix Ca^{2+}, sensitivity to Pi as an inducer (ind) or an inhibitor (inhib), the occurrence of PT desensitization by CsA, the presence of a mitochondrial cyclophilin (Mt CyP), and the presence of thiol-dependent, redox-sensitive (S) sites. For further explanation see text.

	PT	Ca^{2+} Unip	Matrix Ca^{2+}	Pi (ind)	CsA	Mt CyP	Pi (inhib)	S site
S. cerevisiae	Yes	No	Yes[a]	Yes	No	Yes	Yes	Yes
D. melanogaster	Yes	Yes	Yes	No	No	?	Yes	Yes
D. rerio	Yes	Yes	Yes	Yes	Yes	Yes	Yes[b]	Yes
Potato	Yes	Yes	Yes	Yes	Yes	Yes	–[c]	Yes
Mammals	Yes	Yes	Yes	Yes	Yes	Yes	Yes[b]	Yes

[a] In the presence of ETH129.
[b] In the presence of CsA.
[c] –: Not tested.

redox effectors represent the minimum requirements for defining the PT, and unifying features that bridge the gap between yeast and higher eukaryotes. If our view proves to be correct, genetic strategies available in yeast, *Drosophila* and zebrafish could be of tremendous help in the identification of the molecular components of the PTP.

Acknowledgments

Supported by Grants from the Fondazione Cariparo (Padova), the University of Padova Progetti di Eccellenza "Models of mitochondrial diseases", Telethon-Italy and AIRC (to P.B.) and by the NIH-PHS (grant GM69883 to M.A.F. and P.B.).

References

[1] Rasola, A. and Bernardi, P. (2007) The mitochondrial permeability transition pore and its involvement in cell death and in disease pathogenesis. Apoptosis 12, 815–833.
[2] Bernardi, P., Krauskopf, A., Basso, E., Petronilli, V., Blachly-Dyson, E., Di Lisa, F. and Forte, M.A. (2006) The mitochondrial permeability transition from in vitro artifact to disease target. FEBS J. 273, 2077–2099.
[3] Scorrano, L., Ashiya, M., Buttle, K., Weiler, S., Oakes, S.A., Mannella, C.A. and Korsmeyer, S.J. (2002) A distinct pathway remodels mitochondrial cristae and mobilizes cytochrome c during apoptosis. Dev. Cell 2, 55–67.
[4] Petronilli, V., Penzo, D., Scorrano, L., Bernardi, P. and Di Lisa, F. (2001) The mitochondrial permeability transition, release of cytochrome c and cell death. Correlation with the duration of pore openings in situ. J. Biol. Chem. 276, 12030–12034.
[5] Raaflaub, J. (1953) Die schwellung isolierter leberzell mitochondrien und ihre physikalisch beeinflubarkeit. Helv. Physiol. Pharmacol. Acta 11, 142–156.
[6] Raaflaub, J. (1953) Über den wirkungsmechanismus von adenosintriphosphat (ATP) als cofaktor isolierter mitochondrien. Helv. Physiol. Pharmacol. Acta 11, 157–165.
[7] Brenner-Holzach, O. and Raaflaub, J. (1954) Die korrelation zwischen der schwellung isolierter mitochondrien und dem abbau intramitochondrialen adenosinnucleotide (ATP, ADP, AMP, CoA). Helv. Physiol. Pharmacol. Acta 12, 242–252.
[8] Hunter Jr., F.E. and Ford, L. (1955) Inactivation of oxidative and phosphorylative systems in mitochondria by preincubation with phosphate and other ions. J. Biol. Chem. 216, 357–369.
[9] Tapley, D.F. (1956) The effect of thyroxine and other substances on the swelling of isolated rat liver mitochondria. J. Biol. Chem. 222, 325–339.
[10] Lehninger, A.L. and Remmert, L.F. (1959) An endogenous uncoupling and swelling agent in liver mitochondria and its enzymic function. J. Biol. Chem. 234, 2459–2464.
[11] Lehninger, A.L. (1959) Reversal of various types of mitochondrial swelling by adenosine triphosphate. J. Biol. Chem. 234, 2465–2471.
[12] Wojtczak, L. and Lehninger, A.L. (1961) Formation and disappearance of an endogenous uncoupling factor during swelling and contraction of mitochondria. Biochim. Biophys. Acta 51, 442–456.
[13] Zborowski, J. and Wojtczak, L. (1963) Induction of swelling of liver mitochondria by fatty acids of various chain length. Biochim. Biophys. Acta 70, 596–598.
[14] Azzi, A. and Azzone, G.F. (1965) Swelling and shrinkage phenomena in liver mitochondria. I. Large amplitude swelling induced by inorganic phosphate and by ATP. Biochim. Biophys. Acta 105, 253–264.
[15] Azzone, G.F. and Azzi, A. (1965) Volume changes in liver mitochondria. Proc. Natl. Acad. Sci. USA 53, 1084–1089.
[16] Mitchell, P. (1961) Coupling of phosphorylation to electron and hydrogen transfer by a chemio-osmotic type of mechanism. Nature 191, 144–148.
[17] Mitchell, P. (1966) Chemiosmotic Coupling in Oxidative and Photosynthetic Phosphorylation, Glynn Research, Bodmin (Cornwall), England.
[18] Mitchell, P. (1979) Keilin's respiratory chain concept and its chemiosmotic consequences. Science 206, 1148–1159.
[19] Bernardi, P. (1999) Mitochondrial transport of cations: channels, exchangers and permeability transition. Physiol. Rev. 79, 1127–1155.
[20] Vinogradov, A., Scarpa, A. and Chance, B. (1972) Calcium and pyridine nucleotide interaction in mitochondrial membranes. Arch. Biochem. Biophys. 152, 646–654.
[21] Pfeiffer, D.R. and Tchen, T.T. (1973) The role of Ca^{2+} in control of malic enzyme activity in bovine adrenal cortex mitochondria. Biochem. Biophys. Res. Commun. 50, 807–813.
[22] Pfeiffer, D.R. and Tchen, T.T. (1975) The activation of adrenal cortex mitochondrial malic enzyme by Ca^{2+} and Mg^{2+}. Biochemistry 14, 89–96.
[23] Pfeiffer, D.R., Kuo, T.H. and Tchen, T.T. (1976) Some effects of Ca^{2+}, Mg^{2+}, and Mn^{2+} on the ultrastructure, light-scattering properties, and malic enzyme activity of adrenal cortex mitochondria. Arch. Biochem. Biophys. 176, 556–563.
[24] Hunter, D.R., Haworth, R.A. and Southard, J.H. (1976) Relationship between configuration, function, and permeability in calcium-treated mitochondria. J. Biol. Chem. 251, 5069–5077.
[25] Hunter, D.R. and Haworth, R.A. (1979) The Ca^{2+}-induced membrane transition in mitochondria. I. The protective mechanisms. Arch. Biochem. Biophys. 195, 453–459.
[26] Haworth, R.A. and Hunter, D.R. (1979) The Ca^{2+}-induced membrane transition of rat liver mitochondria. II. Nature of the Ca^{2+} trigger site. Arch. Biochem. Biophys. 195, 460–467.
[27] Hunter, D.R. and Haworth, R.A. (1979) The Ca^{2+}-induced membrane transition in mitochondria. III. Transitional Ca^{2+} release. Arch. Biochem. Biophys. 195, 468–477.
[28] Fournier, N., Ducet, G. and Crevat, A. (1987) Action of cyclosporine on mitochondrial calcium fluxes. J. Bioenergy Biomembrane 19, 297–303.
[29] Crompton, M., Ellinger, H. and Costi, A. (1988) Inhibition by cyclosporin A of a Ca^{2+}-dependent pore in heart mitochondria activated by inorganic phosphate and oxidative stress. Biochem. J. 255, 357–360.
[30] Broekemeier, K.M., Dempsey, M.E. and Pfeiffer, D.R. (1989) Cyclosporin A is a potent inhibitor of the inner membrane permeability transition in liver mitochondria. J. Biol. Chem. 264, 7826–7830.
[31] Davidson, A.M. and Halestrap, A.P. (1990) Partial inhibition by cyclosporin A of the swelling of liver mitochondria in vivo and in vitro induced by submicromolar $[Ca^{2+}]$, but not by butyrate. Evidence for two distinct swelling mechanisms. Biochem. J. 268, 147–152.
[32] Broekemeier, K.M., Carpenter Deyo, L., Reed, D.J. and Pfeiffer, D.R. (1992) Cyclosporin A protects hepatocytes subjected to high Ca^{2+} and oxidative stress. FEBS Lett. 304, 192–194.
[33] Imberti, R., Nieminen, A.L., Herman, B. and Lemasters, J.J. (1992) Synergism of cyclosporin A and phospholipase inhibitors in protection against lethal injury to rat hepatocytes from oxidant chemicals. Res. Commun. Chem. Pathol. Pharmacol. 78, 27–38.
[34] Pastorino, J.G., Snyder, J.W., Serroni, A., Hoek, J.B. and Farber, J.L. (1993) Cyclosporin and carnitine prevent the anoxic death of cultured hepatocytes by inhibiting the mitochondrial permeability transition. J. Biol. Chem. 268, 13791–13798.
[35] Duchen, M.R., McGuinness, O., Brown, L.A. and Crompton, M. (1993) On the involvement of a cyclosporin A sensitive mitochondrial pore in myocardial reperfusion injury. Cardiovasc. Res. 27, 1790–1794.
[36] Zoeteweij, J.P., van de Water, B., de Bont, H.J., Mulder, G.J. and Nagelkerke, J.F. (1993) Calcium-induced cytotoxicity in hepatocytes after exposure to extracellular ATP is dependent on inorganic phosphate. Effects on mitochondrial calcium. J. Biol. Chem. 268, 3384–3388.
[37] Griffiths, E.J. and Halestrap, A.P. (1995) Mitochondrial non-specific pores remain closed during cardiac ischaemia, but open upon reperfusion. Biochem. J. 307, 93–98.
[38] Szabó, I. and Zoratti, M. (1991) The giant channel of the inner mitochondrial membrane is inhibited by cyclosporin A. J. Biol. Chem. 266, 3376–3379.
[39] Szabó, I., Bernardi, P. and Zoratti, M. (1992) Modulation of the mitochondrial megachannel by divalent cations and protons. J. Biol. Chem. 267, 2940–2946.
[40] Szabó, I. and Zoratti, M. (1992) The mitochondrial megachannel is the permeability transition pore. J. Bioenergy Biomembrane 24, 111–117.

[41] Prieto, S., Bouillaud, F., Ricquier, D. and Rial, E. (1992) Activation by ATP of a proton-conducting pathway in yeast mitochondria. Eur. J. Biochem. 208, 487–491.

[42] Guerin, B., Bunoust, O., Rouqueys, V. and Rigoulet, M. (1994) ATP-induced unspecific channel in yeast mitochondria. J. Biol. Chem. 269, 25406–25410.

[43] Prieto, S., Bouillaud, F. and Rial, E. (1996) The nature and regulation of the ATP-induced anion permeability in *Saccharomyces cerevisiae* mitochondria. Arch. Biochem. Biophys. 334, 43–49.

[44] Jung, D.W., Bradshaw, P.C. and Pfeiffer, D.R. (1997) Properties of a cyclosporin-insensitive permeability transition pore in yeast mitochondria. J. Biol. Chem. 272, 21104–21112.

[45] Roucou, X., Manon, S. and Guerin, M. (1997) Conditions allowing different states of ATP- and GDP-induced permeability in mitochondria from different strains of *Saccharomyces cerevisiae*. Biochim. Biophys. Acta 1324, 120–132.

[46] Manon, S., Roucou, X., Guerin, M., Rigoulet, M. and Guerin, B. (1998) Characterization of the yeast mitochondria unselective channel: a counterpart to the mammalian permeability transition pore? J. Bioenergy Biomembrane 30, 419–429.

[47] Kowaltowski, A.J., Vercesi, A.E., Rhee, S.G. and Netto, L.E. (2000) Catalases and thioredoxin peroxidase protect *Saccharomyces cerevisiae* against Ca^{2+}-induced mitochondrial membrane permeabilization and cell death. FEBS Lett. 473, 177–182.

[48] Deryabina, Y.I., Bazhenova, E.N., Saris, N.E. and Zvyagilskaya, R.A. (2001) Ca^{2+} efflux in mitochondria from the yeast *Endomyces magnusii*. J. Biol. Chem. 276, 47801–47806.

[49] Perez-Vazquez, V., Saavedra-Molina, A. and Uribe, S. (2003) In *Saccharomyces cerevisiae*, cations control the fate of the energy derived from oxidative metabolism through the opening and closing of the yeast mitochondrial unselective channel. J. Bioenergy Biomembrane 35, 231–241.

[50] Gutierrez-Aguilar, M., Perez-Vazquez, V., Bunoust, O., Manon, S., Rigoulet, M. and Uribe, S. (2007) In yeast, Ca^{2+} and octylguanidine interact with porin (VDAC) preventing the mitochondrial permeability transition. Biochim. Biophys. Acta 1767, 1245–1251.

[51] Kovaleva, M.V., Sukhanova, E.I., Trendeleva, T.A., Zyl'kova, M.V., Ural'skaya, L.A., Popova, K.M., Saris, N.E. and Zvyagilskaya, R.A. (2009) Induction of a non-specific permeability transition in mitochondria from *Yarrowia lipolytica* and *Dipodascus* (*Endomyces*) *magnusii* yeasts. J. Bioenergy Biomembrane 41, 239–249.

[52] Yamada, A., Yamamoto, T., Yoshimura, Y., Gouda, S., Kawashima, S., Yamazaki, N., Yamashita, K., Kataoka, M., Nagata, T., Terada, H., Pfeiffer, D.R. and Shinohara, Y. (2009) Ca^{2+}-induced permeability transition can be observed even in yeast mitochondria under optimized experimental conditions. Biochim. Biophys. Acta 1787, 1486–1491.

[53] Cabrera-Orefice, A., Guerrero-Castillo, S., Luevano-Martinez, L.A., Pena, A. and Uribe-Carvajal, S. (2010) Mitochondria from the salt-tolerant yeast *Debaryomyces hansenii* (halophilic organelles?). J. Bioenergy Biomembrane.

[54] Gutierrez-Aguilar, M., Perez-Martinez, X., Chavez, E. and Uribe-Carvajal, S. (2010) In *Saccharomyces cerevisiae*, the phosphate carrier is a component of the mitochondrial unselective channel. Arch. Biochem. Biophys. 494, 184–191.

[55] Velours, J., Rigoulet, M. and Guerin, B. (1977) Protection of yeast mitochondrial structure by phosphate and other H^+-donating anions. FEBS Lett. 81, 18–22.

[56] Vianello, A., Macri, F., Braidot, E. and Mokhova, E.N. (1995) Effect of cyclosporin A on energy coupling in pea stem mitochondria. FEBS Lett. 371, 258–260.

[57] Fortes, F., Castilho, R.F., Catisti, R., Carnieri, E.G. and Vercesi, A.E. (2001) Ca^{2+} induces a cyclosporin A-insensitive permeability transition pore in isolated potato tuber mitochondria mediated by reactive oxygen species. J. Bioenergy Biomembrane 33, 43–51.

[58] Arpagaus, S., Rawyler, A. and Braendle, R. (2002) Occurrence and characteristics of the mitochondrial permeability transition in plants. J. Biol. Chem. 277, 1780–1787.

[59] Curtis, M.J. and Wolpert, T.J. (2002) The oat mitochondrial permeability transition and its implication in victorin binding and induced cell death. Plant J. 29, 295–312.

[60] Saviani, E.E., Orsi, C.H., Oliveira, J.F., Pinto-Maglio, C.A. and Salgado, I. (2002) Participation of the mitochondrial permeability transition pore in nitric oxide-induced plant cell death. FEBS Lett. 510, 136–140.

[61] Tiwari, B.S., Belenghi, B. and Levine, A. (2002) Oxidative stress increased respiration and generation of reactive oxygen species, resulting in ATP depletion, opening of mitochondrial permeability transition, and programmed cell death. Plant Physiol. 128, 1271–1281.

[62] Virolainen, E., Blokhina, O. and Fagerstedt, K. (2002) Ca^{2+}-induced high amplitude swelling and cytochrome c release from wheat (*Triticum aestivum* L.) mitochondria under anoxic stress. Ann. Bot. 90, 509–516.

[63] Koulintchenko, M., Konstantinov, Y. and Dietrich, A. (2003) Plant mitochondria actively import DNA via the permeability transition pore complex. EMBO J. 22, 1245–1254.

[64] Curtis, M.J. and Wolpert, T.J. (2004) The victorin-induced mitochondrial permeability transition precedes cell shrinkage and biochemical markers of cell death, and shrinkage occurs without loss of membrane integrity. Plant J. 38, 244–259.

[65] Petrussa, E., Casolo, V., Peresson, C., Braidot, E., Vianello, A. and Macri, F. (2004) The K_{ATP} channel is involved in a low-amplitude permeability transition in plant mitochondria. Mitochondrion 3, 297–307.

[66] Kim, M., Lim, J.H., Ahn, C.S., Park, K., Kim, G.T., Kim, W.T. and Pai, H.S. (2006) Mitochondria-associated hexokinases play a role in the control of programmed cell death in *Nicotiana benthamiana*. Plant Cell 18, 2341–2355.

[67] Lin, J., Wang, Y. and Wang, G. (2006) Salt stress-induced programmed cell death in tobacco protoplasts is mediated by reactive oxygen species and mitochondrial permeability transition pore status. J. Plant Physiol. 163, 731–739.

[68] Contran, N., Cerana, R., Crosti, P. and Malerba, M. (2007) Cyclosporin A inhibits programmed cell death and cytochrome *c* release induced by fusicoccin in sycamore cells. Protoplasma 231, 193–199.

[69] Gao, C., Xing, D., Li, L. and Zhang, L. (2008) Implication of reactive oxygen species and mitochondrial dysfunction in the early stages of plant programmed cell death induced by ultraviolet-C overexposure. Planta 227, 755–767.

[70] Panda, S.K., Yamamoto, Y., Kondo, H. and Matsumoto, H. (2008) Mitochondrial alterations related to programmed cell death in tobacco cells under aluminium stress. C.R. Biol 331, 597–610.

[71] Scott, I. and Logan, D.C. (2008) Mitochondrial morphology transition is an early indicator of subsequent cell death in *Arabidopsis*. New Phytol. 177, 90–101.

[72] Toninello, A., Salvi, M. and Colombo, L. (2000) The membrane permeability transition in liver mitochondria of the great green goby *Zosterisessor ophiocephalus* (Pallas). J. Exp. Biol. 203, 3425–3434.

[73] Krumschnabel, G., Manzl, C., Berger, C. and Hofer, B. (2005) Oxidative stress, mitochondrial permeability transition, and cell death in Cu-exposed trout hepatocytes. Toxicol. Appl. Pharmacol. 209, 62–73.

[74] Hanada, H., Katsu, K., Kanno, T., Sato, E.F., Kashiwagi, A., Sasaki, J., Inoue, M. and Utsumi, K. (2003) Cyclosporin A inhibits thyroid hormone-induced shortening of the tadpole tail through membrane permeability transition. Comp. Biochem. Physiol. B: Biochem. Mol. Biol. 135, 473–483.

[75] Savina, M.V., Emelyanova, L.V. and Belyaeva, E.A. (2006) Bioenergetic parameters of lamprey and frog liver mitochondria during metabolic depression and activity. Comp. Biochem. Physiol. B: Biochem. Mol. Biol. 145, 296–305.

[76] Menze, M.A., Hutchinson, K., Laborde, S.M. and Hand, S.C. (2005) Mitochondrial permeability transition in the crustacean *Artemia franciscana*: absence of a calcium-regulated pore in the face of profound calcium storage. Am. J. Physiol. 289, R68–R76.

[77] Borel, J.F., Feurer, C., Gubler, H.U. and Stahelin, H. (1976) Biological effects of cyclosporin A: a new antilymphocytic agent. Agents Actions 6, 468–475.

[78] Liu, J., Farmer, J.D.J., Lane, W.S., Friedman, J., Weissman, I. and Schreiber, S.L. (1991) Calcineurin is a common target of cyclophilin–cyclosporin A and FKBP–FK506 complexes. Cell 66, 807–815.

[79] Clipstone, N.A. and Crabtree, G.R. (1992) Identification of calcineurin as a key signalling enzyme in T-lymphocyte activation. Nature 357, 695–697.

[80] Walsh, C.T., Zydowsky, L.D. and McKeon, F.D. (1992) Cyclosporin A, the cyclophilin class of peptidyl-prolyl isomerases, and blockade of T cell signal transduction. J. Biol. Chem. 267, 13115–13118.

[81] Wang, P. and Heitman, J. (2005) The cyclophilins. Genome Biol. 6, 226.1–226.6.

[82] Fischer, G., Wittmann-Liebold, B., Lang, K., Kiefhaber, T. and Schmid, F.X. (1989) Cyclophilin and peptidyl-prolyl cis–trans isomerase are probably identical proteins. Nature 337, 476–478.

[83] Takahashi, N., Hayano, T. and Suzuki, M. (1989) Peptidyl-prolyl cis–trans isomerase is the cyclosporin A-binding protein cyclophilin. Nature 337, 473–475.

[84] Borel, J.F., Feurer, C., Magnee, C. and Stahelin, H. (1977) Effects of the new anti-lymphocytic peptide cyclosporin A in animals. Immunology 32, 1017–1025.

[85] Zydowsky, L.D., Etzkorn, F.A., Chang, H.Y., Ferguson, S.B., Stolz, L.A., Ho, S.I. and Walsh, C.T. (1992) Active site mutants of human cyclophilin A separate peptidyl-prolyl isomerase activity from cyclosporin A binding and calcineurin inhibition. Protein Sci. 1, 1092–1099.

[86] Jin, Z.G., Lungu, A.O., Xie, L., Wang, M., Wong, C. and Berk, B.C. (2004) Cyclophilin A is a proinflammatory cytokine that activates endothelial cells. Arterioscler. Thromb. Vasc. Biol. 24, 1186–1191.

[87] Kim, S.H., Lessner, S.M., Sakurai, Y. and Galis, Z.S. (2004) Cyclophilin A as a novel biphasic mediator of endothelial activation and dysfunction. Am. J. Pathol. 164, 1567–1574.

[88] Kim, H., Kim, W.J., Jeon, S.T., Koh, E.M., Cha, H.S., Ahn, K.S. and Lee, W.H. (2005) Cyclophilin A may contribute to the inflammatory processes in rheumatoid arthritis through induction of matrix degrading enzymes and inflammatory cytokines from macrophages. Clin. Immunol. 116, 217–224.

[89] Arora, K., Gwinn, W.M., Bower, M.A., Watson, A., Okwumabua, I., MacDonald, H.R., Bukrinsky, M.I. and Constant, S.L. (2005) Extracellular cyclophilins contribute to the regulation of inflammatory responses. J. Immunol. 175, 517–522.

[90] Damsker, J.M., Bukrinsky, M.I. and Constant, S.L. (2007) Preferential chemotaxis of activated human CD^{4+} T cells by extracellular cyclophilin A. J. Leukoc. Biol. 82, 613–618.

[91] Kong, W., Li, S., Longaker, M.T. and Lorenz, H.P. (2007) Cyclophilin C-associated protein is up-regulated during wound healing. J. Cell Physiol. 210, 153–160.

[92] Sokolskaja, E. and Luban, J. (2006) Cyclophilin, TRIM5, and innate immunity to HIV-1. Curr. Opin. Microbiol. 9, 404–408.

[93] Flisiak, R., Dumont, J.M. and Crabbe, R. (2007) Cyclophilin inhibitors in hepatitis C viral infection. Exp. Opin. Invest. Drugs 16, 1345–1354.
[94] Bell, A., Monaghan, P. and Page, A.P. (2006) Peptidyl-prolyl cis–trans isomerases (immunophilins) and their roles in parasite biochemistry, host-parasite interaction and antiparasitic drug action. Int. J. Parasitol. 36, 261–276.
[95] Yao, Q., Li, M., Yang, H., Chai, H., Fisher, W. and Chen, C. (2005) Roles of cyclophilins in cancers and other organ systems. World J. Surg. 29, 276–280.
[96] Connern, C.P. and Halestrap, A.P. (1992) Purification and N-terminal sequencing of peptidyl-prolyl cis–trans-isomerase from rat liver mitochondrial matrix reveals the existence of a distinct mitochondrial cyclophilin. Biochem. J. 284, 381–385.
[97] Nicolli, A., Basso, E., Petronilli, V., Wenger, R.M. and Bernardi, P. (1996) Interactions of cyclophilin with the mitochondrial inner membrane and regulation of the permeability transition pore, a cyclosporin A-sensitive channel. J. Biol. Chem. 271, 2185–2192.
[98] Woodfield, K.Y., Price, N.T. and Halestrap, A.P. (1997) CDNA cloning of rat mitochondrial cyclophilin. Biochim. Biophys. Acta 1351, 27–30.
[99] Waldmeier, P.C., Zimmermann, K., Qian, T., Tintelnot-Blomley, M. and Lemasters, J.J. (2003) Cyclophilin D as a drug target. Curr. Med. Chem 10, 1485–1506.
[100] Baines, C.P., Kaiser, R.A., Purcell, N.H., Blair, N.S., Osinska, H., Hambleton, M.A., Brunskill, E.W., Sayen, M.R., Gottlieb, R.A., Dorn, G.W., Robbins, J. and Molkentin, J.D. (2005) Loss of cyclophilin D reveals a critical role for mitochondrial permeability transition in cell death. Nature 434, 658–662.
[101] Basso, E., Fante, L., Fowlkes, J., Petronilli, V., Forte, M.A. and Bernardi, P. (2005) Properties of the permeability transition pore in mitochondria devoid of cyclophilin D. J. Biol. Chem. 280, 18558–18561.
[102] Nakagawa, T., Shimizu, S., Watanabe, T., Yamaguchi, O., Otsu, K., Yamagata, H., Inohara, H., Kubo, T. and Tsujimoto, Y. (2005) Cyclophilin D-dependent mitochondrial permeability transition regulates some necrotic but not apoptotic cell death. Nature 434, 652–658.
[103] Schinzel, A.C., Takeuchi, O., Huang, Z., Fisher, J.K., Zhou, Z., Rubens, J., Hetz, C., Danial, N.N., Moskowitz, M.A. and Korsmeyer, S.J. (2005) Cyclophilin D is a component of mitochondrial permeability transition and mediates neuronal cell death after focal cerebral ischemia. Proc. Natl. Acad. Sci. USA 102, 12005–12010.
[104] Giorgio, V., Soriano, M.E., Basso, E., Bisetto, E., Lippe, G., Forte, M.A. and Bernardi, P. (2010) Cyclophilin D in Mitochondrial Pathophysiology. Biochim. Biophys. Acta. doi:10.1016/j.bbabio.2009.12.006.
[105] Basso, E., Petronilli, V., Forte, M.A. and Bernardi, P. (2008) Phosphate is essential for inhibition of the mitochondrial permeability transition pore by cyclosporin A and by cyclophilin D ablation. J. Biol. Chem. 283, 26307–26311.
[106] Gunter, T.E. and Pfeiffer, D.R. (1990) Mechanisms by which mitochondria transport calcium. Am. J. Physiol. 258, C755–C786.
[107] Bernardi, P., Broekemeier, K.M. and Pfeiffer, D.R. (1994) Recent progress on regulation of the mitochondrial permeability transition pore; a cyclosporin-sensitive pore in the inner mitochondrial membrane. J. Bioenergy Biomembrane 26, 509–517.
[108] Zoratti, M. and Szabó, I. (1995) The mitochondrial permeability transition. Biochim. Biophys. Acta 1241, 139–176.
[109] Halestrap, A.P., Kerr, P.M., Javadov, S. and Woodfield, K.Y. (1998) Elucidating the molecular mechanism of the permeability transition pore and its role in reperfusion injury. Biochim. Biophys. Acta 1366, 79–94.
[110] Bernardi, P., Scorrano, L., Colonna, R., Petronilli, V. and Di Lisa, F. (1999) Mitochondria and cell death. Mechanistic aspects and methodological issues. Eur. J. Biochem. 264, 687–701.
[111] Crompton, M. (1999) The mitochondrial permeability transition pore and its role in cell death. Biochem. J. 341, 233–249.
[112] Forte, M. and Bernardi, P. (2005) Genetic dissection of the permeability transition pore. J. Bioenergy Biomembrane 37, 121–128.
[113] Leung, A.W. and Halestrap, A.P. (2008) Recent progress in elucidating the molecular mechanism of the mitochondrial permeability transition pore. Biochim. Biophys. Acta 1777, 946–952.
[114] Abramov, A.Y., Fraley, C., Diao, C.T., Winkfein, R., Colicos, M.A., Duchen, M.R., French, R.J. and Pavlov, E. (2007) Targeted polyphosphatase expression alters mitochondrial metabolism and inhibits calcium-dependent cell death. Proc. Natl. Acad. Sci. USA 104, 18091–18096.
[115] Pavlov, E., Aschar-Sobbi, R., Campanella, M., Turner, R.J., Gomez-Garcia, M.R. and Abramov, A.Y. (in press) Inorganic polyphosphate and energy metabolism in mammalian cells. J. Biol. Chem. doi:10.1074/jbc.M109.013011.
[116] Bernardi, P., Veronese, P. and Petronilli, V. (1993) Modulation of the mitochondrial cyclosporin A-sensitive permeability transition pore. I. Evidence for two separate Me^{2+} binding sites with opposing effects on the pore open probability. J. Biol. Chem. 268, 1005–1010.
[117] Costantini, P., Chernyak, B.V., Petronilli, V. and Bernardi, P. (1995) Selective inhibition of the mitochondrial permeability transition pore at the oxidation–reduction sensitive dithiol by monobromobimane. FEBS Lett. 362, 239–242.
[118] Costantini, P., Chernyak, B.V., Petronilli, V. and Bernardi, P. (1996) Modulation of the mitochondrial permeability transition pore by pyridine nucleotides and dithiol oxidation at two separate sites. J. Biol. Chem. 271, 6746–6751.
[119] Costantini, P., Colonna, R. and Bernardi, P. (1998) Induction of the mitochondrial permeability transition pore by N-ethylmaleimide depends on secondary oxidation of critical thiol groups. Potentiation by copper-*ortho*-phenanthroline without dimerization of the adenine nucleotide translocase. Biochim. Biophys. Acta 1365, 385–392.
[120] Petronilli, V., Šileikyte, J., Zulian, A., Dabbeni-Sala, F., Jori, G., Gobbo, S., Tognon, G., Nikolov, P., Bernardi, P. and Ricchelli, F. (2009) Switch from inhibition to activation of the mitochondrial permeability transition during hematoporphyrin-mediated photooxidative stress. Unmasking pore-regulating external thiols. Biochim. Biophys. Acta 1787, 897–904.
[121] Lenartowicz, E., Bernardi, P. and Azzone, G.F. (1991) Phenylarsine oxide induces the cyclosporin A-sensitive membrane permeability transition in rat liver mitochondria. J. Bioenergy Biomembrane 23, 679–688.
[122] Matouschek, A., Rospert, S., Schmid, K., Glick, B.S. and Schatz, G. (1995) Cyclophilin catalyzes protein folding in yeast mitochondria. Proc. Natl. Acad. Sci. USA 92, 6319–6323.
[123] Kokoszka, J.E., Waymire, K.G., Levy, S.E., Sligh, J.E., Cai, J., Jones, D.P., MacGregor, G.R. and Wallace, D.C. (2004) The ADP/ATP translocator is not essential for the mitochondrial permeability transition pore. Nature 427, 461–465.
[124] Baines, C.P., Kaiser, R.A., Sheiko, T., Craigen, W.J. and Molkentin, J.D. (2007) Voltage-dependent anion channels are dispensable for mitochondrial-dependent cell death. Nat. Cell Biol. 9, 550–555.
[125] Bernardi, P., Vassanelli, S., Veronese, P., Colonna, R., Szabo, I. and Zoratti, M. (1992) Modulation of the mitochondrial permeability transition pore. Effect of protons and divalent cations. J. Biol. Chem. 267, 2934–2939.
[126] Bernardi, P. (1992) Modulation of the mitochondrial cyclosporin A-sensitive permeability transition pore by the proton electrochemical gradient. Evidence that the pore can be opened by membrane depolarization. J. Biol. Chem. 267, 8834–8839.
[127] Bazhenova, E.N., Deryabina, Y.I., Eriksson, O., Zvyagilskaya, R.A. and Saris, N.E. (1998) Characterization of a high capacity calcium transport system in mitochondria of the yeast *Endomyces magnusii*. J. Biol. Chem. 273, 4372–4377.
[128] Chiara, F., Castellaro, D., Marin, O., Petronilli, V., Brusilow, W.S., Juhaszova, M., Sollott, S.J., Forte, M., Bernardi, P. and Rasola, A. (2008) Hexokinase II detachment from mitochondria triggers apoptosis through the permeability transition pore independent of voltage-dependent anion channels. PLoS One 3, e1852.
[129] Pemberton, T.J. and Kay, J.E. (2005) Identification and comparative analysis of the peptidyl-prolyl cis/trans isomerase repertoires of *H. Sapiens*, *D. melanogaster*, *C. elegans*, *S. cerevisiae* and *Sz. pombe*. Comp. Funct. Genomics 6, 277–300.

B. Publication 3

Cell Calcium 52 (2012) 22–27

Contents lists available at SciVerse ScienceDirect

Cell Calcium

journal homepage: www.elsevier.com/locate/ceca

The permeability transition pore as a Ca^{2+} release channel: New answers to an old question

Paolo Bernardi*, Sophia von Stockum

Department of Biomedical Sciences and CNR Institute of Neuroscience, University of Padova, Padova, Italy

ARTICLE INFO

Article history:
Received 16 February 2012
Received in revised form 21 March 2012
Accepted 21 March 2012
Available online 17 April 2012

Keywords:
Mitochondria
Permeability transition
Ca^{2+} release

ABSTRACT

Mitochondria possess a sophisticated array of Ca^{2+} transport systems reflecting their key role in physiological Ca^{2+} homeostasis. With the exception of most yeast strains, energized organelles are endowed with a very fast and efficient mechanism for Ca^{2+} uptake, the ruthenium red (RR)-sensitive mitochondrial Ca^{2+} uniporter (MCU); and one main mechanism for Ca^{2+} release, the RR-insensitive $3Na^+$–Ca^{2+} antiporter. An additional mechanism for Ca^{2+} release is provided by a Na^+ and RR-insensitive release mechanism, the putative $3H^+$–Ca^{2+} antiporter. A potential kinetic imbalance is present, however, because the V_{max} of the MCU is of the order of 1400 nmol Ca^{2+} mg^{-1} protein min^{-1} while the combined V_{max} of the efflux pathways is about 20 nmol Ca^{2+} mg^{-1} protein min^{-1}. This arrangement exposes mitochondria to the hazards of Ca^{2+} overload when the rate of Ca^{2+} uptake exceeds that of the combined efflux pathways, *e.g.* for sharp increases of cytosolic $[Ca^{2+}]$. In this short review we discuss the hypothesis that transient opening of the Ca^{2+}-dependent permeability transition pore may provide mitocondria with a fast Ca^{2+} release channel preventing Ca^{2+} overload. We also address the relevance of a mitochondrial Ca^{2+} release channel recently discovered in *Drosophila melanogaster*, which possesses intermediate features between the permeability transition pore of yeast and mammals.

1. Mitochondria have a large Ca^{2+} problem

In energized mitochondria Ca^{2+} uptake is an electrophoretic process driven by the Ca^{2+} electrochemical gradient, $\Delta\tilde{\mu}Ca$:

$$\Delta\tilde{\mu}Ca = zF\Delta\Psi + RT \ln \frac{[Ca^{2+}]_i}{[Ca^{2+}]_o} \quad (1)$$

In respiring, coupled mitochondria the $\Delta\psi$ (negative inside) drives uptake of Ca^{2+}, which is transported with a net charge of 2 [1,2] *via* an inner membrane channel [3], the mitochondrial Ca^{2+} uniporter, MCU [4,5]. Ca^{2+} uptake is charge-compensated by increased H^+ pumping by the respiratory chain [1,2], resulting in increased matrix pH that prevents the recovery of $\Delta\psi$, limiting the further ability to accumulate Ca^{2+} [6–8]. Uptake of substantial amounts of Ca^{2+} therefore requires both buffering of matrix pH (to allow regeneration of the $\Delta\psi$); and buffering of matrix Ca^{2+} (to prevent the buildup of a Ca^{2+} concentration gradient) [6–8]. Buffering of matrix pH is achieved by the simultaneous uptake of protons and anions *via* diffusion of the undissociated acid through the inner membrane (as in the case of acetate), of CO_2 (which then regenerates bicarbonate and H^+ in the matrix) or through transport proteins (like the H^+–Pi symporter) [9]. Buffering of accumulated Ca^{2+} (and therefore the final $[Ca^{2+}]$ in the matrix) thus depends in part on the cotransported anion and in part on remarkably ill-characterized matrix constituents. If Pi is the prevailing anion, free matrix $[Ca^{2+}]$ becomes invariant with the matrix Ca^{2+} load [10] and the $\Delta\tilde{\mu}Ca$ favors the accumulation of large loads of both Ca^{2+} and Pi [11], with a predicted Ca^{2+} equilibrium accumulation of 10^6 if the $\Delta\psi$ is −180 mV [6]. This is never reached because at resting cytosolic Ca^{2+} levels the rate of Ca^{2+} uptake is comparable to that of the efflux pathways, and Ca^{2+} distribution is governed by a kinetic steady state rather than by thermodynamic equilibrium [6,7]. Thus, in energized mitochondria coupling of Ca^{2+} uptake with Ca^{2+} efflux on separate pathways allows regulation of both cytosolic and matrix $[Ca^{2+}]$. Energy is required both for Ca^{2+} uptake and for Ca^{2+} release, owing to the electrophoretic nature of transport on MCU and the $3Na^+$–$1Ca^{2+}$ stoichiometry of NCLX [12], which dissipates the $\Delta\psi$; the requirement for H^+ extrusion posed by operation of the Na^+–H^+ exchanger (NHE) coupled to NCLX; and the fact that Ca^{2+} efflux on the putative H^+–Ca^{2+} exchanger is favored by the $\Delta\psi$ [13,14], suggesting a H^+–Ca^{2+} stoichiometry higher than $2H^+$ per Ca^{2+}. A kinetic imbalance is apparent, however, because the V_{max} of the MCU is of the order of 1400 nmol Ca^{2+} mg^{-1} protein min^{-1} while the combined V_{max} of the efflux pathways is about

* Corresponding author at: Department of Biomedical Sciences, University of Padova, Viale Giuseppe Colombo 3, I-35121 Padova, Italy. Tel.: +39 049 827 6365; fax: +39 049 827 6361.
E-mail address: bernardi@bio.unipd.it (P. Bernardi).

0143-4160/$ – see front matter © 2012 Elsevier Ltd. All rights reserved.
http://dx.doi.org/10.1016/j.ceca.2012.03.004

20 nmol Ca^{2+} mg^{-1} protein min^{-1}. This arrangement exposes mitochondria to the hazards of Ca^{2+} overload when the rate of Ca^{2+} uptake exceeds that of the combined efflux pathways, e.g. for sharp increases of cytosolic [Ca^{2+}]. Why is then the rate of Ca^{2+} efflux so slow?

The rate of Ca^{2+} uptake *via* the MCU is a steep function of extramitochondrial [Ca^{2+}] [15]. Increasing rates of Ca^{2+} efflux would increase extramitochondrial Ca^{2+}, stimulate Ca^{2+} uptake *via* MCU and increase overall Ca^{2+} cycling, resulting in energy dissipation [16]. This can be observed by adding the electroneutral $2H^+$–Ca^{2+} ionophore A23187 to respiring mitochondria that have accumulated Ca^{2+}, a condition where Ca^{2+} is released and all of the respiratory capacity can be diverted into Ca^{2+} cycling [17]. Thus (and as long as the membrane potential is high) net Ca^{2+} efflux through stimulation of the efflux pathways would have a high energetic cost. The low V_{max} and early saturation of the efflux pathways by matrix Ca^{2+} are probably designed to pose an upper limit to the energy that can be spent in regulation of matrix and cytosolic [Ca^{2+}] through mitochondrial "Ca^{2+} cycling". As mentioned above, however, this situation exposes mitochondria to the constant threat of Ca^{2+} overload. We have proposed that this event may be prevented by transient openings of the permeability transition pore (PTP), which does mediate mitochondrial depolarization and fast Ca^{2+} release *in vitro* and possibly *in vivo* [18].

2. Properties of the permeability transition pore in mammals

The PTP is a high-conductance (≈1.3 nS) inner membrane channel [19–21]. In the fully open state its apparent diameter is about 3 nm [22] and its solute exclusion size ≈ 1500 Da. The PTP open-closed transitions are regulated by physiological effectors, and the consequences of pore opening vary dramatically depending on the open time [16]. Here we shall cover only the basic features of PTP modulation, and we refer the Reader to previous reviews for more information on the rise of the PTP from the status of *in vitro* artifact to that of effector mechanism of cell death regulated by key signaling cascades [23–25].

Matrix modulators of the PTP include Ca^{2+} through a "permissive" site for opening that can be competitively inhibited by other Me^{2+} ions like Mg^{2+}, Sr^{2+} and Mn^{2+}; and Pi, which in most species acts as a powerful PTP inducer through a still undefined mechanism. Pore opening is promoted by an oxidized state of pyridine nucleotides and of critical dithiols at discrete sites, both effects being individually reversed by proper reductants [26]. Pore opening can also *cause* production of reactive oxygen species, as shown by the occurrence of "superoxide flashes" triggered by transient openings of the PTP in cardiomyocytes [27]. The permeability transition is strictly modulated by matrix pH with an optimum at pH 7.4, while the open probability decreases both below pH 7.4 (through reversible protonation of critical histidyl residues [28,29]) and above pH 7.4 (through an unknown mechanism). Opening of the PTP is inhibited by cyclosporin (Cs) A after binding of the latter to cyclophilin (CyP) D, a matrix peptidyl-prolyl *cis-trans* isomerase encoded by the *Ppif* gene that facilitates PTP opening [30–32]; indeed, ablation of CyPD approximately doubles the threshold Ca^{2+} load required to open the PTP, which becomes identical to that of CsA-treated, strain-matched wild type mitochondria, while no effect of CsA is observed in CyPD-null mitochondria [33–36]. Major *membrane* effectors are the inside-negative $\Delta\psi_m$, which tends to stabilize the PTP in the closed conformation [28]; and electron flux within respiratory chain complex I, with an increased open probability when flux increases [37]. The latter finding led to the discovery that the PT is regulated by quinones [38], possibly through a specific binding site whose occupancy affects the open-closed transitions depending on the bound species [39].

The only primary consequence of PTP opening is mitochondrial depolarization. Unless single channel events are being recorded openings of short duration may not be detected by potentiometric probes. Since opening events are not synchronized for individual mitochondria [40,41] in population studies they may also be missed due to probe redistribution. We refer the reader to a series of specific studies about the occurrence of PTP openings of different durations in mitochondria *in situ*, and their consequences on cell viability [40–44]. For openings of longer duration depolarization can be easily measured both in isolated mitochondria and intact cells. As long as the pore is open collapse of the $\Delta\tilde{\mu}H$ prevents ATP synthesis, and ATP hydrolysis by the mitochondrial ATPase worsens ATP depletion, which together with altered Ca^{2+} homeostasis is a key factor in various paradigms of cell death [45]. Persistent PTP opening is also followed by loss of matrix pyridine nucleotides with respiratory inhibition [46], by equilibration of ion gradients, and by diffusion of solutes with molecular masses lower than about 1500 Da and possible occurrence of swelling, cristae unfolding and outer membrane rupture. This, however, is not an inevitable consequence of PTP opening. Cristae remodeling due to PTP opening can also occur in the absence of outer membrane rupture [47] with mobilization of the large pool of cytochrome *c* usually compartmentalized in the intracristal spaces [48] allowing increased release of cytochrome *c* through BAX/BAK channels in an otherwise intact outer membrane [47]. Furthermore, osmotic swelling requires the existence of a colloidosmotic gradient between the matrix and the intermembrane space that may not exist (or may not be large enough) to cause outer membrane rupture *in situ*.

The possible role of the PTP in physiological Ca^{2+} homeostasis has not been studied thoroughly, in part because the nature of the PTP has remained elusive [23] and therefore modulation of the "channel" itself by genetic methods has not been possible; in part because true PTP blockers have not been developed. Great hopes were raised by the discovery that the PTP is inhibited by CsA [49–51], but it is now clear that CyPD is a key modulator but not an obligatory component of the PTP. It should therefore be borne in mind that *Ppif*$^{-/-}$ *(CyPD-null) mice are not PTP-null mice*, as a permeability transition can still occur, e.g. after an increased Ca^{2+} load [33–36]. This consideration has dramatic implications for the interpretation of results obtained with CsA; similar to the absence of CyPD, CsA can desensitize but not block the PTP, and therefore lack of sensitivity to CsA does not necessarily mean that the PTP is not involved in the event under study. Little attention has also been paid to the fact that expression of CyPD can be modulated (e.g. by muscle denervation [52]), and that only CyPD-expressing mitochondria are expected to respond to CsA. A further element of complexity is that CsA also affects mitochondria *in situ* by preventing calcineurin-dependent dephosphorylation of the pro-fission protein DRP1, which is essential for its translocation to mitochondria [53]. The resulting inhibition of mitochondrial fission by CsA may thus be a cytoprotective event that is independent of inhibition of CyPD and desensitization of the PTP [53], a finding that should induce some caution in evaluating *in situ* and *in vivo* studies based only on CsA rather than on genetic ablation of CyPD or on the use of CyP inhibitors devoid of effects on calcineurin [54–56].

3. The mitochondrial permeability transition pore as a Ca^{2+} release channel: is lack of selectivity a problem or an advantage?

If a Ca^{2+} concentration gradient exists between the matrix and the external medium (or the cytosol) PTP opening leads to Ca^{2+} release. In 1996 we have proposed that the PTP may serve as a

mitochondrial Ca^{2+} release channel [18], and a specific point that needs to be discussed is whether the lack of selectivity is a real problem, or rather an essential feature that allows fast and effective release of matrix Ca^{2+}. Ca^{2+} efflux down its concentration gradient *via* a Ca^{2+}-selective channel would be opposed by the buildup of a Ca^{2+} diffusion potential [57]. According to the Nernst equation, the magnitude of the Ca^{2+} diffusion potential when no charge-compensating species are present is −30 mV per decade of the matrix/cytosol Ca^{2+} concentration ratio. This diffusion potential is reduced to less negative values (with corresponding increase of the Ca^{2+} efflux rate) by any charge-compensating current (influx of positive charges, efflux of negative charges, or both). Since the inner membrane has a very low permeability to charged species, the rate of Ca^{2+} efflux would be extremely slow and essentially limited by the H^+ permeability. In other words, to obtain a significant rate of Ca^{2+} efflux *via* a Ca^{2+}-selective channel the inner membrane permeability should be increased as well. An unselective pore of large size like the PTP confers the advantage of providing charge compensation within the channel itself, thus allowing maximal Ca^{2+} flux (*i.e.* Ca^{2+} release would occur at zero potential). This would make Ca^{2+} release possible even for vanishingly small $[Ca^{2+}]$ gradients, regulation being achieved through modulation of the pore open time. It should be noted that no K^+ and Na^+ concentration gradients exist across the inner membrane because the slow electrophoretic uptake of K^+ and Na^+ is compensated by the K^+–H^+ exchanger and the NHE, respectively. Thus, PTP opening can lead to selective Ca^{2+} release without perturbation of K^+ and Na^+ homeostasis, and no evolutionary pressure may have existed for the development of cation selectivity. In this respect the PTP is strikingly similar to the Ca^{2+} release channel of the sarcoplasmic reticulum, which operates as a Ca^{2+}-selective channel despite its large size (>38 Å), high conductance for monovalent cations (≈1 nS at saturating K^+), permeability to solutes like glucose and low permeability ratio when both K^+ and Ca^{2+} are present ($P_{Ca}/P_K \approx 6$) [58].

4. A Ca^{2+} release channel in *Drosophila* mitochondria: the missing link between the PTP of yeast and mammals?

We have recently argued that, in spite of clear differences between species, the PTP has been conserved in evolution from yeast to mammals [59]. Yeast mitochondria do possess a permeability pathway that resembles the mammalian PTP, also called the Yeast Mitochondrial Unselective Channel (YMUC) [60,61]. Based on the features of the PTP of yeast and mammals as of 1998, Manon et al. concluded that regulation of YMUC is too different from that of the mammalian PTP for yeast to be a good model of the latter [60]; in the light of new results we believe that the differences are not as fundamental as suspected earlier, and we refer the reader to a recent review specifically devoted to this aspect [59]. Other than in mammals and yeast, occurrence of a permeability transition has been established in plants, amphibians and fish including zebrafish (*Danio rerio*) [62] (see [59] for references). A mitochondrial Ca^{2+} release channel (mCRC) that we recently identified in cells from *Drosophila melanogaster* [63] deserves a special mention, as it may represent an evolutionary variant of the PTP displaying remarkable selectivity toward Ca^{2+} and H^+.

Mitochondria were studied in digitonin-permeabilized S_2R^+ cells [63], which are derived from Drosophila late embryonic stages and represent a variety of tissue precursors [64]. Of interest, mitochondria of S_2R^+ cells possess all the classical Ca^{2+} transport pathways found in mammalian mitochondria, *i.e.* (i) the RR-sensitive Ca^{2+} uniporter (which is consistent with the existence of orthologs of MCU [4,5] and of MICU1 [65] in the Drosophila genome); (ii) the Na^+–Ca^{2+} antiporter recently identified as NCLX [12], whose ortholog also exists in Drosophila; (iii) the RR-insensitive putative H^+–Ca^{2+} antiporter mediating Ca^{2+} release at high membrane potential; (iv) a tetracaine-sensitive, RR-insensitive Ca^{2+} release pathway that opens in response to matrix Ca^{2+} loading or to depolarization, and mediates Ca^{2+} release [63]. The properties of the Drosophila mCRC appear to be intermediate between those of the PTP of mammals and yeast. Like the mammalian PTP, the Drosophila Ca^{2+} release pathway is inhibited by tetracaine [66] and opens in response to matrix Ca^{2+} loading, inner membrane depolarization, thiol oxidation and treatment with relatively high concentrations of NEM [63]. Like the yeast PTP (and at striking variance from the mammalian pore) the Drosophila mCRC is *inhibited* rather than stimulated by Pi; and is insensitive to ADP, quinones and to CsA [63], a finding that matches the absence of a mitochondrial CyP in Drosophila. Together with the inhibitory effect of Pi, the most striking difference between the Drosophila mCRC and the PTP is the selectivity for the transported species. At the onset of Ca^{2+}-dependent Ca^{2+} release Drosophila mitochondria undergo depolarization, suggesting that the putative channel is also permeable to H^+; yet no matrix swelling is observed even in KCl-based medium, indicating that the channel is not permeable to K^+ (and to Cl^-) in spite of the fact that the hydrated radius of Ca^{2+} is larger than that of K^+ [63]. Lack of swelling was confirmed by lack of cytochrome *c* release and by ultrastructural analysis, and was not due to peculiar structural features of Drosophila mitochondria because matrix swelling and cytochrome *c* release readily followed the addition of the pore-forming peptide alamethicin [63].

Table 1
Properties of mammalian and yeast PTP, and of the Drosophila mCRC.

	Mammals	Yeast	Drosophila
Permeability to solutes up to ≈1500 Da	Yes	Yes	No
Selective Ca^{2+} release	No	No	Yes
Matrix Ca^{2+}	Required	May be required	Required
Matrix Pi	Inducer	Inhibitor	Inhibitor
mt Cyp	Yes	Yes	No
CsA	Inhibitor	No effect	No effect
Tetracaine	Inhibitor	Not tested	Inhibitor
Redox sites	Yes	Yes	Yes

The key features of the yeast and mammalian PTP, and of the Drosophila mCRC are summarized in Table 1. The most remarkable differences are the permeability to solutes, the selectivity for Ca^{2+} and the effects of Pi. Since nearly all yeast strains lack an MCU, the Ca^{2+}-dependence of the yeast PTP has not been easy to assess although it was known that the yeast PT is favored by added Ca^{2+} [67]. Recent work using the Ca^{2+} ionophore ETH129, which mediates electrophoretic Ca^{2+} transport, has demonstrated that the PTP is favored by Ca^{2+} uptake in mitochondria from *Saccharomyces cerevisiae* [68], and based on this finding we suggest that matrix Ca^{2+} may be required for onset of the PT in yeast as well (Table 1). Lack of inhibition of Drosophila mCRC by CsA can be easily explained by the lack of a mitochondrial CyP. On the other hand, since a matrix CyP is found in yeast and its enzymatic activity is inhibited by CsA [69] we suspect that the CyP ability to interact with the PTP occurred later in evolution.

5. The PTP as a mitochondrial Ca^{2+} release channel: only a hypothesis?

In 1992, Altschuld et al. demonstrated that CsA significantly increases net Ca^{2+} uptake and decreases Ca^{2+} efflux in isolated cardiomyocytes, as measured by radiolabeled $^{45}Ca^{2+}$, without having any impact on cell morphology or viability [70]. The effect of CsA was concentration-dependent and specific to mitochondria, as

ATP-dependent Ca^{2+} uptake by the sarcoplasmatic reticulum was not affected. The selectivity of the effects for mitochondrial Ca^{2+} and the very short incubation time with CsA (15 min) suggest that the PTP was being affected, and these data may represent the first piece of evidence that the pore contributes to Ca^{2+} cycling in mitochondria of living cardiomyocytes, and that reversible pore opening may be a physiological process in heart cells [70]. On the other hand, Eriksson et al. found that fluxes of Ca^{2+}, Mg^{2+} and adenine nucleotides in perfused rat livers following hormonal stimulation were unaffected by previous administration of CsA, even if the PTP was demonstrably desensitized by CsA in mitochondria isolated from the same CsA-perfused livers [71]. The Authors concluded that regulation of mitochondrial ion and metabolite homeostasis is independent of the PTP [71], yet as discussed above a negative result is not as informative.

Two recent publications based on *Ppif*$^{-/-}$ cells and mice do provide clear support for a role of the PTP in Ca^{2+} homeostasis [72,73]. Adult cortical neurons from wild type and *Ppif*$^{-/-}$ mice were treated with either ATP (to activate P2Y purinergic receptors) or with depolarizing concentrations of KCl (to open plasma membrane voltage-dependent Ca^{2+} channels), both stimuli causing a robust increase of both cytosolic and mitochondrial [Ca^{2+}] that was indistinguishable in neurons of the two genotypes [73]. Application of the two stimuli together, however, resulted in much higher levels of mitochondrial [Ca^{2+}] in the *Ppif*$^{-/-}$ neurons, suggesting that the threshold for PTP activation had been reached in the wild type but not in the CyPD-null mitochondria *in situ*. Thus, it appears that the regulatory role of CyPD (and of PTP opening) becomes crucial only for relatively large mitochondrial Ca^{2+} loads exceeding the capacity of NCLX and of the Na^+-insensitive release pathway [73]. In other words, the PTP could be silent unless high Ca^{2+} loads saturate the NCLX and the H^+–Ca^{2+} exchanger, allowing matrix [Ca^{2+}] to rise enough to trigger pore opening. It should be noted that the transient stimulation of these Ca^{2+}-mobilizing pathways did not induce cell death either in wild type or in CyPD-null neurons, suggesting that the mitochondrial PTP-activating response was part of a physiological process that is consistent with occurrence of reversible PTP opening [42].

In adult mice ablation of CyPD increases resistance to acute ischemia-reperfusion injury both in the heart and brain [33,35,36,74], while in neonatal mice, where the membrane-permeabilizing effects of BAX predominate, *Ppif*$^{-/-}$ mice were instead remarkably sensitized suggesting age-related changes in the mitochondrial response to injury [74]. An age-related phenotype was also discovered in the hearts of *Ppif*$^{-/-}$ mice, which displayed an intriguing decrease of maximum contractile reserve matched by increased shortening and relaxation times with longer decay of cytosolic Ca^{2+} transients [72]. *Ppif*$^{-/-}$ mice were also unable to compensate for the increase in afterload caused by transaortic constriction, displaying a larger reduction in fractional shortening, decompensation, ventricular dilation, fibrosis and congestive heart failure; all consequences of CyPD ablation were cured by heart-selective reexpression of CyPD, strongly indicating that the maladaptive phenotype of *Ppif*$^{-/-}$ mice depends on a primary disturbance of myocyte mitochondria rather than on an underlying systemic response [72]. Metabolic *in vivo* analysis demonstrated a significant increase in the glucose to palmitate ratio, suggesting a metabolic shift from fatty acid oxidation to glycolysis associated with increased activity of pyruvate dehydrogenase and α-ketoglutarate dehydrogenase. Direct measurement of total mitochondrial Ca^{2+} content of *Ppif*$^{-/-}$ hearts showed a 2.6-fold increase, which was matched by greater mitochondrial Ca^{2+} transients in myocytes treated with CsA. Very importantly, under continuous pacing PTP desensitization with CsA decreased the rise time in Ca^{2+} accumulation and prolonged the recovery time after pacing, findings that are entirely consistent with the PTP acting as a Ca^{2+} release channel to prevent Ca^{2+} overload [72].

6. Summary and conclusions

The hypothesis that transient opening of the PTP may serve the physiological function of regulating matrix Ca^{2+} by preventing Ca^{2+} overload appears theoretically justified, and supported by a limited but extremely solid set of experimental results. Confusion may have arisen from the interpretation of results based on the use of CsA as well as of *Ppif*$^{-/-}$ mice, which have too often been erroneously considered null for the PTP as well. Much more work is obviously needed, and we hope that this short review will help rekindle interest and experimental testing of this subject.

Acknowledgments

Work in our laboratory is supported by funds from the MIUR (FIRB and PRIN), Telethon Grants GPP10005 and GGP11082, AIRC Investigator Grant 8722, the University of Padova and the Fondazione Cariparo.

References

[1] A. Scarpa, G.F. Azzone, The mechanism of ion translocation in mitochondria. 4. Coupling of K^+ efflux with Ca^{2+} uptake, Eur. J. Biochem. 12 (1970) 328–335.
[2] D.E. Wingrove, J.M. Amatruda, T.E. Gunter, Glucagon effects on the membrane potential and calcium uptake rate of rat liver mitochondria, J. Biol. Chem. 259 (1984) 9390–9394.
[3] Y. Kirichok, G. Krapivinsky, D.E. Clapham, The mitochondrial calcium uniporter is a highly selective ion channel, Nature 427 (2004) 360–364.
[4] D. De Stefani, A. Raffaello, E. Teardo, I. Szabó, R. Rizzuto, A forty-kilodalton protein of the inner membrane is the mitochondrial calcium uniporter, Nature 476 (2011) 336–340.
[5] J.M. Baughman, F. Perocchi, H.S. Girgis, M. Plovanich, C.A. Belcher-Timme, Y. Sancak, X.R. Bao, L. Strittmatter, O. Goldberger, R.L. Bogorad, V. Koteliansky, V.K. Mootha, Integrative genomics identifies MCU as an essential component of the mitochondrial calcium uniporter, Nature 476 (2011) 341–345.
[6] G.F. Azzone, T. Pozzan, S. Massari, M. Bragadin, P. Dell'Antone, H^+/site ratio and steady state distribution of divalent cations in mitochondria, FEBS Lett. 78 (1977) 21–24.
[7] D.G. Nicholls, The regulation of extramitochondrial free calcium ion concentration by rat liver mitochondria, Biochem. J. 176 (1978) 463–474.
[8] P. Bernardi, D. Pietrobon, On the nature of Pi-induced, Mg^{2+}-prevented Ca^{2+} release in rat liver mitochondria, FEBS Lett. 139 (1982) 9–12.
[9] P. Mitchell, Keilin's respiratory chain concept and its chemiosmotic consequences, Science 206 (1979) 1148–1159.
[10] S. Chalmers, D.G. Nicholls, The relationship between free and total calcium concentrations in the matrix of liver and brain mitochondria, J. Biol. Chem. 278 (2003) 19062.
[11] E.J. Harris, B. Zaba, The phosphate requirement for Ca^{2+}-uptake by heart and liver mitochondria, FEBS Lett. 79 (1977) 284–290.
[12] R. Palty, W.F. Silverman, M. Hershfinkel, T. Caporale, S.L. Sensi, J. Parnis, C. Nolte, D. Fishman, V. Shoshan-Barmatz, S. Herrmann, D. Khananshvili, I. Sekler, NCLX is an essential component of mitochondrial Na^+/Ca^{2+} exchange, Proc. Natl. Acad. Sci. U.S.A. 107 (2010) 436–441.
[13] P. Bernardi, G.F. Azzone, A membrane potential-modulated pathway for Ca^{2+} efflux in rat liver mitochondria, FEBS Lett. 139 (1982) 13–16.
[14] P. Bernardi, G.F. Azzone, Regulation of Ca^{2+} efflux in rat liver mitochondria. Role of membrane potential, Eur. J. Biochem. 134 (1983) 377–383.
[15] M. Bragadin, T. Pozzan, G.F. Azzone, Kinetics of Ca^{2+} carrier in rat liver mitochondria, Biochemistry 18 (1979) 5972–5978.
[16] P. Bernardi, Mitochondrial transport of cations: channels, exchangers, and permeability transition, Physiol. Rev. 79 (1999) 1127–1155.
[17] G.M Heaton, D.G. Nicholls, The calcium conductance of the inner membrane of rat liver mitochondria and the determination of the calcium electrochemical gradient, Biochem. J. 156 (1976) 635–646.
[18] P. Bernardi, V. Petronilli, The permeability transition pore as a mitochondrial calcium release channel: a critical appraisal, J. Bioenerg. Biomembr. 28 (1996) 131–138.
[19] V. Petronilli, I. Szabó, M. Zoratti, The inner mitochondrial membrane contains ion-conducting channels similar to those found in bacteria, FEBS Lett. 259 (1989) 137–143.

[20] K.W. Kinnally, M.L. Campo, H. Tedeschi, Mitochondrial channel activity studied by patch-clamping mitoplasts, J. Bioenerg. Biomembr. 21 (1989) 497–506.
[21] I. Szabó, M. Zoratti, The giant channel of the inner mitochondrial membrane is inhibited by cyclosporin A, J. Biol. Chem. 266 (1991) 3376–3379.
[22] S. Massari, G.F. Azzone, The equivalent pore radius of intact and damaged mitochondria and the mechanism of active shrinkage, Biochim. Biophys. Acta 283 (1972) 23–29.
[23] P. Bernardi, A. Krauskopf, E. Basso, V. Petronilli, E. Blachly-Dyson, F. Di Lisa, M.A. Forte, The mitochondrial permeability transition from in vitro artifact to disease target, FEBS J. 273 (2006) 2077–2099.
[24] A. Rasola, M. Sciacovelli, B. Pantic, P. Bernardi, Signal transduction to the permeability transition pore, FEBS Lett. 584 (2010) 1989–1996.
[25] A. Rasola, P. Bernardi, Mitochondrial permeability transition in Ca^{2+}-dependent apoptosis and necrosis, Cell Calcium 50 (2011) 222–233.
[26] P. Costantini, B.V. Chernyak, V. Petronilli, P. Bernardi, Modulation of the mitochondrial permeability transition pore by pyridine nucleotides and dithiol oxidation at two separate sites, J. Biol. Chem. 271 (1996) 6746–6751.
[27] W. Wang, H. Fang, L. Groom, A. Cheng, W. Zhang, J. Liu, X. Wang, K. Li, P. Han, M. Zheng, J. Yin, W. Wang, M.P. Mattson, J.P. Kao, E.G. Lakatta, S.S. Sheu, K. Ouyang, J. Chen, R.T. Dirksen, H. Cheng, Superoxide flashes in single mitochondria, Cell 134 (2008) 279–290.
[28] P. Bernardi, Modulation of the mitochondrial cyclosporin A-sensitive permeability transition pore by the proton electrochemical gradient. Evidence that the pore can be opened by membrane depolarization, J. Biol. Chem. 267 (1992) 8834–8839.
[29] A. Nicolli, V. Petronilli, P. Bernardi, Modulation of the mitochondrial cyclosporin A-sensitive permeability transition pore by matrix pH. Evidence that the pore open-closed probability is regulated by reversible histidine protonation, Biochemistry 32 (1993) 4461–4465.
[30] A.P. Halestrap, A.M. Davidson, Inhibition of Ca^{2+}-induced large-amplitude swelling of liver and heart mitochondria by cyclosporin is probably caused by the inhibitor binding to mitochondrial-matrix peptidyl-prolyl cis-trans isomerase and preventing it interacting with the adenine nucleotide translocase, Biochem. J. 268 (1990) 153–160.
[31] E.J. Griffiths, A.P. Halestrap, Further evidence that cyclosporin A protects mitochondria from calcium overload by inhibiting a matrix peptidyl-prolyl cis-trans isomerase. Implications for the immunosuppressive and toxic effects of cyclosporin, Biochem. J. 274 (1991) 611–614.
[32] A. Nicolli, E. Basso, V. Petronilli, R.M. Wenger, P. Bernardi, Interactions of cyclophilin with the mitochondrial inner membrane and regulation of the permeability transition pore, a cyclosporin A-sensitive channel, J. Biol. Chem. 271 (1996) 2185–2192.
[33] C.P. Baines, R.A. Kaiser, N.H. Purcell, N.S. Blair, H. Osinska, M.A. Hambleton, E.W. Brunskill, M.R. Sayen, R.A. Gottlieb, G.W. Dorn, J. Robbins, J.D. Molkentin, Loss of cyclophilin D reveals a critical role for mitochondrial permeability transition in cell death, Nature 434 (2005) 658–662.
[34] E. Basso, L. Fante, J. Fowlkes, V. Petronilli, M.A. Forte, P. Bernardi, Properties of the permeability transition pore in mitochondria devoid of cyclophilin D, J. Biol. Chem. 280 (2005) 18558–18561.
[35] T. Nakagawa, S. Shimizu, T. Watanabe, O. Yamaguchi, K. Otsu, H. Yamagata, H. Inohara, T. Kubo, Y. Tsujimoto, Cyclophilin D-dependent mitochondrial permeability transition regulates some necrotic but not apoptotic cell death, Nature 434 (2005) 652–658.
[36] A.C. Schinzel, O. Takeuchi, Z. Huang, J.K. Fisher, Z. Zhou, J. Rubens, C. Hetz, N.N. Danial, M.A. Moskowitz, S.J. Korsmeyer, Cyclophilin D is a component of mitochondrial permeability transition and mediates neuronal cell death after focal cerebral ischemia, Proc. Natl. Acad. Sci. U.S.A. 102 (2005) 12005–12010.
[37] E. Fontaine, O. Eriksson, F. Ichas, P. Bernardi, Regulation of the permeability transition pore in skeletal muscle mitochondria. Modulation by electron flow through the respiratory chain complex I, J. Biol. Chem. 273 (1998) 12662–12668.
[38] E. Fontaine, F. Ichas, P. Bernardi, A ubiquinone-binding site regulates the mitochondrial permeability transition pore, J. Biol. Chem. 273 (1998) 25734–25740.
[39] L. Walter, H. Miyoshi, X. Leverve, P. Bernardi, E. Fontaine, Regulation of the mitochondrial permeability transition pore by ubiquinone analogs. A progress report, Free Radic. Res. 36 (2002) 405–412.
[40] J. Hüser, C.E. Rechenmacher, L.A. Blatter, Imaging the permeability pore transition in single mitochondria, Biophys. J. 74 (1998) 2129–2137.
[41] J. Hüser, L.A. Blatter, Fluctuations in mitochondrial membrane potential caused by repetitive gating of the permeability transition pore, Biochem. J. 343 (Pt 2) (1999) 311–317.
[42] V. Petronilli, G. Miotto, M. Canton, M. Brini, R. Colonna, P. Bernardi, F. Di Lisa, Transient and long-lasting openings of the mitochondrial permeability transition pore can be monitored directly in intact cells by changes in mitochondrial calcein fluorescence, Biophys. J. 76 (1999) 725–734.
[43] V. Petronilli, D. Penzo, L. Scorrano, P. Bernardi, F. Di Lisa, The mitochondrial permeability transition, release of cytochrome c and cell death. Correlation with the duration of pore openings in situ, J. Biol. Chem. 276 (2001) 12030–12034.
[44] L. Scorrano, D. Penzo, V. Petronilli, F. Pagano, P. Bernardi, Arachidonic acid causes cell death through the mitochondrial permeability transition. Implications for tumor necrosis factor-α apoptotic signaling, J. Biol. Chem. 276 (2001) 12035–12040.
[45] P. Bernardi, V. Petronilli, F. Di Lisa, M. Forte, A mitochondrial perspective on cell death, Trends Biochem. Sci. 26 (2001) 112–117.
[46] A. Vinogradov, A. Scarpa, B. Chance, Calcium and pyridine nucleotide interaction in mitochondrial membranes, Arch. Biochem. Biophys. 152 (1972) 646–654.
[47] L. Scorrano, M. Ashiya, K. Buttle, S. Weiler, S.A. Oakes, C.A. Mannella, S.J. Korsmeyer, A distinct pathway remodels mitochondrial cristae and mobilizes cytochrome c during apoptosis, Dev. Cell 2 (2002) 55–67.
[48] P. Bernardi, G.F. Azzone, Cytochrome c as an electron shuttle between the outer and inner mitochondrial membranes, J. Biol. Chem. 256 (1981) 7187–7192.
[49] N. Fournier, G. Ducet, A. Crevat, Action of cyclosporine on mitochondrial calcium fluxes, J. Bioenerg. Biomembr. 19 (1987) 297–303.
[50] M. Crompton, H. Ellinger, A. Costi, Inhibition by cyclosporin A of a Ca^{2+}-dependent pore in heart mitochondria activated by inorganic phosphate and oxidative stress, Biochem. J. 255 (1988) 357–360.
[51] K.M. Broekemeier, M.E. Dempsey, D.R. Pfeiffer, Cyclosporin A is a potent inhibitor of the inner membrane permeability transition in liver mitochondria, J. Biol. Chem. 264 (1989) 7826–7830.
[52] K. Csukly, A. Ascah, J. Matas, P.F. Gardiner, E. Fontaine, Y. Burelle, Muscle denervation promotes opening of the permeability transition pore and increases the expression of cyclophilin D, J. Physiol. 574 (2006) 319–327.
[53] G.M. Cereghetti, A. Stangherlin, O. Martins de Brito, C.R. Chang, C. Blackstone, P. Bernardi, L. Scorrano, Dephosphorylation by calcineurin regulates translocation of Drp1 to mitochondria, Proc. Natl. Acad. Sci. U.S.A. 105 (2008) 15803–15808.
[54] P.C. Waldmeier, J.J. Feldtrauer, T. Qian, J.J. Lemasters, Inhibition of the mitochondrial permeability transition by the nonimmunosuppressive cyclosporin derivative NIM811, Mol. Pharmacol. 62 (2002) 22–29.
[55] M.J. Hansson, G. Mattiasson, R. Mansson, J. Karlsson, M.F. Keep, P. Waldmeier, U.T. Ruegg, J.M. Dumont, K. Besseghir, E. Elmer, The nonimmunosuppressive cyclosporin analogs NIM811 and UNIL025 display nanomolar potencies on permeability transition in brain-derived mitochondria, J. Bioenerg. Biomembr. 36 (2004) 407–413.
[56] T. Tiepolo, A. Angelin, E. Palma, P. Sabatelli, L. Merlini, L. Nicolosi, F. Finetti, P. Braghetta, G. Vuagniaux, J.M. Dumont, C.T. Baldari, P. Bonaldo, P. Bernardi, The cyclophilin inhibitor Debio 025 normalizes mitochondrial function, muscle apoptosis and ultrastructural defects in *Col6a1*$^{-/-}$ myopathic mice, Br. J. Pharmacol. 157 (2009) 1045–1052.
[57] K.E.O. Akerman, Changes in membrane potential during calcium ion influx and efflux across the mitochondrial membrane, Biochim. Biophys. Acta: Bioenerg 502 (1978) 359–366.
[58] J.S. Smith, T. Imagawa, J. Ma, M. Fill, K.P. Campbell, R. Coronado, Purified ryanodine receptor from rabbit skeletal muscle is the calcium-release channel of sarcoplasmic reticulum, J. Gen. Physiol. 92 (1988) 1–26.
[59] L. Azzolin, S. von Stockum, E. Basso, V. Petronilli, M.A. Forte, P. Bernardi, The mitochondrial permeability transition from yeast to mammals, FEBS Lett. 584 (2010) 2504–2509.
[60] S. Manon, X. Roucou, M. Guerin, M. Rigoulet, B. Guerin, Characterization of the yeast mitochondria unselective channel: a counterpart to the mammalian permeability transition pore? J. Bioenerg. Biomembr. 30 (1998) 419–429.
[61] S. Uribe-Carvajal, L.A. Luévano-Martínez, S. Guerrero-Castillo, A. Cabrera-Orefice, N.A. Corona-de-la-Peña, M. Gutiérrez-Aguilar, Mitochondrial unselective channels throughout the eukaryotic domain, Mitochondrion 11 (2011) 382–390.
[62] L. Azzolin, E. Basso, F. Argenton, P. Bernardi, Mitochondrial Ca^{2+} transport and permeability transition in zebrafish (*Danio rerio*), Biochim. Biophys. Acta 1797 (2010) 1775–1779.
[63] S. von Stockum, E. Basso, V. Petronilli, P. Sabatelli, M.A. Forte, P. Bernardi, Properties of Ca^{2+} Transport in Mitochondria of *Drosophila melanogaster*, J. Biol. Chem. 286 (2011) 41163–41170.
[64] I. Schneider, Cell lines derived from late embryonic stages of *Drosophila melanogaster*, J. Embryol. Exp. Morphol. 27 (1972) 353–365.
[65] F. Perocchi, V.M. Gohil, H.S. Girgis, X.R. Bao, J.E. McCombs, A.E. Palmer, V.K. Mootha, MICU1 encodes a mitochondrial EF hand protein required for Ca^{2+} uptake, Nature 467 (2010) 291–296.
[66] A.P. Dawson, M.J. Selwyn, D.V. Fulton, Inhibition of Ca^{2+} efflux from mitochondria by nupercaine and tetracaine, Nature 277 (1979) 484–486.
[67] A.J. Kowaltowski, A.E. Vercesi, S.G. Rhee, L.E. Netto, Catalases and thioredoxin peroxidase protect *Saccharomyces cerevisiae* against Ca^{2+}-induced mitochondrial membrane permeabilization and cell death, FEBS Lett. 473 (2000) 177–182.
[68] A. Yamada, T. Yamamoto, Y. Yoshimura, S. Gouda, S. Kawashima, N. Yamazaki, K. Yamashita, M. Kataoka, T. Nagata, H. Terada, D.R. Pfeiffer, Y. Shinohara, Ca^{2+}-induced permeability transition can be observed even in yeast mitochondria under optimized experimental conditions, Biochim. Biophys. Acta 1787 (2009) 1486–1491.
[69] M. Tropschug, I.B. Barthelmess, W. Neupert, Sensitivity to cyclosporin A is mediated by cyclophilin in *Neurospora crassa* and *Saccharomyces cerevisiae*, Nature 342 (1989) 953–955.
[70] R.A. Altschuld, C.M. Hohl, L.C. Castillo, A.A. Garleb, R.C. Starling, G.P. Brierley, Cyclosporin inhibits mitochondrial calcium efflux in isolated adult rat ventricular cardiomyocytes, Am. J. Physiol. 262 (1992) H1699–H1704.
[71] O. Eriksson, P. Pollesello, E. Geimonen, Regulation of total mitochondrial Ca^{2+} in perfused liver is independent of the permeability transition pore, Am. J. Physiol. 276 (1999) C1297–C1302.

[72] J.W. Elrod, R. Wong, S. Mishra, R.J. Vagnozzi, B. Sakthievel, S.A. Goonasekera, J. Karch, S. Gabel, J. Farber, T. Force, J.H. Brown, E. Murphy, J.D. Molkentin, Cyclophilin D controls mitochondrial pore-dependent Ca^{2+} exchange, metabolic flexibility, and propensity for heart failure in mice, J. Clin. Investig. 120 (2010) 3680–3687.
[73] A. Barsukova, A. Komarov, G. Hajnoczky, P. Bernardi, D. Bourdette, M. Forte, Activation of the mitochondrial permeability transition pore modulates Ca^{2+} responses to physiological stimuli in adult neurons, Eur. J. Neurosci. 33 (2011) 831–842.
[74] X. Wang, Y. Carlsson, E. Basso, C. Zhu, C.I. Rousset, A. Rasola, B.R. Johansson, K. Blomgren, C. Mallard, P. Bernardi, M.A. Forte, H. Hagberg, Developmental shift of cyclophilin D contribution to hypoxic-ischemic brain injury, J. Neurosci. 29 (2009) 2588–2596.